SHOCK AND VIBRATION SIGNAL ANALYSIS

By Tom Irvine

Email: tomirvine@aol.com

www.vibrationdata.com

September 12, 2005

PREFACE

Engineers collect accelerometer data in a variety of settings. Examples include:

1. Aerospace vehicle flight data
2. Automotive proving grounds
3. Machinery condition monitoring
4. Building and bridge response to seismic and wind excitation
5. Modal testing of structures

In addition, engineers acquire dynamic data from microphones, pressure transducers, geophones, strain gages and other sensors.

The sensors measure the time history data in analog form. The analog signal is sent through a signal conditioner. The signal conditioner should have an analog lowpass filter for anti-aliasing. The analog data is then converted to digital form.

The next step is to post-process the data in order to extract useful information. The primary metrics of interest are typically the spectral frequencies and corresponding amplitudes. The Fourier transform is a tool for identifying these spectral components, particularly if the data has some distinct sinusoidal content.

Furthermore, the power spectral density of signal can be calculated using the Fourier transform as an intermediate calculation step. The power spectral density is useful for analyzing random vibration.

This report presents both the Fourier transform and the power spectral density function. It also provides some data acquisition guidelines in terms of sampling rate and anti-alias filtering.

The remainder of the report discusses digital filtering, which can be used for many purposes.

The main purpose of filtering is to clarify the response of a particular spectral component, which may be an excitation function or a modal response frequency. Note that a given structure's natural frequency, or frequencies, may be excited by an applied force, base motion, or initial velocity or displacement. A structure may also experience "self-excited" vibration, such as flutter. Resonance is a special case where the excitation frequency matches the structural frequency. Bandpass filtering may be used to improve the signal-to-noise ratio of the frequency component of interest.

On the other hand, notch filtering can be used to suppress an unwanted frequency. Consider a rocket vehicle with a closed-loop guidance system. The autopilot has an internal navigation system which uses accelerometers and gyroscopes to determine the vehicle's attitude and direction. The navigation system then sends commands to actuators which rotate the exhaust nozzle to steer the vehicle during its powered flight. Feedback sensors measure the position of the nozzle. The data is sent back to the navigation computer. Unfortunately, the feedback sensors, accelerometers, and gyroscopes could be affected by the vehicle's body-bending vibration. Specifically, instability could result if the vibration frequency coincides with the control frequency. The body-bending frequencies must thus be removed from the sensor data via digital filtering.

Furthermore, digital filtering can also be used to calculate a power spectral density. This method is useful for educational purposes. A power spectral density is more commonly calculated from a Fourier transform, however.

CHAPTER 1

AN INTRODUCTION TO THE FOURIER TRANSFORM

Introduction

Stationary vibration signals can be placed along a continuum in terms of their qualitative characteristics.

A pure sine oscillation is at one end of the continuum. A form of broadband random vibration called white noise is at the other end.

Reasonable examples of each extreme occur in the physical world. Most signals, however, are somewhere in the middle of the continuum. An example is shown in Figure 1-1.

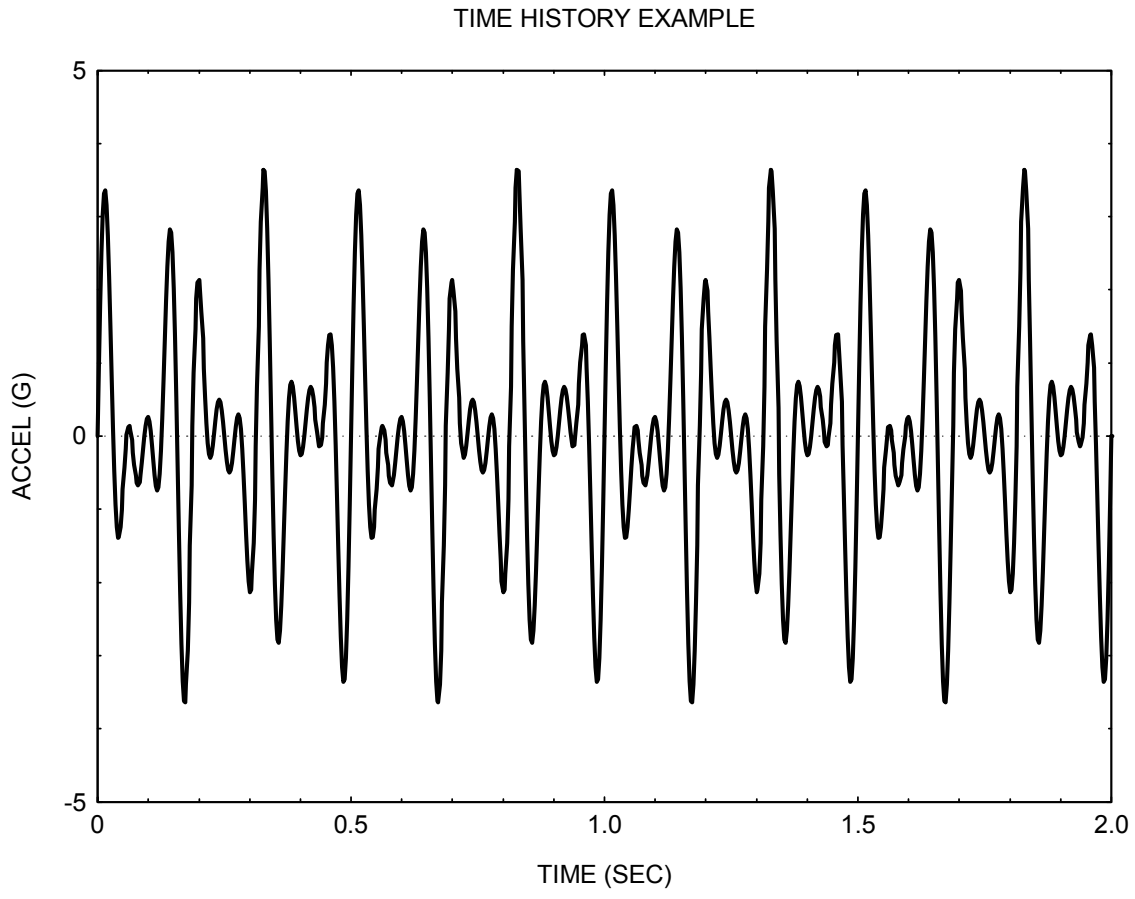

Figure 1-1.

The time history in Figure 1-1 appears to be the sum of several sine functions. The goal of this chapter is to resolve the frequencies and amplitudes of the components.

At the risk of short-circuiting the process, the equation of the signal in Figure 1-1 is

$$y(t) = 1.0 \sin[2\pi(10)t] + 1.5 \sin[2\pi(16)t] + 1.2 \sin[2\pi(22)t] \qquad (1\text{-}1)$$

The signal thus consists of three components with frequencies of 10, 16, and 22 Hz, respectively. The respective amplitudes are 1.0, 1.5, and 1.2 G.

In addition, each component could have had a phase angle. In this example, the phase angle was zero for each component.

A "spectral function" is thus needed to display the frequency and amplitude data. Ideally, the spectral function would have the form shown in Figure 1-2.

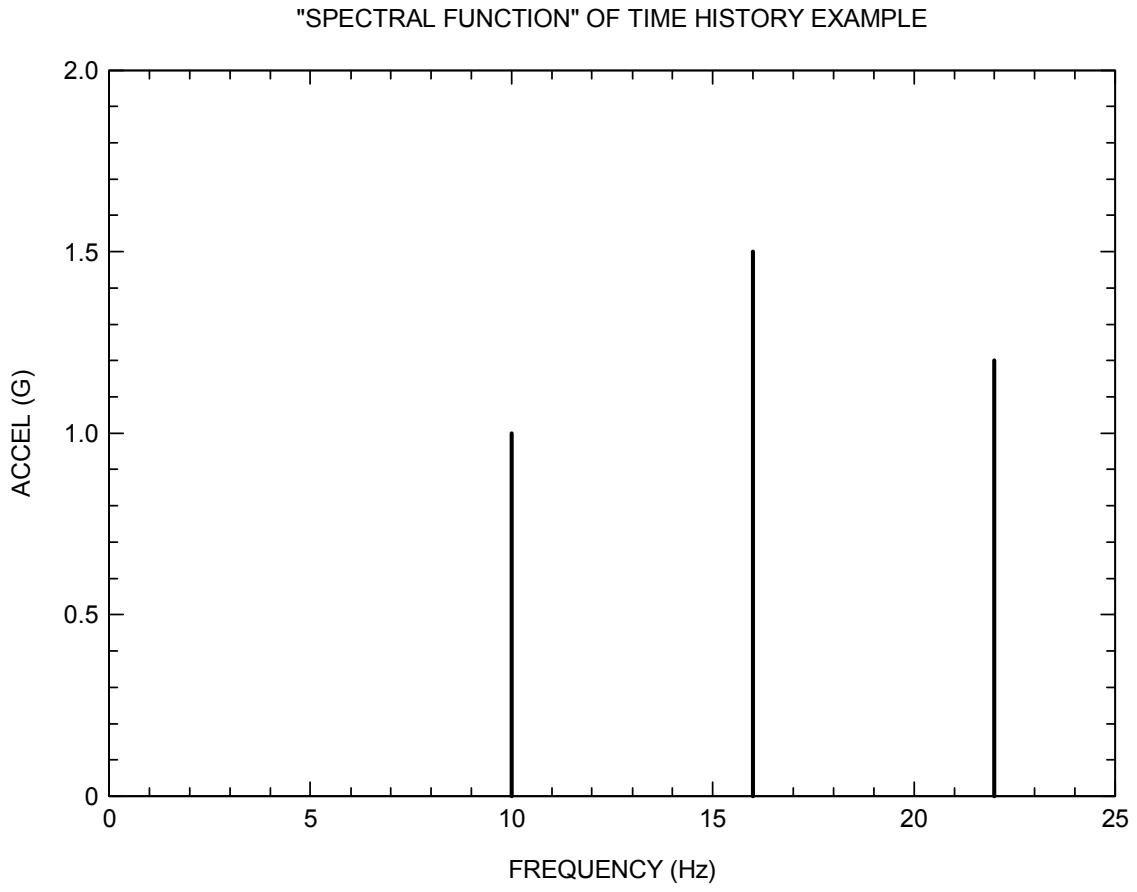

Figure 1-2.

Some engineers would claim that Figure 1-2 is the Fourier transform of the signal in equation (1-1). In some sense, this is true.

The Fourier transform, however, is a methodology which can be applied via many different forms and formulas.

Mathematicians and engineers make such different use of Fourier transforms that a mathematician would likely be unable to comprehend an engineer's application and vice versa.

This Unit will attempt to bridge the gap. A method will eventually be derived to transform the time history in Figure 1-1 to the frequency domain "spectral function" in Figure 1-2. The desired "spectral function" will be shown to be based on the Fourier transform. Nevertheless, the phrase which most aptly describes this process is "some assembly required."

Continuous Fourier Transform

The Fourier transform is a method for representing a time history signal in terms of a frequency domain function.

The Fourier transform is a complex exponential transform which is related to the Laplace transform.

The Fourier transform is also referred to as a trigonometric transformation since the complex exponential function can be represented in terms of trigonometric functions. Specifically,

$$\exp[j\omega t] = \cos(\omega t) + j\sin(\omega t) \tag{1-2a}$$

$$\exp[-j\omega t] = \cos(\omega t) - j\sin(\omega t) \tag{1-2b}$$

where $j = \sqrt{-1}$

The Fourier transform X(f) for a continuous time series x(t) is defined as

$$X(f) = \int_{-\infty}^{\infty} x(t)\exp[-j2\pi f t]dt \tag{1-3}$$

where $-\infty < f < \infty$

Thus, the Fourier transform is continuous over an infinite frequency range.

The inverse transform is

$$x(t) = \int_{-\infty}^{\infty} X(f)\exp[+j2\pi ft]df \tag{1-4}$$

Equations (1-3) and (1-4) are taken from Reference 1-1. Note that X(f) has dimensions of [amplitude-time].

Also note that X(f) is a complex function. It may be represented in terms of real and imaginary components, or in terms of magnitude and phase.

The conversion to magnitude and phase is made as follows for a complex variable V.

$$V = a + jb \tag{1-5}$$

$$\text{Magnitude } V = \sqrt{a^2 + b^2} \tag{1-6}$$

$$\text{Phase } V = \arctan(b / a) \tag{1-7}$$

Note that the inverse Fourier transform in equation (1-4) calculates the original time history in a complex form. The inverse Fourier transform will be entirely real if the original time history was real, however.

Continuous Example

Consider a sine function

$$x(t) = A\sin\left[2\pi \hat{f}\, t\right] \tag{1-8}$$

where $\infty < t < \infty$

The Fourier transform of the sine function is

$$X(f) = \left\{\frac{jA}{2}\right\}\left\{-\delta\left(f - \hat{f}\right) + \delta\left(-f - \hat{f}\right)\right\} \tag{1-9}$$

where δ is the Dirac delta function.

Note that

$$\delta\left(f - \hat{f}\right) = 0 \quad \text{for } f \neq \hat{f} \tag{1-10}$$

And

$$\int_{-\infty}^{\infty} \delta\left(f - \hat{f}\right) dt = 1 \tag{1-11}$$

The derivation is given in Appendix A. The Fourier transform is plotted in Figure 1-3.

Imaginary X(f)

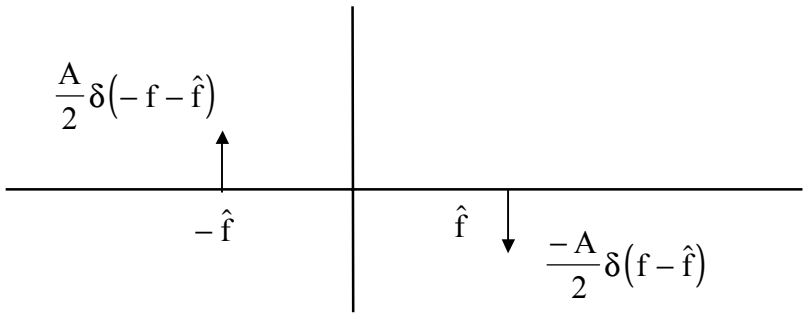

Figure 1-3. Fourier Transform of a Sine Function

The transform of a sine function is purely imaginary. The real component, which is zero, is not plotted.

On the other hand, the Fourier transform of a cosine function is

$$X(f) = \left\{\frac{A}{2}\right\}\left\{\delta\left(f - \hat{f}\right) + \delta\left(-f - \hat{f}\right)\right\} \tag{1-12}$$

The Fourier transform is plotted in Figure 1-4.

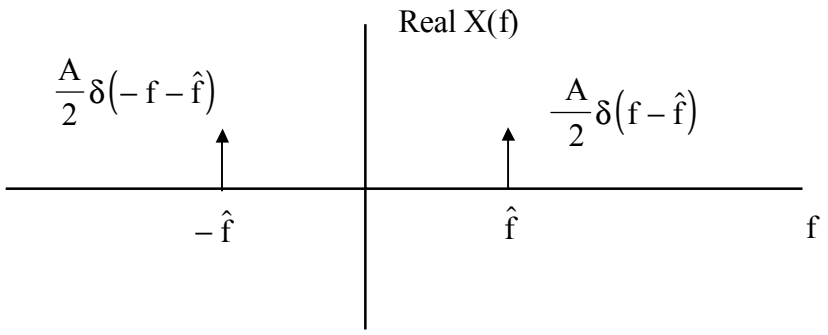

Figure 1-4. Fourier Transform of a Cosine Function

The transform of a cosine function is purely real. The imaginary component, which is zero, is not plotted.

Characteristics of the Continuous Fourier Transform

The plots in Figures 1-1 and 1-2 demonstrate two characteristics of the Fourier transforms of real time history functions:

1. The real Fourier transform is symmetric about the f = 0 line.
2. The imaginary Fourier transform is antisymmetric about the f = 0 line.

As an aside, the Dirac delta function is purely delightful from a mathematics point of view. Some mathematicians even promote it from a lowly function to a "distribution."

The Dirac delta distribution is of little or no use to the engineer in the test lab, however. A different approach is needed for engineers.

Discrete Fourier Transform (DFT)

An accelerometer returns an analog signal. The analog signal could be displayed in a continuous form on a traditional oscilloscope.

Current practice, however, is to digitize the signal, which allows for post-processing on a digital computer. Thus, the Fourier transform equation must be modified to accommodate digital data. This is essentially the dividing line between mathematicians and engineers in regard Fourier transformation methodology. Nevertheless, further assembly is required to meet the engineering goal, which is still the "spectral function" in Figure 1-2.

The discrete Fourier Transform $\hat{F}_k$ for a digital time series x_n is

$$\hat{F}_k = \Delta t \sum_{n=0}^{N-1} \left\{ x_n \exp\left(- j \frac{2\pi}{N} nk \right) \right\}, \quad \text{for } k = 0, 1, \ldots, N-1 \tag{1-13}$$

where

N	is the number of time domain samples
n	is the time domain sample index
k	is the frequency domain index
Δt	is the frequency domain index

Note that $\hat{F}_k$ has dimensions of [amplitude-time].

The corresponding inverse transform is

$$x_n = \Delta f \sum_{n=0}^{N-1} \left\{ \hat{F}_k \exp\left(+ j \frac{2\pi}{N} nk \right) \right\}, \text{ for } n = 0, 1, \ldots, N-1 \tag{1-14}$$

Note that the frequency increment Δf is equal to the time domain period T as follows

$$\Delta f = \frac{1}{T} \tag{1-15}$$

The frequency is obtained from the index parameter k as follows

$$\text{frequency } (k) = k \Delta f \tag{1-16}$$

The discrete Fourier transform in equation (1-13) requires further modification to meet the engineering goal set forth in Figure 1-2.

The following equation set is taken from Reference 1-2. As an alternate form, the Fourier transform F_k for a discrete time series x_n can be expressed as

$$F_k = \frac{1}{N} \sum_{n=0}^{N-1} \left\{ x_n \exp\left(- j \frac{2\pi}{N} nk \right) \right\}, \text{ for } k = 0, 1, \ldots, N-1 \tag{1-17}$$

The corresponding inverse transform is

$$x_n = \sum_{k=0}^{N-1} \left\{ F_k \exp\left(+ j \frac{2\pi}{N} nk \right) \right\}, \text{ for } n = 0, 1, ..., N-1 \qquad (1\text{-}18)$$

Note that F_k has dimensions of [amplitude]. Thus, an important milestone is reached.

Discrete Example

The discrete Fourier transform of a sine wave is given in Figure 1-5.

A characteristic of the discrete Fourier transform is that the frequency domain is taken from 0 to (N-1)Δf. The line of symmetry is at a frequency of

$$\left[\frac{N-1}{2} \right] \Delta f \qquad (1\text{-}19)$$

Nyquist Frequency

Note that the line of symmetry in Figure 1-5 marks the Nyquist frequency. The Nyquist frequency is equal to one-half of the sampling rate. Shannon's sampling theorem states that a sampled time signal must not contain components at frequencies above half the Nyquist frequency, from Reference 1-3.

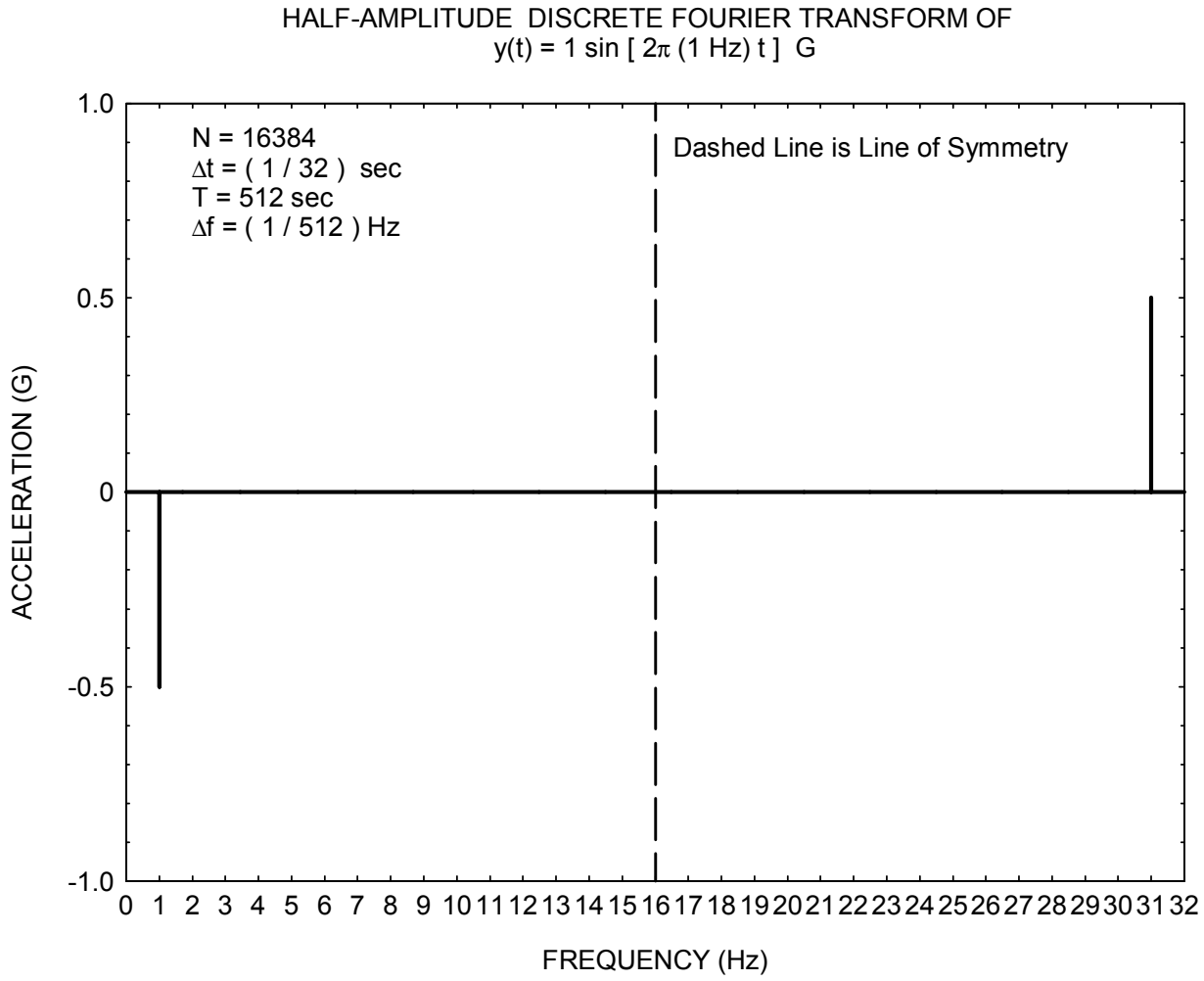

Figure 1-5. Fourier Transform of a Sine Wave

Note that the sine wave has a frequency of 1 Hz. The total number of cycles is 512, with a resulting period of 512 seconds. Again, the Fourier transform of a sine wave is imaginary and antisymmetric. The real component, which is zero, is not plotted.

Spectrum Analyzer Approach

Spectrum analyzer devices typically represent the Fourier transform in terms of magnitude and phase rather than real and imaginary components. Furthermore, spectrum analyzers typically only show one-half the total frequency band due to the symmetry relationship.

The spectrum analyzer amplitude may either represent the *half-amplitude* or the *full-amplitude* of the spectral components. Care must be taken to understand the particular convention of the spectrum analyzer. Note that the half-amplitude convention has been represented in the equations thus far, particularly equations (1-14) and (1-17).

The full-amplitude Fourier transform magnitude G_k would be calculated as

$$G_k = \begin{cases} \text{magnitude}\left\{ \left[\frac{1}{N} \right] \sum_{n=0}^{N-1} \{x_n\} \right\} \quad \text{for } k = 0 \\ 2 \text{ magnitude} \left\{ \left[\frac{2}{N} \right] \sum_{n=0}^{N-1} \left\{ x_n \ \exp\left(- j \frac{2\pi}{N} nk \right) \right\} \right\} \quad \text{for } k = 1, \ ..., \frac{N}{2} - 1 \end{cases}$$

with N as an even integer. (1-20)

Note that k = 0 is a special case. The Fourier transform at this frequency is already at full-amplitude.

For example, a sine wave with amplitude of 1 G and a frequency of 1 Hz would simply have a full-amplitude Fourier magnitude of 1 G at 1 Hz, as shown in Figure 1-6.

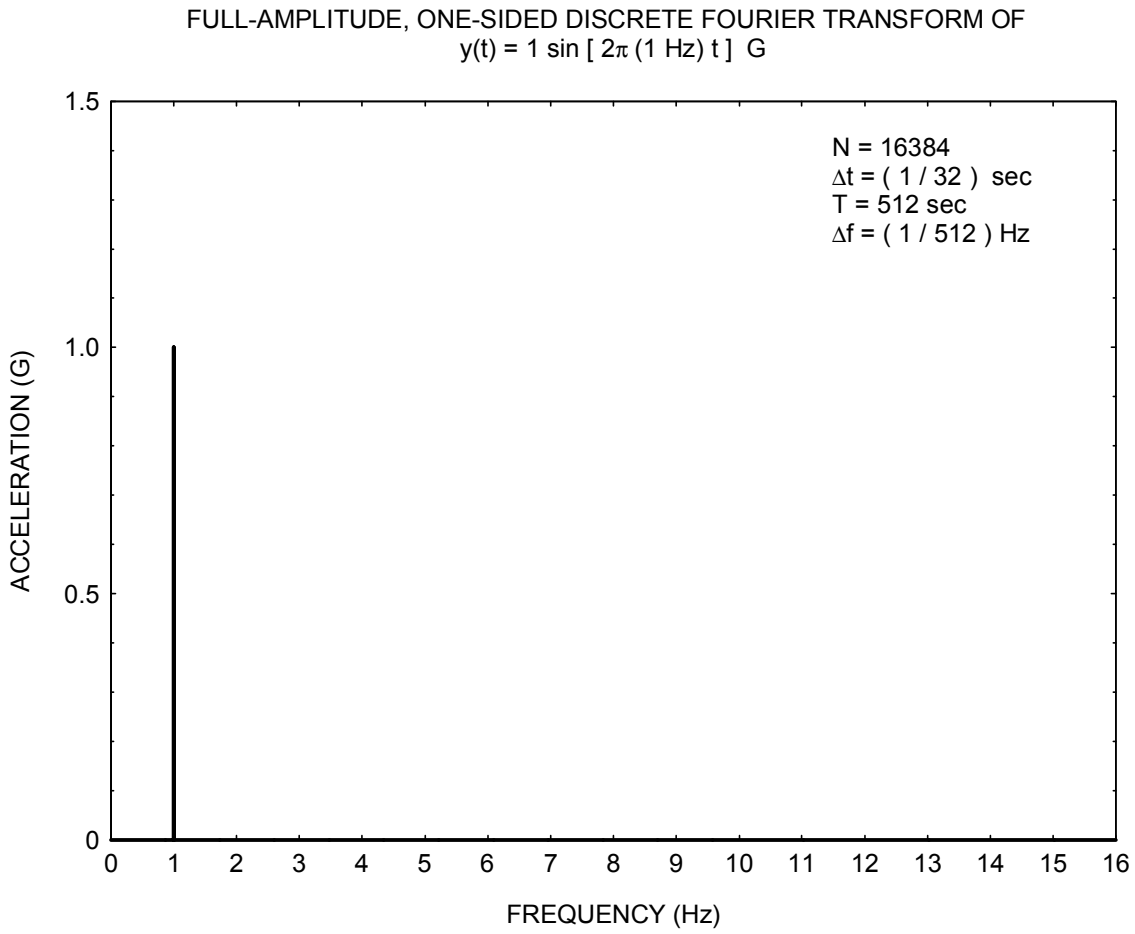

Figure 1-6.

Goal

The sine function considered in Figures 1-5 and 1-6 had a long duration of 512 seconds. The time history in Figure 1-1 has a duration of only 2 seconds, however. Note that the Fourier transform frequency resolution is the inverse of the duration, as given in equation (1-15). The frequency resolution is thus 0.5 Hz for a duration of 2 seconds.

The full-amplitude Fourier transform of the time history in Figure 1-1 is given in Figure 1-7. The "spectral function" goal is thus reasonably met, at least for this example. The course frequency resolution, however, gives the spectral lines a triangular shape.

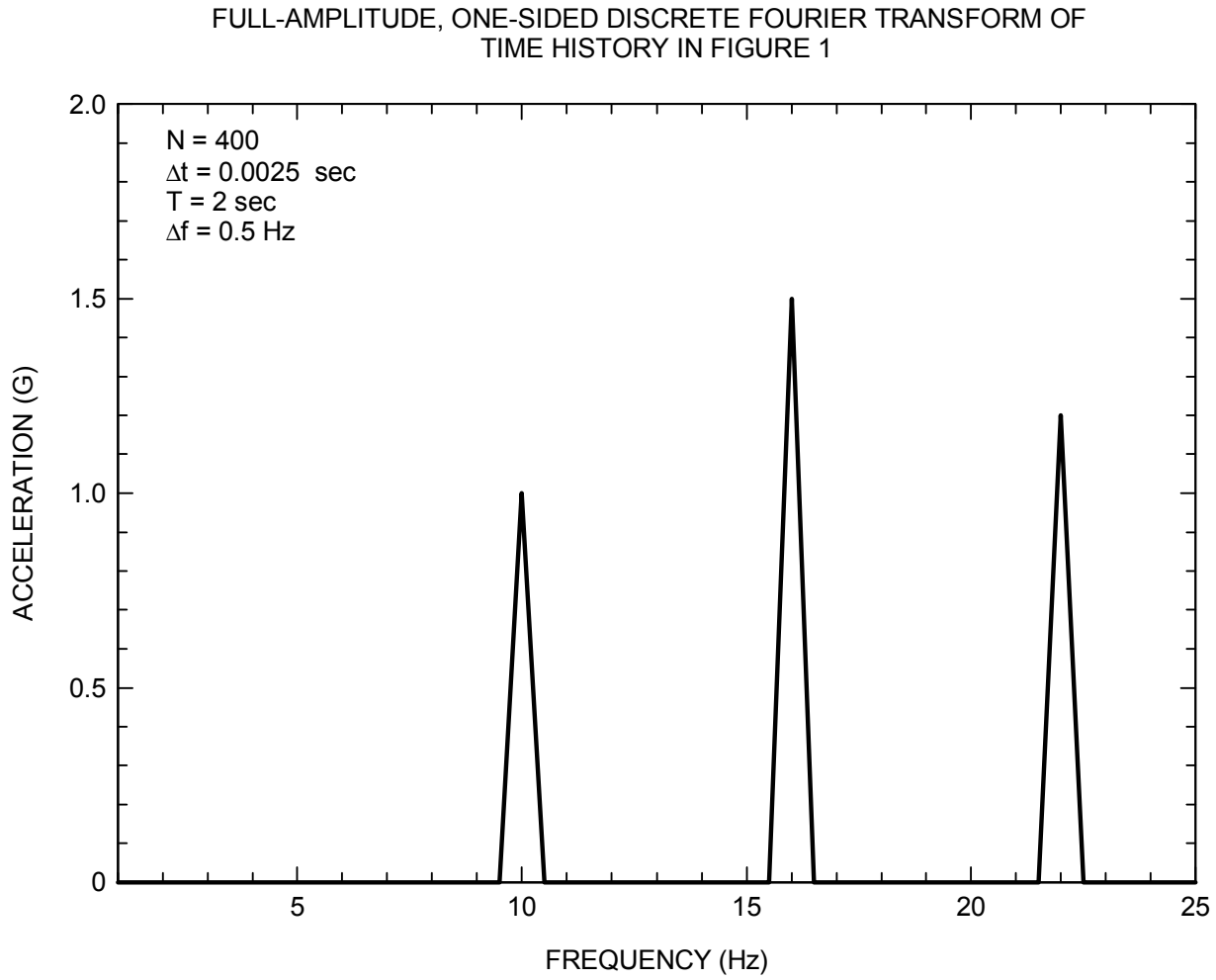

Figure 1-7.

The 10, 16, and 22 Hz sinusoidal frequencies are thus clearly apparent in Figure 1-7. The corresponding amplitudes are also correct per equation (1-1).

Note that this example is somewhat idealistic. The Fourier transform data in Figure 1-7 is defined at each 0.5 Hz frequency increment, beginning at 0. Thus, three of the spectral lines occur exactly at 10, 16, and 22 Hz.

What if the 10 Hz component in equation (1-1) were shifted to 9.75 Hz? The answer is that some of the energy would be shifted to 9.5 Hz and some to 10.0 Hz in the Fourier transform. This effect is one of several error sources in the Fourier transform. This error can be avoided by taking a longer duration.

Magnetostriction Example

Figure 1-8.

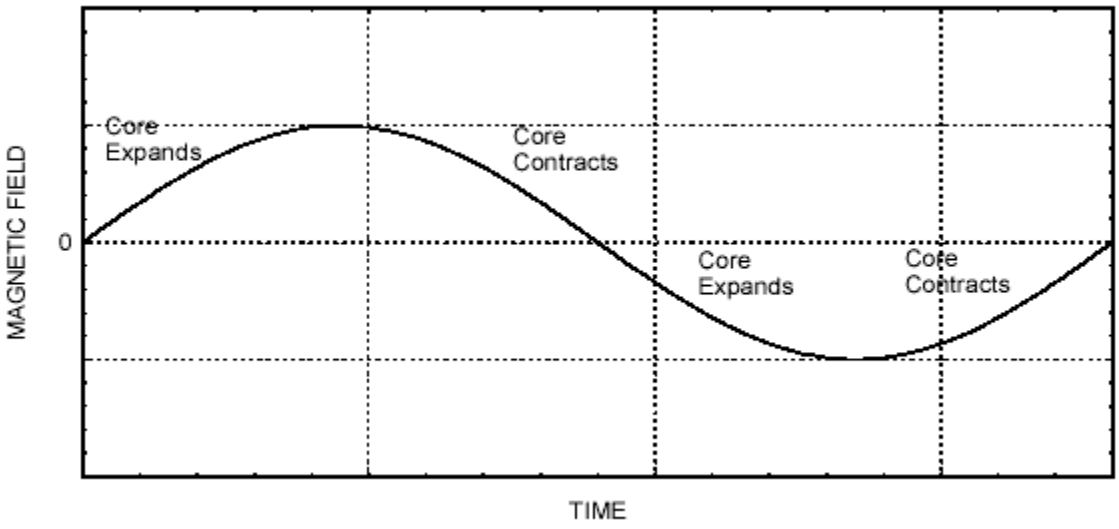

Figure 1-9.

The residential transformer in Figure 1-8 supplies 60 Hz electrical power to several homes. The transformer core experiences two mechanical vibration cycles per each electromagnetic cycle, as shown in Figure 1-9.

The resulting acoustic noise measured via a microphone is shown in Figure 1-10. The amplitude scale is uncalibrated. The time history appears to be somewhat periodic. The Fourier transform magnitude in Figure 1-11 reveals spectral peaks at 120, 360 and 480 Hz.

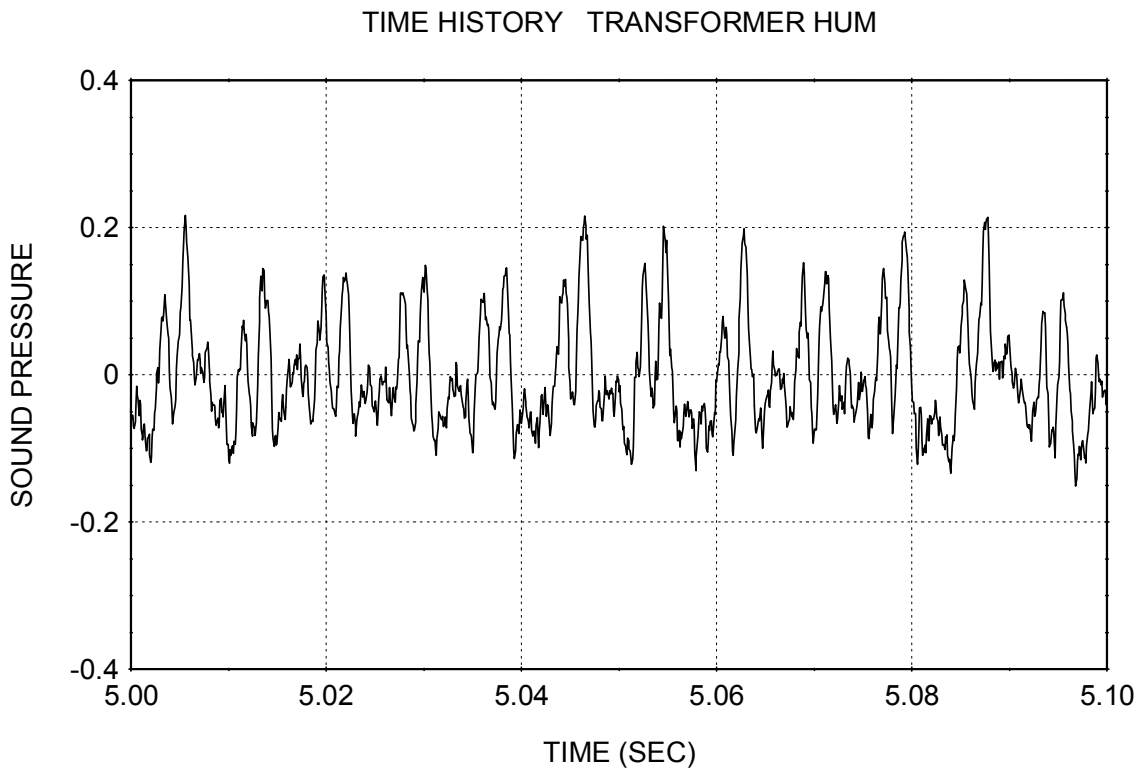

Figure 1-10.

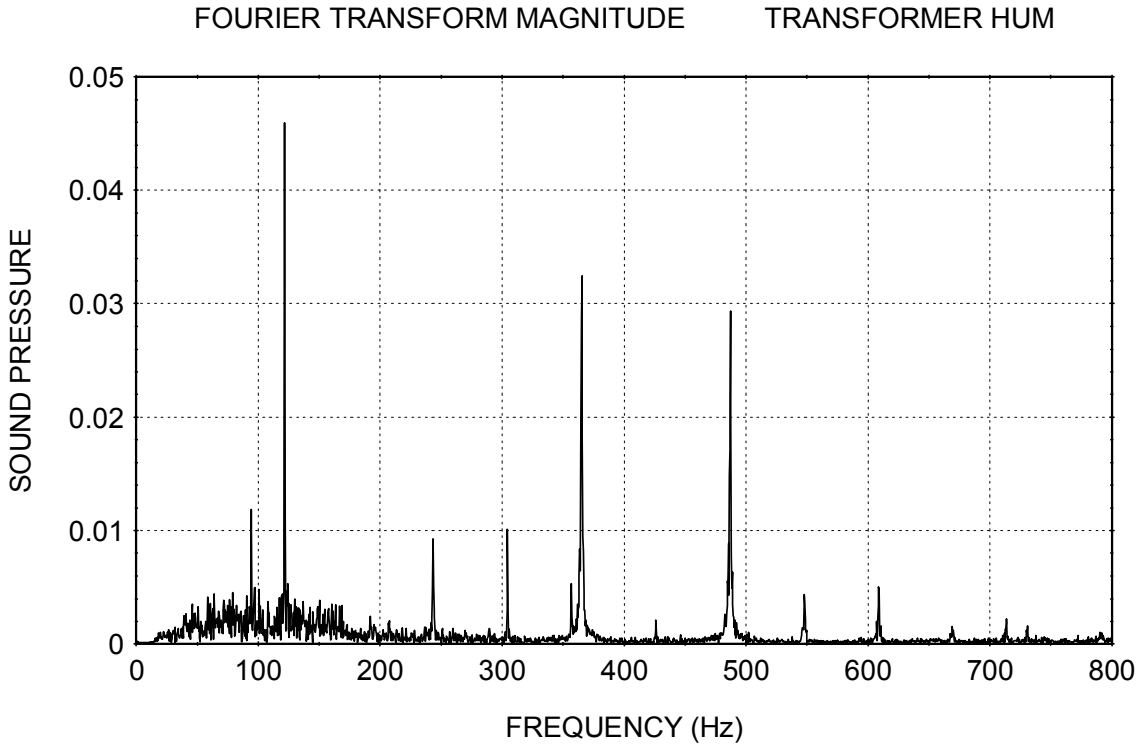

Figure 1-11.

References

1-1. W. Thomson, Theory of Vibration with Applications, 2nd Ed, Prentice-Hall, 1981.

1-2. GenRad TSL25 Time Series Language for 2500-Series Systems, Santa Clara, California, 1981.

1-3. R. Randall, Frequency Analysis 3rd edition, Bruel & Kjaer, 1987.

1-4. F. Harris, Trigonometric Transforms, Scientific-Atlanta, Technical Publication DSP-005, San Diego, CA.

1-5. T. Irvine, Statistical Degrees of Freedom, Vibrationdata Publications, 1998.

CHAPTER 2

NOTES ON THE FOURIER TRANSFORM MAGNITUDE

Introduction

Fourier transforms, which were introduced in Chapter 1, have a number of potential error sources and other peculiar characteristics. The purpose of this chapter is to discuss the Fourier transform magnitude, which must be interpreted with great care.

Sine Example

Consider a sine function with a 1 Hz frequency and 1 G amplitude. Let the period be 20 seconds, which is equivalent to 20 cycles. Thus, $\Delta f = 0.05$ Hz. The corresponding Fourier transform magnitude is shown in Figure 2-1.

Now define the same sine function over a period of 40 seconds. Thus, $\Delta f = 0.025$ Hz. The Fourier transform magnitude is shown in Figure 2-2.

The Fourier transform magnitude at 1 Hz is 1 G in each case, independent of the duration difference. Thus, the Fourier transform magnitude is shown to be a good tool for resolving sinusoidal amplitudes.

In each Fourier transform, there is a spectral line exactly at a frequency of 1 Hz. Otherwise, the acceleration amplitude would be smeared between frequencies adjacent to 1 Hz. This smearing effect is not a concern if the duration is sufficiently long and hence the frequency resolution is sufficiently narrow.

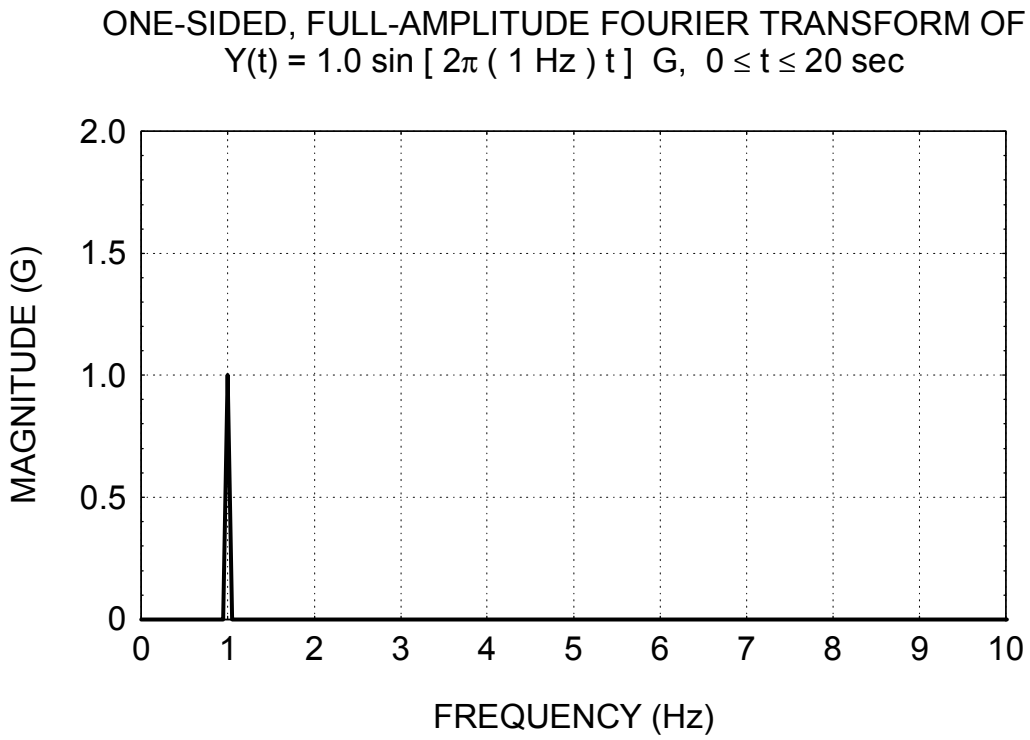

Figure 2-1.

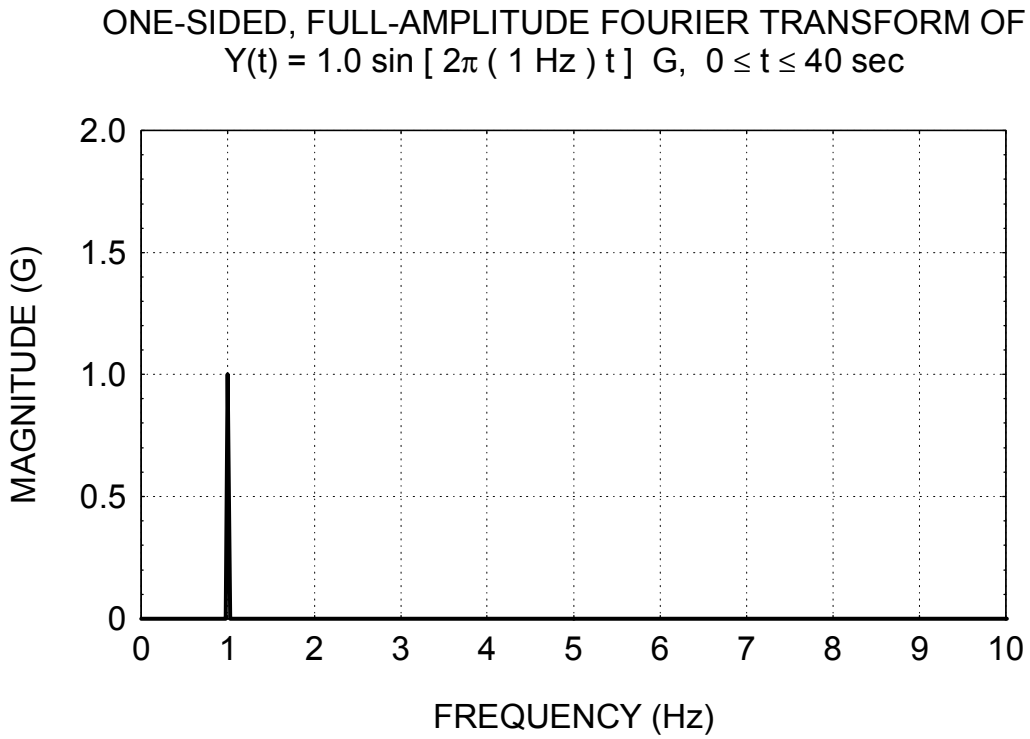

Figure 2-2.

White Noise Example

Consider the two white noise time histories in Figures 2-3 and 2-4. Each has a sample rate of 200 samples per second. Each has a standard deviation of 1 G. The overall level is 1 GRMS since the mean is zero, in each case.

The parameters for the Fourier transform calculation are given in Table 2-1.

Table 2-1. White Noise Parameters for Fourier Transform

Parameter	Figure 2-3	Figure 2-4
Overall Level	1 GRMS	1 GRMS
Duration	5 sec	10 sec
Δf	0.2 Hz	0.1 Hz
Sample Rate	200 sps	200 sps
Frequency Domain (Hz)	0 to 100 Hz	0 to 100 Hz
Number of Spectral Lines	500	1000

sps = samples per second.

Recall that the frequency resolution Δf is the inverse of the duration T.

$$\Delta f = 1/T \tag{2-1}$$

The frequency domain is taken from zero to one-half the sample rate.

The number of spectral lines N is equal to the maximum frequency divided by the frequency resolution.

$$N = \frac{F\,max}{\Delta f} \tag{2-2}$$

The Fourier transforms of the respective white noise time histories are shown in Figures 2-5 and 2-6.

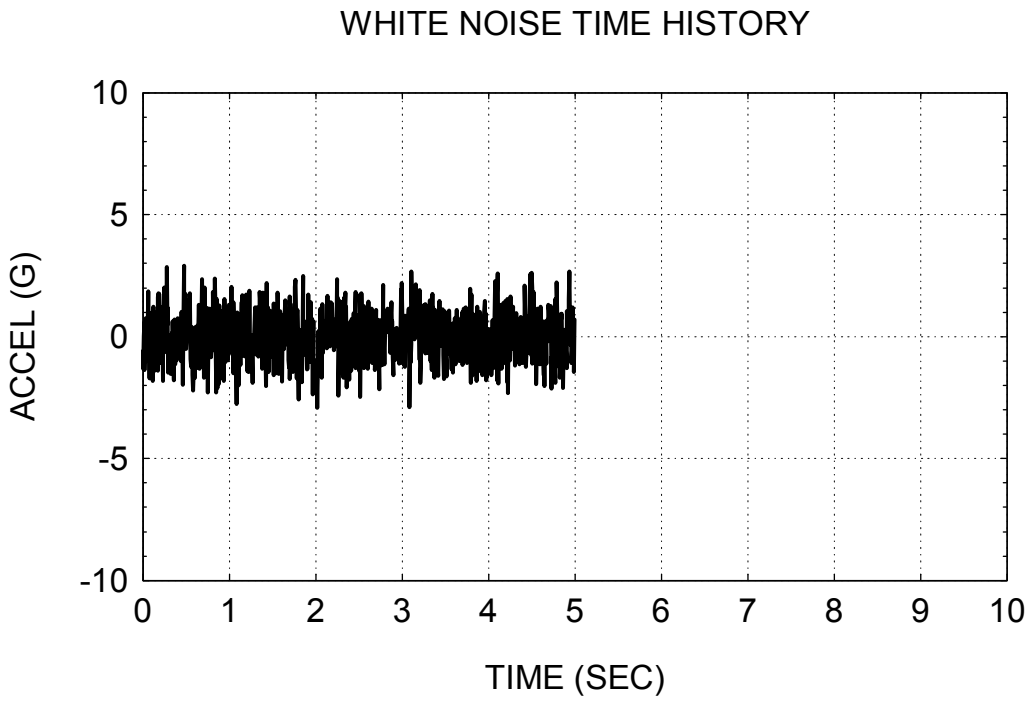

Figure 2-3.

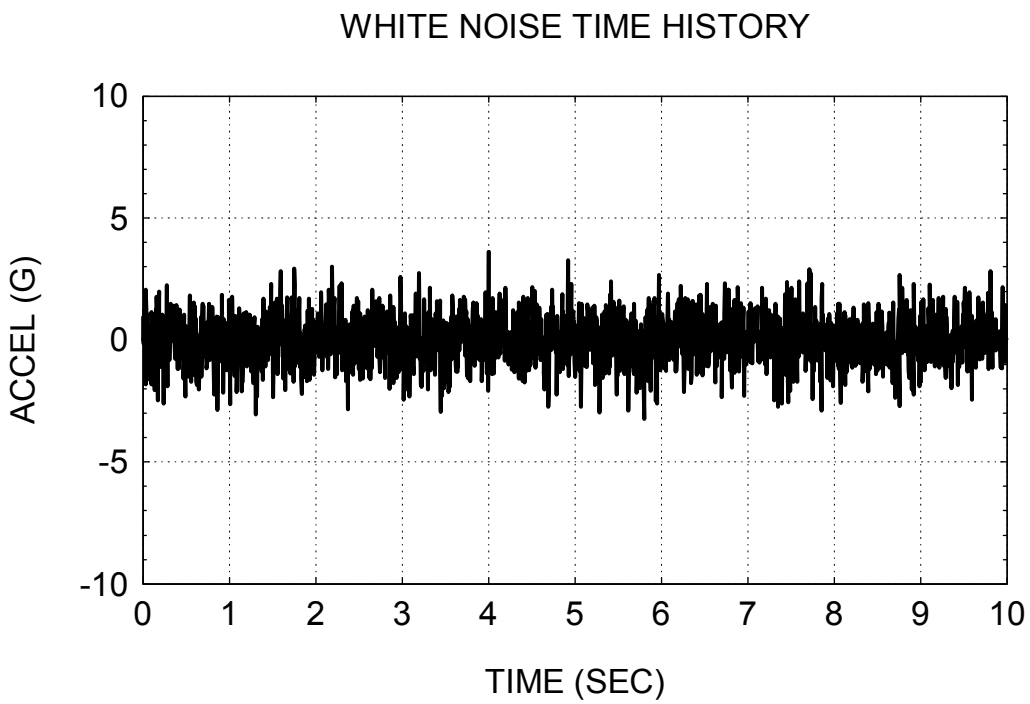

Figure 2-4.

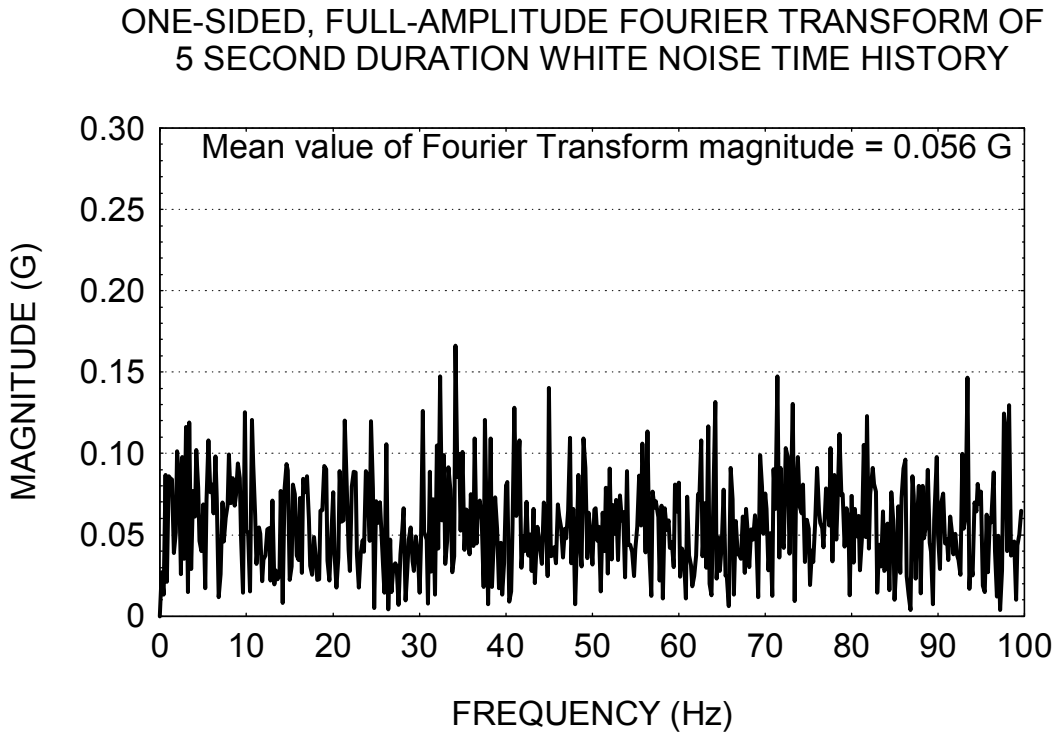

Figure 2-5.

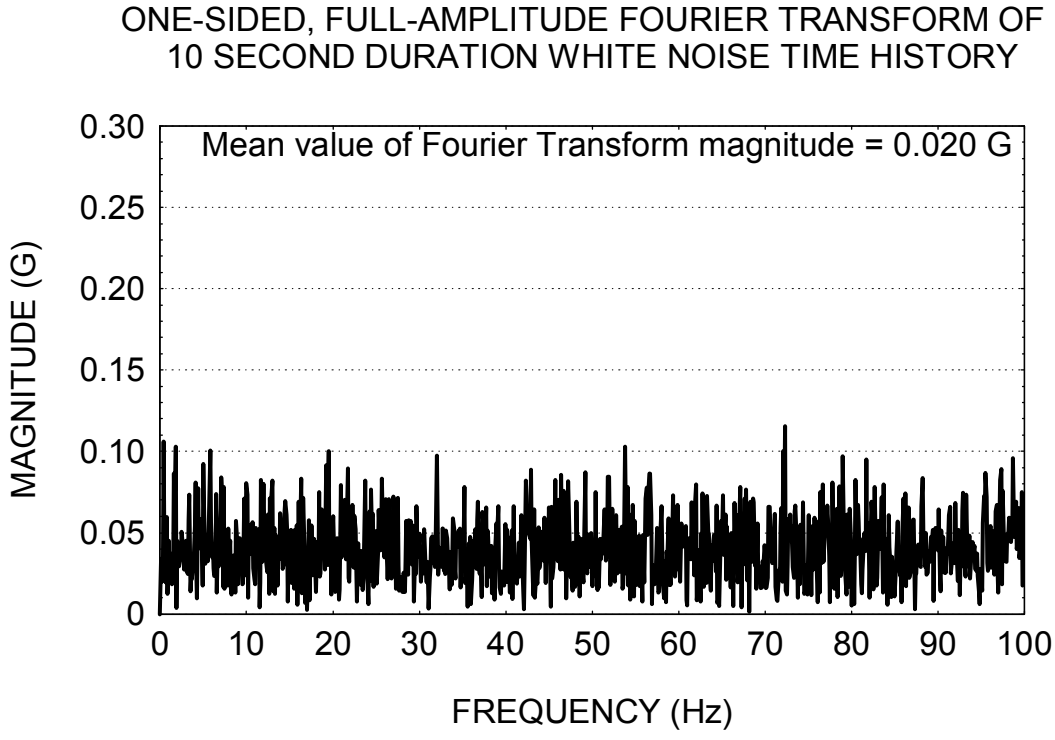

Figure 2-6.

Ideally, the "white noise" would have a constant Fourier transform magnitude with respect to frequency. The fact that there is some variation within Figures 2-5 and within Figure 2-6 is unimportant for this example. The pertinent point is that the mean magnitude decreases by about one-half, comparing the transform in Figure 2-6 to the transform in Figure 2-5.

The reason for the decrease is that the transform in Figure 2-6 has 1000 spectral lines compared to the 500 spectral lines in the Figure 2-5 transform. Thus, the "energy" is divided into a greater number of spectral lines in the Figure 2-6 transform.

Each transform, however, yields the same overall value of 1 GRMS. This is found as follows:

1. Divide each spectral magnitude by $\sqrt{2}$ to convert from peak to RMS.
2. Square each spectral RMS value to convert to mean square.
3. Sum the mean square values.
4. Take the square root of the sum.

For a random signal, the Fourier transform magnitude depends on the number of spectral lines. This drawback is overcome by the power spectral density function, discussed in Chapter 8.

CHAPTER 3

LEAKAGE ERROR IN FOURIER TRANSFORMS

Introduction

Several error sources are associated with the Fourier transform. One error source is called "leakage."

Leakage is a smearing of energy throughout the frequency domain. Leakage results when both of the following conditions are present:

1. The signal is taken over a finite duration.
2. The signal is "non-periodic" in the time record.

Both these conditions are usually present in engineering data. Thus, leakage usually occurs.

For example, leakage occurs if a Fourier transform is calculated for a non-integral number of sine function cycles.

Sine Function Example 1

Consider that a data acquisition system is used to monitor a continuous sine function. The sine function has amplitude of 1 G and a frequency of 1 Hz, as shown in Figure 3-1. The sample rate is 32 samples per second.

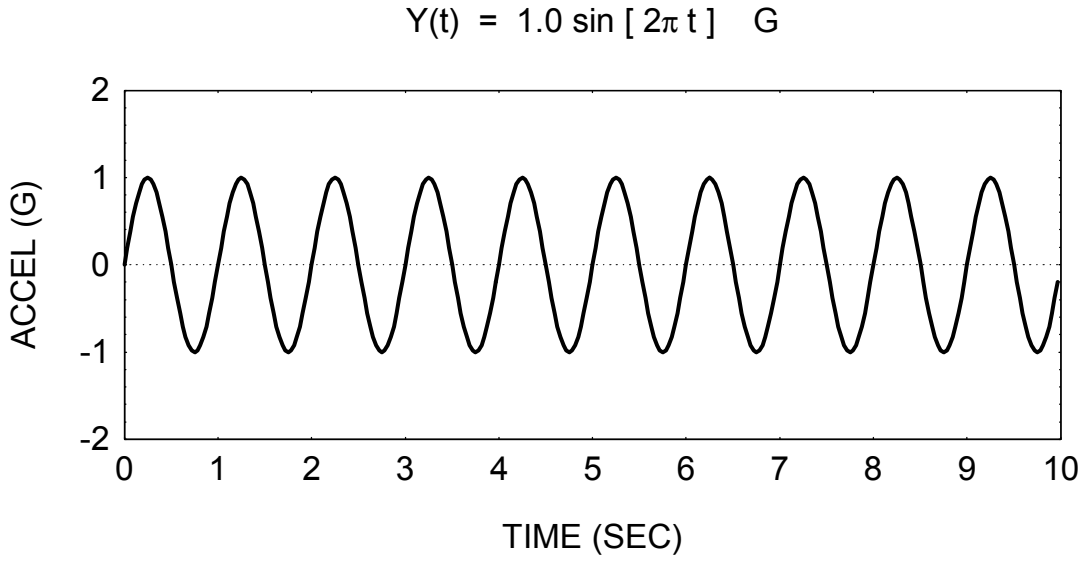

Figure 3-1.

Now consider that the data acquisition system measures three cycles as shown in Figure 3-2. Note that the time history amplitude is zero at the start and end of the record.

In essence, the Fourier transform will correctly assume that the original signal is a series of three-cycle segments as shown in the time history in Figure 3-3.

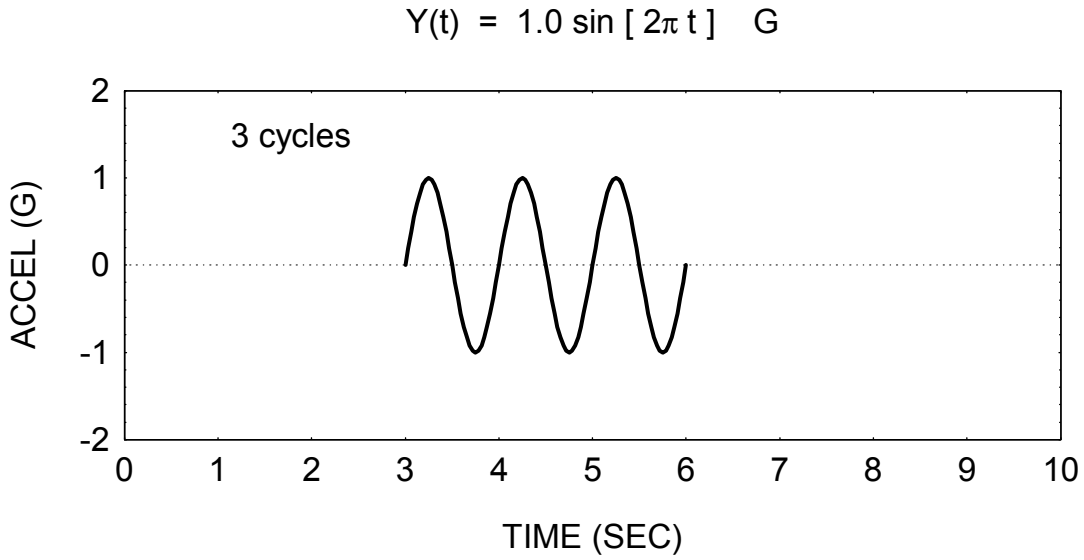

Figure 3-2.

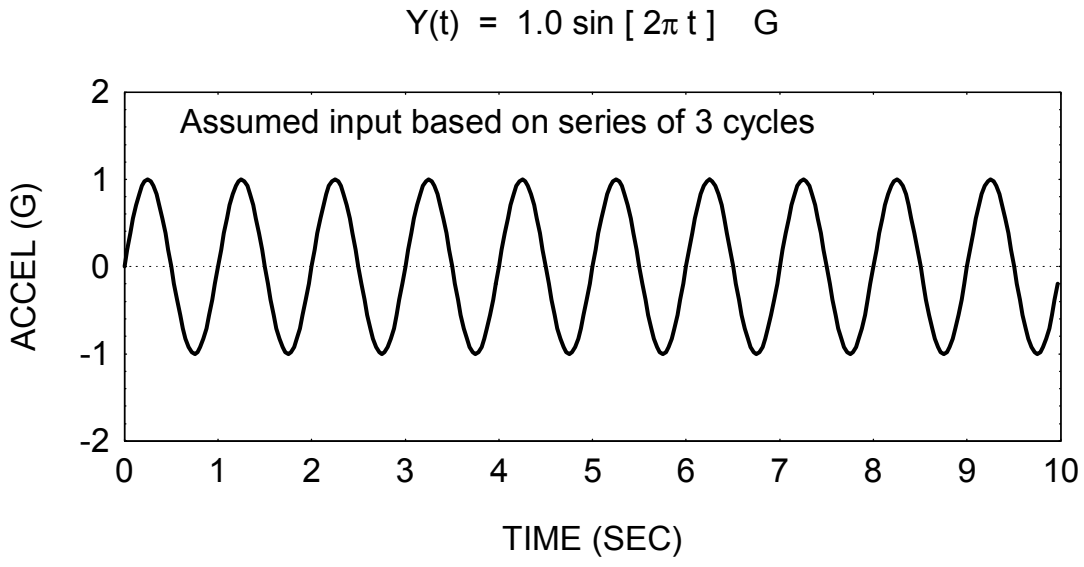

Figure 3-3.

The three-cycle sine function in Figure 3-2 is converted to a Fourier transform in Figure 3-4. As expected, a spectral line of 1 G appears at 1 Hz. Note that $\Delta f = 0.333$ Hz.

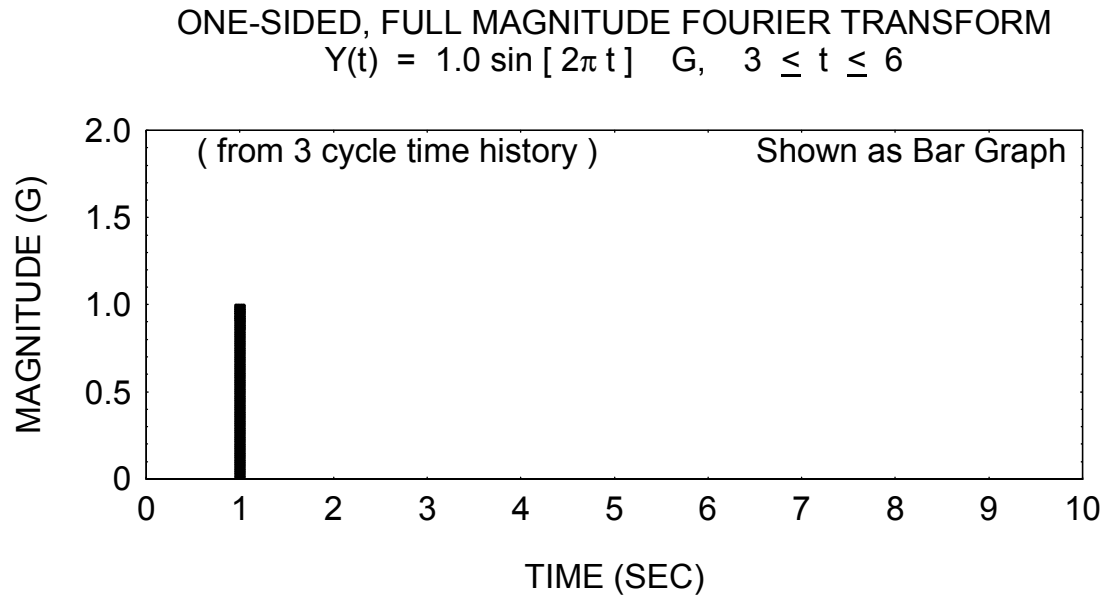

Figure 3-4.

Sine Function Example 2

Now assume that the data acquisition system has a limited memory buffer and is only able to capture 2.5 cycles of the sine function, as shown in Figure 3-5.

In essence, the Fourier transform will assume that the original signal is a series of 2.5 cycle segments as shown in Figure 3-6. Distortion is clearly visible in the time history in Figure 3-6. Specifically, the input signal is not periodic in the time record.

The 2.5 cycle sine function in Figure 3-5 is converted to a Fourier transform in Figure 3-7. Note that leakage occurs as shown by the smearing of energy across the frequency band.

A related problem is that $\Delta f = 0.4$ Hz. Thus, there are spectral lines at the following frequencies in Hz: 0, 0.4, 0.8, 1.2, …. There is no spectral line at 1 Hz, however, which is the frequency of the sine function.

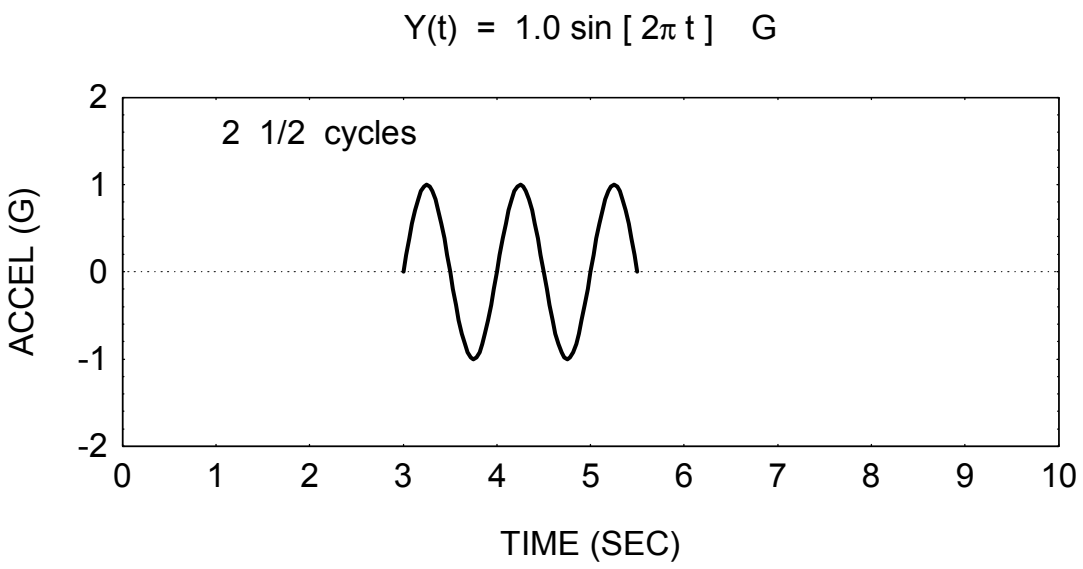

Figure 3-5.

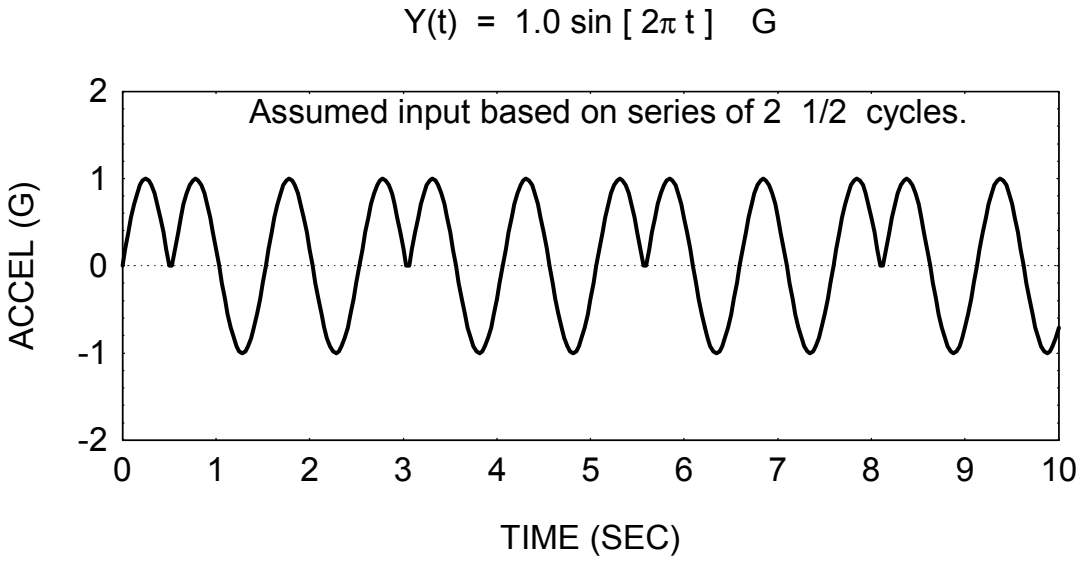

Figure 3-6.

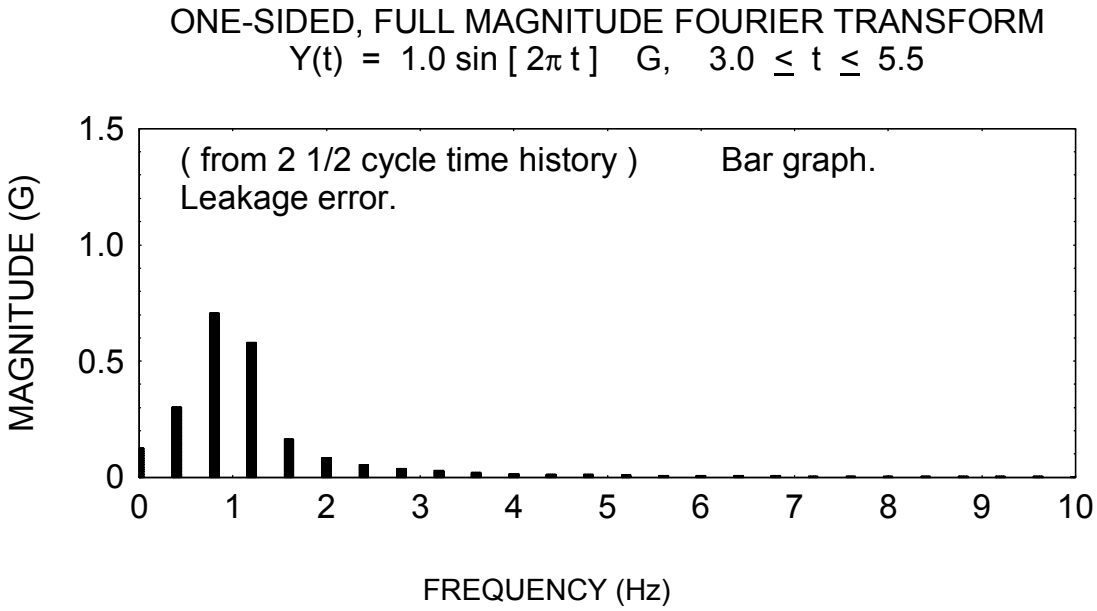
ONE-SIDED, FULL MAGNITUDE FOURIER TRANSFORM
Y(t) = 1.0 sin [2π t] G, 3.0 ≤ t ≤ 5.5
(from 2 1/2 cycle time history)
Bar graph.
Leakage error.
MAGNITUDE (G)
1.5
1.0
0.5
0
0 1 2 3 4 5 6 7 8 9 10
FREQUENCY (Hz)

Figure 3-7.

CHAPTER 4

HANNING WINDOW

Introduction

A Fourier transform may have a leakage error, as discussed in Chapter 3. The leakage error can be reduced by subjecting the time history to a window, as discussed in References 4-1 through 4-6.

Two common types of windows are the rectangular window and the Hanning window.

Rectangular Window

The rectangular, or flat, window leaves the time history data unmodified. Thus, a rectangular window is equivalent to no window at all. A rectangular window is appropriate for transient data or nonstationary data. Ideally, the time history includes some data during the "quiet" periods both before and after the event. An example of a transient event is shown in Figure 4-1.

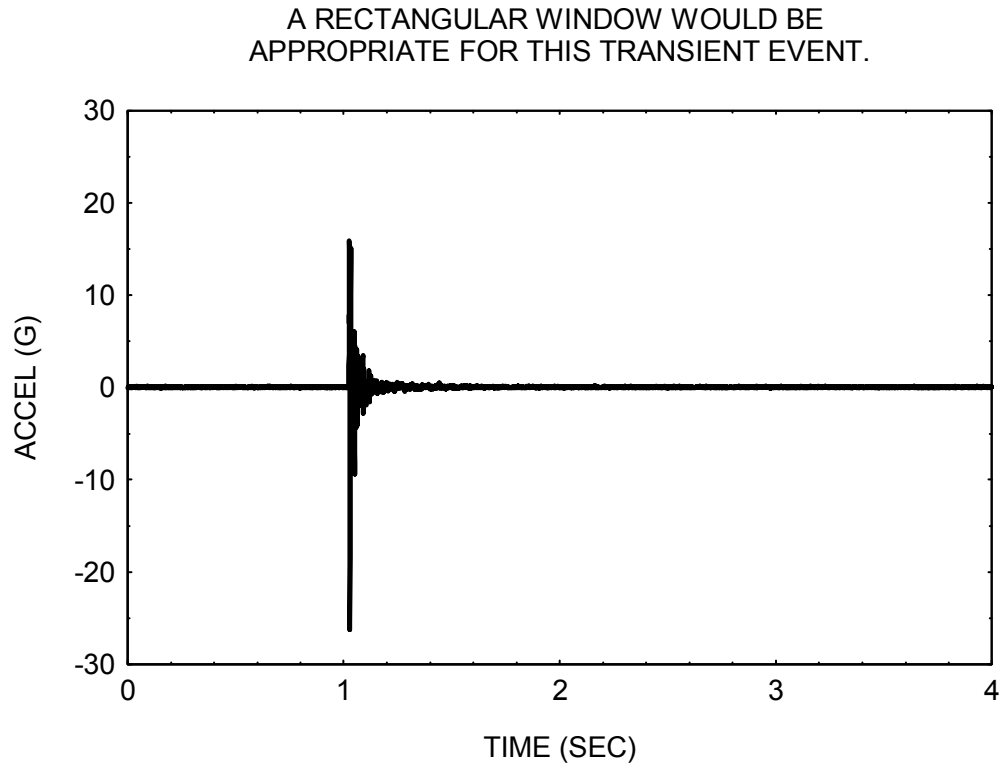

Figure 4-1.

Hanning Window

One of the most common windows is the Hanning window, or the cosine squared window. It is appropriate for stationary vibration.

This window tapers the time history data so that the amplitude envelope decreases to zero at both the beginning and end of the time segment. The Hanning window w(t) can be defined as

$$w(t) = \begin{cases} 1 - \cos^2\left[\pi \dfrac{t}{T}\right], & 0 \le t \le T \\ \\ 0, \quad \text{elsewhere} \end{cases} \tag{4-1}$$

Equation (4-1) is plotted in Figure 4-2.

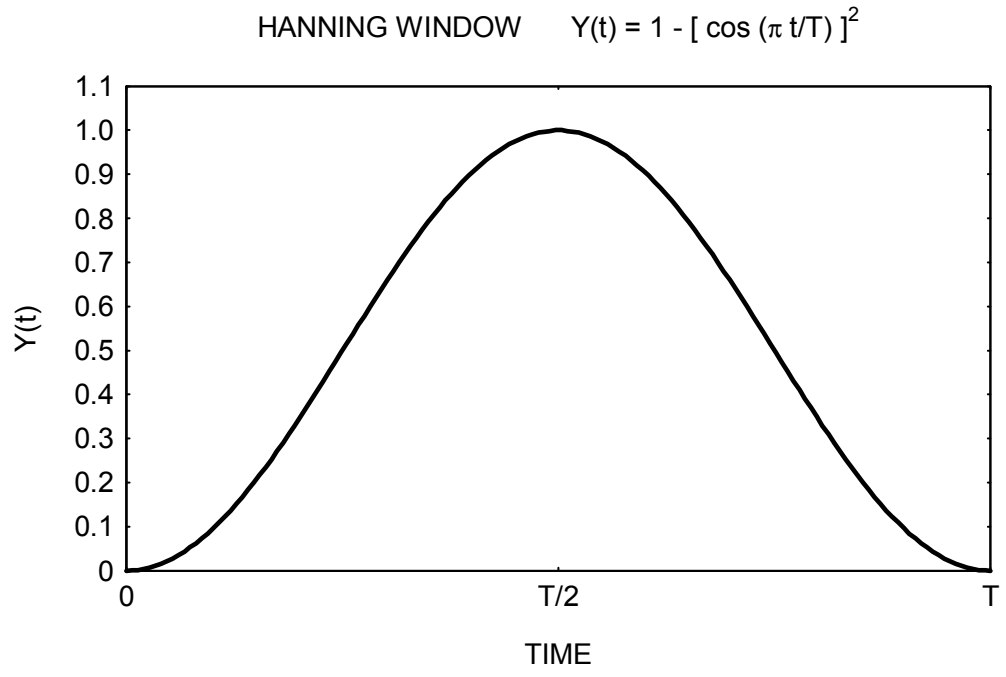

Figure 4-2.

Furthermore, a normalization factor of $\sqrt{8/3}$ may be applied to the Hanned data to compensate for the lost energy, from Reference 4-6.

Example

A 1 Hz sine function is shown in Figure 4-3. The same function is shown after a normalized Hanning window is applied in Figure 4-4.

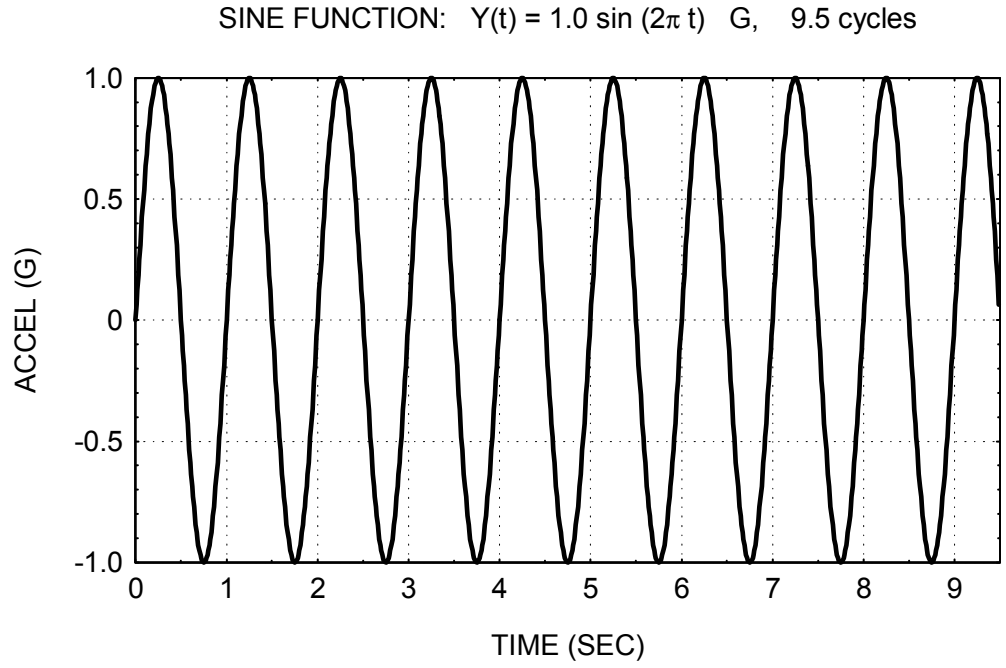

Figure 4-3.

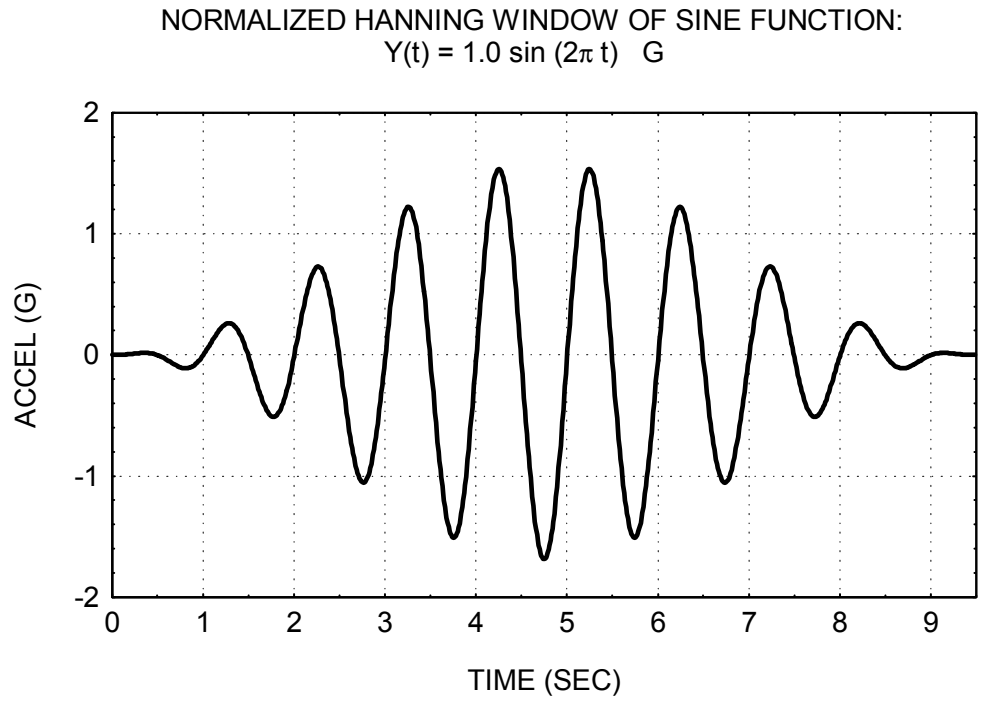

Figure 4-4.

The Fourier transforms of two time histories are shown together in Figure 4-5.

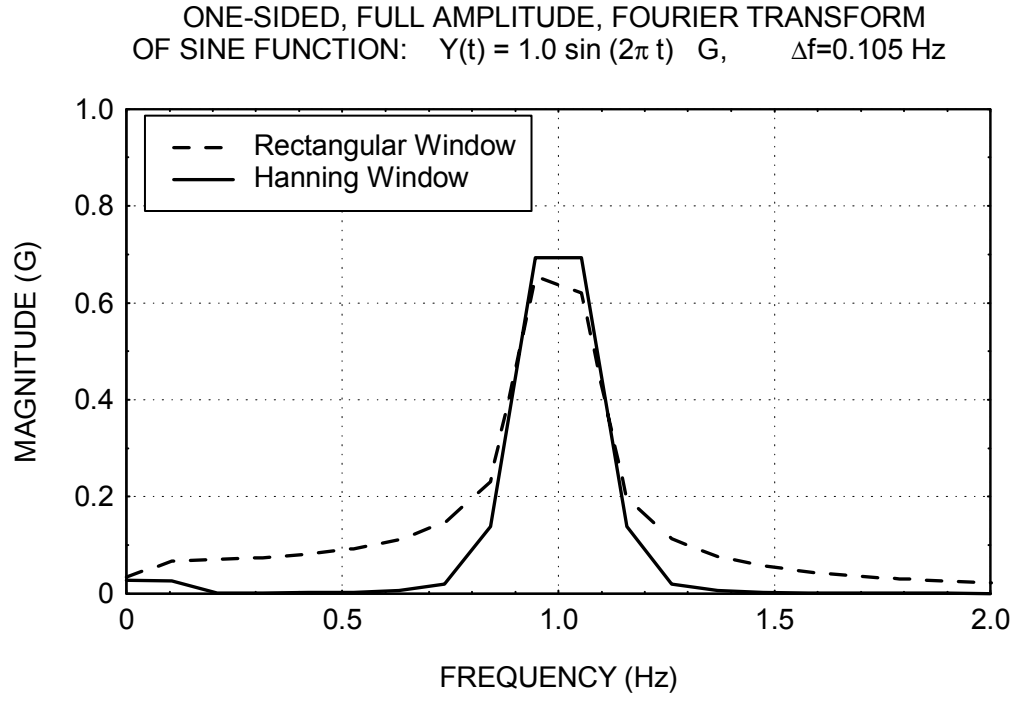

Figure 4-5.

Ideally, the Fourier transform would have a single, discrete line at 1 Hz with amplitude of 1 G.

Both the rectangular and Hanning Fourier transforms have some leakage error, however. The rectangular window produces more leakage error than the Hanning window. Thus, the Hanning window is recommended for stationary data.

References

4-1. C. Harris, editor; Shock and Vibration Handbook, 3rd edition; R. Randall, "Chapter 13 Vibration Measurement Equipment and Signal Analyzers," McGraw-Hill, New York, 1988.

4-2. MAC/RAN Applications Manual Revision 2, University Software Systems, Los Angeles, CA, 1991.

4-3. Vibration Testing, Introduction to Vibration Testing, Section 9 (I), Scientific-Atlanta, Spectral Dynamics Division, San Diego, CA, Rev 5/72.

4-4. R. Randall, Frequency Analysis, Bruel & Kjaer, Denmark, 1987.

4-5. TSL25, Time Series Language for 2500-Series Systems, GenRad, Santa Clara, CA, 1981.

4-6. F. Harris, Trigonometric Transforms, Scientific-Atlanta, Spectral Dynamics Division, Technical Publication DSP-005 (8-81), San Diego, CA.

CHAPTER 5

FAST FOURIER TRANSFORM (FFT)

Introduction

The discrete Fourier transform requires a tremendous amount of calculations. A time history with M coordinates would require M^2 complex multiplication steps.

The discrete Fourier transform can be carried out by a Fast Fourier transform method, however. The method is based on a time series with a number of points equal to 2^N, where N is an integer.

The FFT requires $M \log_2 M$ complex multiplication steps, where $M = 2^N$.

The details of the FFT algorithm are given in Reference 5-1.

Example

Now consider a time history with 1,000,000 points. A regular Fourier transform would require 10^{12} complex multiplication steps. On the other hand, an FFT would only require approximately $2(10^7)$ steps. Thus, the FFT achieves the calculation in $1/50{,}000^{th}$ of the time.

Limitation of the FFT

The above example is not quite correct. Again, the FFT is based on a time series with 2^N coordinates. Note that

$$2^{19} = 524{,}288$$

and

$$2^{20} = 1{,}048{,}576$$

Unfortunately, a time history with 1,000,000 points falls between these two cases.

There are two options for dealing with a time history that is not an integer power of 2.

One option is to truncate the time history. This should be acceptable if the data is stationary. In the above example, the time history would thus be truncated to 524,288 points.

The second option is to pad the time history with trailing zeroes to bring its length to an integer power of 2. A problem with this option is that it artificially reduces the amplitude of the Fourier transform spectral lines.

Reference

5-1. T. Irvine, The Fast Fourier Transform (FFT), Vibrationdata Publications, 1998.

CHAPTER 6

INVERSE FOURIER TRANSFORM

Introduction

Recall that the Fourier transform F_k for a discrete time series x_n can be expressed as

$$F_k = \frac{1}{N}\sum_{n=0}^{N-1}\left\{x_n \exp\left(-j\frac{2\pi}{N}nk\right)\right\}, \text{ for } k = 0, 1, ..., N-1 \tag{6-1}$$

The corresponding inverse transform is

$$x_n = \sum_{k=0}^{N-1}\left\{F_k \exp\left(+j\frac{2\pi}{N}nk\right)\right\}, \text{ for } n = 0, 1, ..., N-1 \tag{6-2}$$

Note that F_k has dimensions of [amplitude].

Points

Here are some important points about the Fourier transform and its inverse:

1. The Fourier transform converts a time history to the frequency domain. The inverse Fourier transform converts the frequency domain function back to a time history.

2. In some cases, an intermediate calculation may be performed on the Fourier transform prior to taking its inverse. This calculation might involve a transfer function.

3. The Fourier transform and its inverse must be a matched pair. This is an absolute requirement since there are many different types of Fourier transforms.

4. The main difference between the two transforms is the polarity of the argument in the exponential function. In addition, the Fourier transform has a scale factor of 1/N.

5. A measured time history consists only of real amplitude. The Fourier transform converts this to a complex function. The inverse Fourier transform converts this complex function to a complex time history, but the resulting imaginary component is zero.

6. An exception to point 5 could occur if some intermediate calculation were performed prior to taking the inverse Fourier transform.

7. Theoretically, the input time history could be complex with a non-zero imaginary component. For practical purposes, this never occurs.

8. A Hanning window may be applied in the Fourier transform, but it is never applied to the inverse calculation.

9. An inverse Fourier transform can be performed as an "inverse Fast Fourier transform" if the number of points is an integer power of 2.

CHAPTER 7

WATERFALL FFT EXAMPLES

Figure 7-1. Minuteman II ICBM at March AFB Museum, California

M57A1 Motor

The M57A1 motor is a solid-fuel motor originally developed as the third stage for the Minuteman II missile program. The Minuteman II is designated as LGM-30F Mk II. The M57A1 motor has since been used on a variety of suborbital vehicles, such as target vehicles.

This motor has a distinct sinusoidal pressure oscillation which forms in its cavity. The oscillation frequency sweeps downward from 530 Hz to 450 Hz over a 16-second duration. A Waterfall FFT plot taken from flight accelerometer data during the M57A1 burn is given in Figures 7-4. The magnitude is the unscaled acceleration.

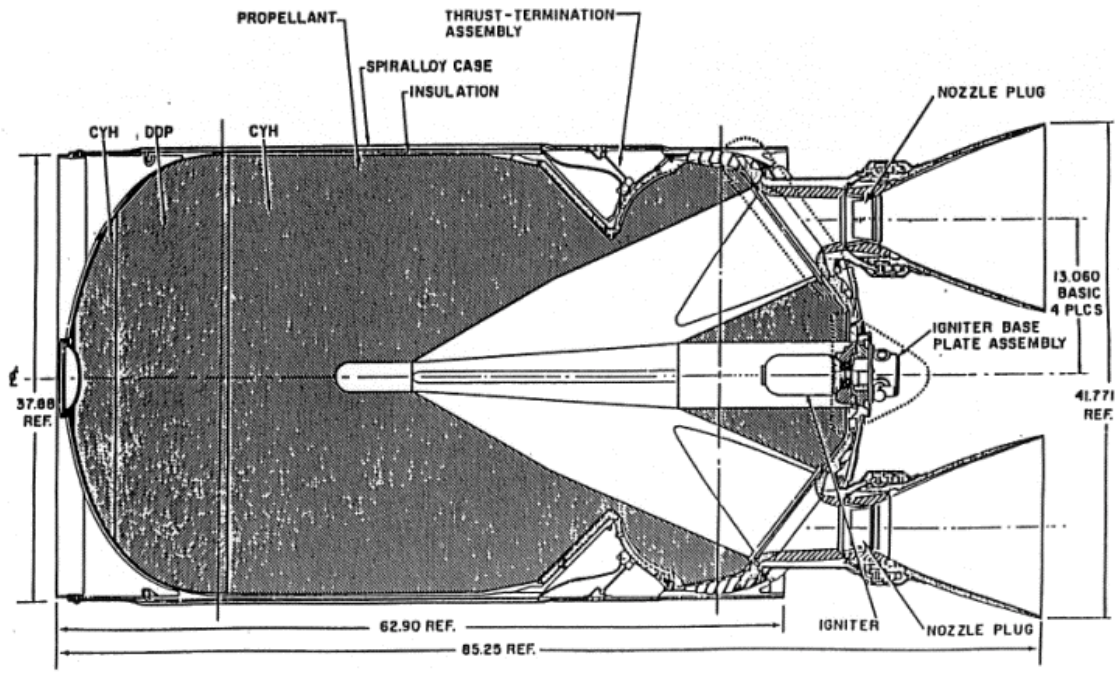
PROPELLANT
THRUST-TERMINATION ASSEMBLY
SPIRALLOY CASE
INSULATION
NOZZLE PLUG
CYH
DDP
CYH
13.060 BASIC 4 PLCS
IGNITER BASE PLATE ASSEMBLY
37.88 REF.
41.771 REF.
62.90 REF.
IGNITER
NOZZLE PLUG
85.25 REF.

Figure 7-2.


H44-2
LOADED
H44-1
ROCKET MOTOR M57-A1
SECTION 44
S/N 0032972
CAUTION
FWD

Figure 7-3.

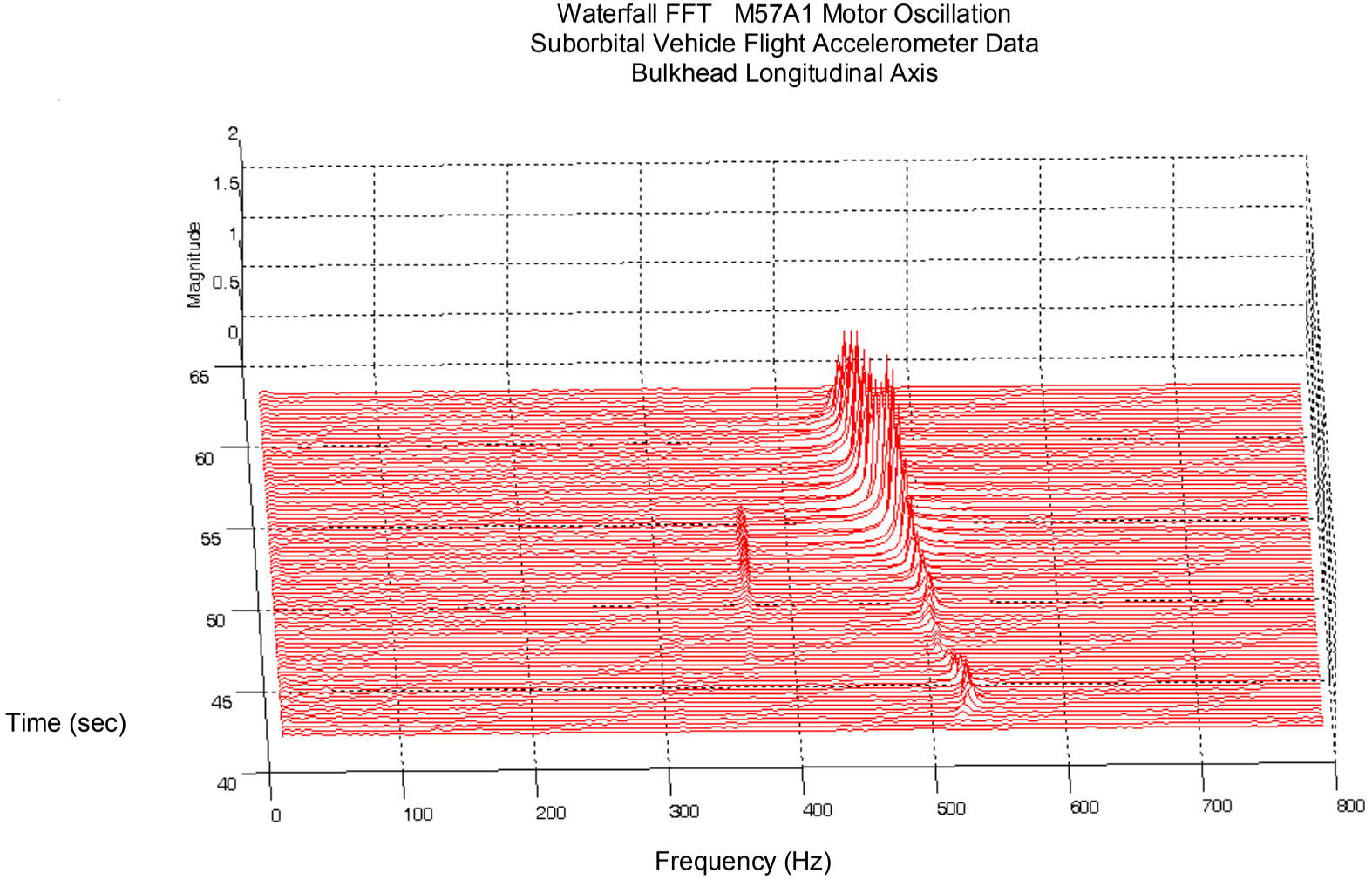
Waterfall FFT M57A1 Motor Oscillation
Suborbital Vehicle Flight Accelerometer Data
Bulkhead Longitudinal Axis
Magnitude
2
1.5
1
0.5
0
Time (sec)
65
60
55
50
45
40
0
100
200
300
400
500
600
700
800
Frequency (Hz)

Figure 7-4.

Figure 7-5.

The SR-19 motor is a solid-fuel motor originally developed as the second stage for the Minuteman II missile program. The SR-19 motor has since been used on a variety of suborbital vehicles, such as target vehicles. The HERA missile in Figure 7-5 had an SR-19 first stage and an M57A1 second stage.

The SR-19 motor has a distinct sinusoidal pressure oscillation which forms in its cavity. The oscillation frequency sweeps downward from 700 Hz to 550 Hz over a 5-second duration, as shown in the Waterfall FFT plot in Figure 7-6. This data is from a static fire test where the motor was mounted to a frame, with the motor horizontal to the ground.

The corresponding GRMS plot is shown in Figure 7-7. The amplitude is high because the accelerometer was mounted to the forward motor dome.

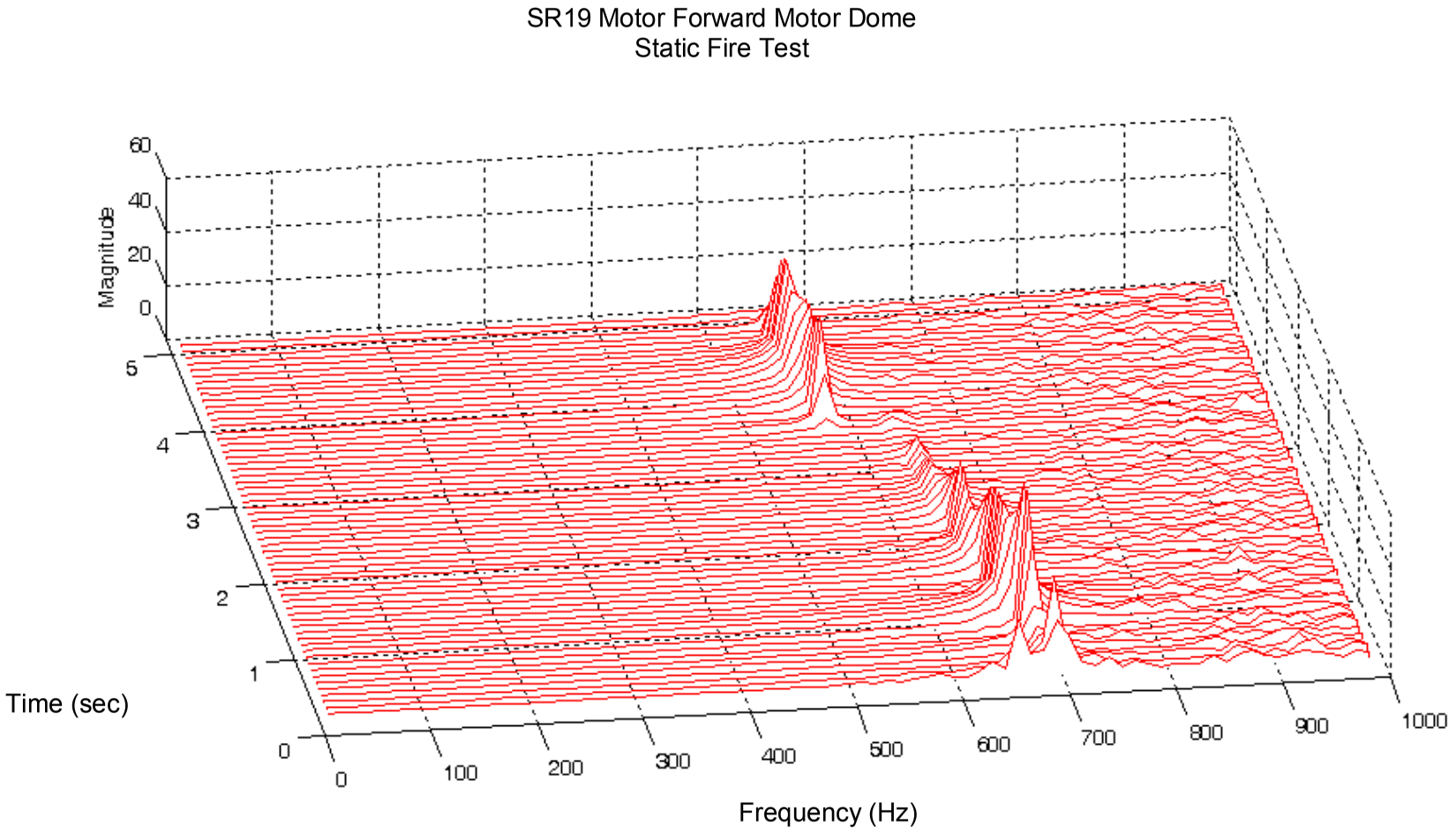
SR19 Motor Forward Motor Dome
Static Fire Test
Magnitude
60
40
20
0
Time (sec)
5
4
3
2
1
0
0
100
200
300
400
500
600
700
800
900
1000
Frequency (Hz)

Figure 7-6.

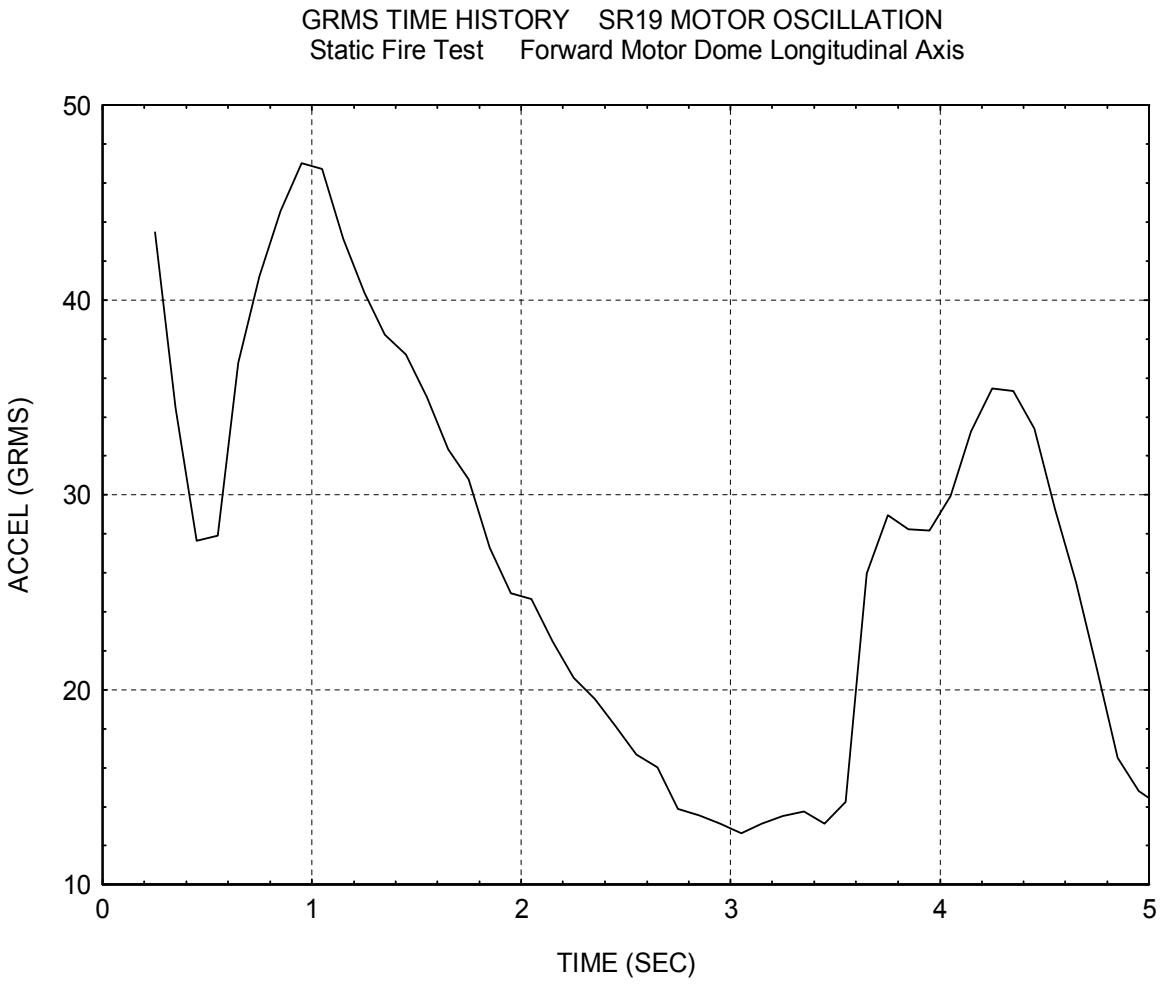
GRMS TIME HISTORY SR19 MOTOR OSCILLATION
Static Fire Test Forward Motor Dome Longitudinal Axis
ACCEL (GRMS)
50
40
30
20
10
0
1
2
3
4
5
TIME (SEC)

Figure 7-7.

CHAPTER 8

POWER SPECTRAL DENSITY FUNCTION

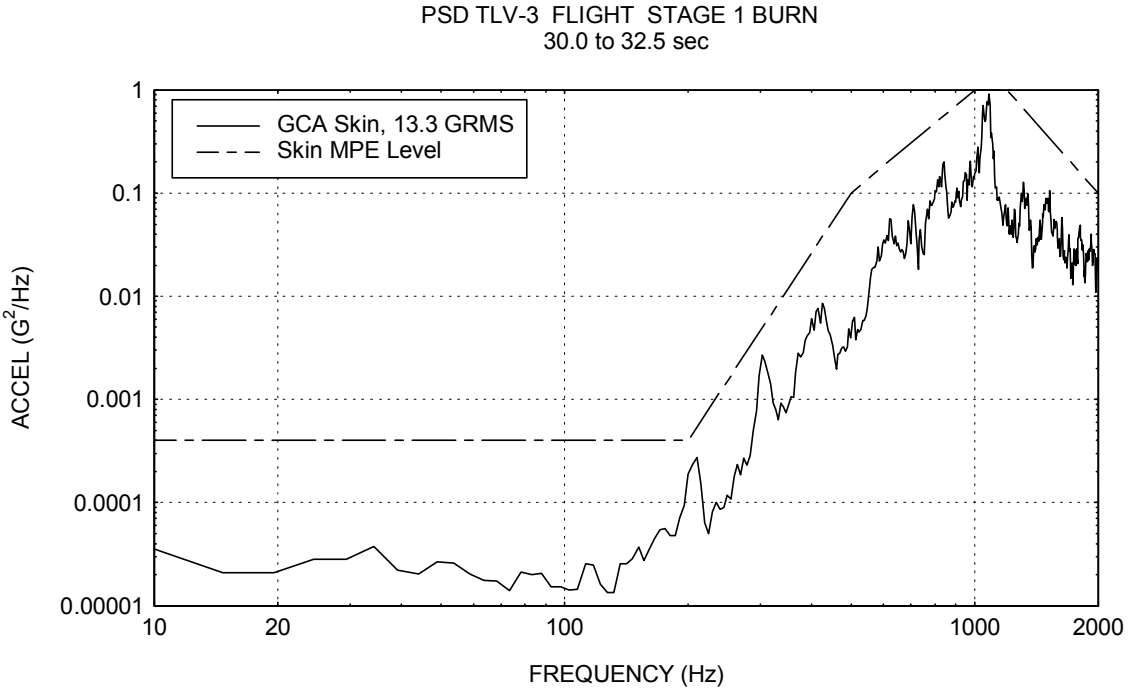

Figure 8-1. Power Spectral Density from a Sample Rocket Vehicle's Flight

The PSD was calculated from flight accelerometer data. The vibration level was driven by aerodynamic buffeting as the vehicle encountered its maximum dynamic pressure condition soon after passing Mach one. The measured overall level is 13.3 GRMS, which is equal to the square root of the area under the PSD curve. The MPE level is the maximum predicted environment.

Introduction

A Fourier transform by itself is a poor format for representing random vibration because the Fourier magnitude depends on the number of spectral lines, as shown in previous chapters.

The power spectral density function, which can be calculated from a Fourier transform, overcomes this limitation. Again, some assembly is required.

Note that the power spectral density function represents the magnitude, but it discards the phase angle. The magnitude is typically represented as G^2/Hz. The G is actually GRMS.

Calculation Method

Power spectral density functions may be calculated via three methods:

1. Measuring the RMS value of the amplitude in successive frequency bands, where the signal in each band has been bandpass filtered.
2. Taking the Fourier transform of the autocorrelation function. This is the Wierner-Khintchine approach.
3. Taking the limit of the Fourier transform X(f) times its complex conjugate divided by its period T as the period approaches infinity. Symbolically, the power spectral density function $X_{PSD}(f)$ is

$$X_{PSD}(f) = \lim_{T \to \infty} \frac{X(f)X^*(f)}{T} \tag{8-1}$$

These methods are summarized in Reference 8-1. Only the third method is considered in this unit.

Fourier Transform Method

Equation (8-1) assumes that the Fourier transform has a dimension of [amplitude-time].

The following equations are taken from Reference 8-2.

The discrete Fourier transform [amplitude-time] is

$$X(k) = \Delta t \sum_{n=0}^{N-1} x(n) \exp(-j\frac{2\pi}{N}nk) \text{ for } k = 0, 1, ..., N-1 \tag{8-2a}$$

Note that the index k can be related to the frequency

$$\text{frequency}(k) = k\,\Delta f \tag{8-2b}$$

The inverse transform is

$$x(n) = \Delta f \sum_{k=0}^{N-1} X(k) \exp(+j\frac{2\pi}{N}nk) \text{ for } n = 0, 1, ..., N-1 \tag{8-3}$$

These equations give the Fourier transform values X(k) at the N discrete frequencies kΔf and give the time series x(n) at the N discrete time points n Δt. The total period of the signal is thus

$$T = N\Delta t \tag{8-4}$$

where

- N is number of samples in the time function and in the Fourier transform
- T is the record length of the time function
- Δt is the time sample separation

Consider a sine wave with a frequency such that one period is equal to the record length. This frequency is thus the smallest sine wave frequency which can be resolved. This frequency Δf is the inverse of the record length.

$$\Delta f = 1/T \tag{8-5}$$

This frequency is also the frequency increment for the Fourier transform.

Alternate Fourier Transform Method

The Fourier transform with dimension of [amplitude-time] is rather awkward.

Fortunately, the power spectral density can be calculated from a Fourier transform with dimension of [amplitude]. The corresponding formula is

$$X_{PSD}(f) = \lim_{\Delta f \to 0} \frac{F(f)F^*(f)}{\Delta f} \tag{8-6}$$

The Fourier transform $F(k)$ for the discrete time series $x(n)$ is

$$F(k) = \frac{1}{N}\sum_{n=0}^{N-1}\left\{x(n)\exp\left(-j\frac{2\pi}{N}nk\right)\right\}, \text{ for } k = 0, 1, ..., N-1 \tag{8-7a}$$

Note that the index k can be related to the frequency

$$\text{frequency}(k) = k\,\Delta f \tag{8-7b}$$

The corresponding inverse transform is

$$x(n) = \sum_{k=0}^{N-1} \left\{ F(k) \exp\left(+ j \frac{2\pi}{N} nk \right) \right\}, \text{ for } n = 0, 1, ..., N-1 \tag{8-8}$$

One-sided Fourier Transform Approach

The power spectral density functions in equations (8-1) and (8-6) were both double-sided. The power spectral density amplitude would be symmetric about the Nyquist frequency.

A one-sided, or single-sided, power spectral density function is desired.

Let $\hat{X}_{PSD}(f)$ be the one-sided power spectral density function.

$$\hat{X}_{PSD}(f) = \lim_{\Delta f \to 0} \frac{G(f)G^*(f)}{\Delta f} \tag{8-9}$$

The one-sided Fourier transform G(k) is

$$G(k) = \begin{cases} \text{magnitude}\left\{ \left[\frac{1}{N} \right] \sum_{n=0}^{N-1} \{x(n)\} \right\} & \text{for } k = 0 \\ 2 \text{ magnitude} \left\{ \left[\frac{1}{N} \right] \sum_{n=0}^{N-1} \left\{ x(n) \exp\left(- j \frac{2\pi}{N} nk \right) \right\} \right\} & \text{for } k = 1, ..., \frac{N}{2} - 1 \end{cases}$$

with

N as an even integer

Frequency (k) = $k\Delta f$

(8-10)

Implementation

Calculation of a power spectral density requires that the user select the Δf value from a list of options. The Δf value is linked to the number of degrees of freedom.

Statistical degrees of freedom

The reliability of the power spectral density data is proportional to the degrees of freedom.

The statistical degree of freedom parameter is defined from References 8-3 and 8-4 as follows:

$$dof = 2BT \tag{8-11}$$

where dof is the number of statistical degrees of freedom and B is the bandwidth of an ideal rectangular filter. This filter is equivalent to taking the time signal "as is," with no tapering applied. Note that the bandwidth B equals Δf, again assuming an ideal rectangular filter.

The 2 coefficient in equation (8-11) results from the fact that a single-sided power spectral density is calculated from a double-sided Fourier transform. The symmetries of the Fourier transform allow this double-sided to single-sided conversion.

For a single time history record, the period is T and the bandwidth B is the reciprocal so that the BT product is unity, which is equal to 2 statistical degrees of freedom from the definition in equation (8-11).

A given time history is thus worth 2 degrees of freedoms, which is poor accuracy per Chi-Square theory, as well as per experimental data per Reference 8-3. Note that the Chi-Square theory is discussed in Reference 8-5.

Breakthrough

The breakthrough is that a given time history record can be subdivided into small records, each yielding 2 degrees of freedom, as discussed in Reference 8-4 for example. The total degrees of freedom value is then equal to twice the number of individual records. The penalty, however, is that the frequency resolution widens as the record is subdivided. Narrow peaks could thus become smeared as the resolution is widened.

An example of this subdivision process is shown in Table 8-1. The process is summarized in equations (8-12) through (8-16).

Table 8-1. Example: 4096 samples taken over 16 seconds, rectangular filter					
Number of Records NR	Number of Time Samples per Record	Period of Each Record T_i (sec)	Frequency Resolution $B_i=1/T_i$ (Hz)	dof per Record $=2B_i T_I$	Total dof
1	4096	16	0.0625	2	2
2	2048	8	0.125	2	4
4	1024	4	0.25	2	6
8	512	2	0.5	2	16
16	256	1	1	2	32
32	128	0.5	2	2	64
64	64	0.25	4	2	128

Notes:

1. The subscript "i" is used to denote "individual" in Table 8-1.
2. The rows in the table could be continued until a single sample per record remained.

Also note that:

$$\text{Total dof} = 2\ NR \tag{8-12}$$

$$NR = T / T_i \tag{8-13}$$

$$B_i = 1 / T_i \tag{8-14}$$

$$NR = B_i\ T \tag{8-15}$$

$$\text{Total dof} = 2\ B_i\ T \tag{8-16}$$

Window

A window is typically applied to each time segment during the power spectral density calculation. The purpose of the window is to reduce a type of error called leakage. One of the most common windows is the Hanning window, or the cosine squared window. This window tapers the data so that the amplitude envelope decreases to zero at both the beginning and end of the time segment.

The Hanning window w(t) can be defined as

$$w(t) = \begin{cases} 1 - \cos^2\left[\pi \dfrac{t}{T}\right], & 0 \le t \le T \\ \\ 0, \quad \text{elsewhere} \end{cases} \tag{8-21}$$

The window operation reduces the leakage error but also has the effect of reducing the statistical degrees-of-freedom.

Also, a normalization factor of $\sqrt{8/3}$ is applied to the Hanned data to compensate for the lost energy.

Overlap

The lost degrees-of-freedom can be recovered by overlapping the time segments, each of which is subjected to a Hanning window. Nearly 90% of the degrees-of-freedom are recovered with a 50% overlap.

The concept of windows and overlapping is represented in Figure 8-2.

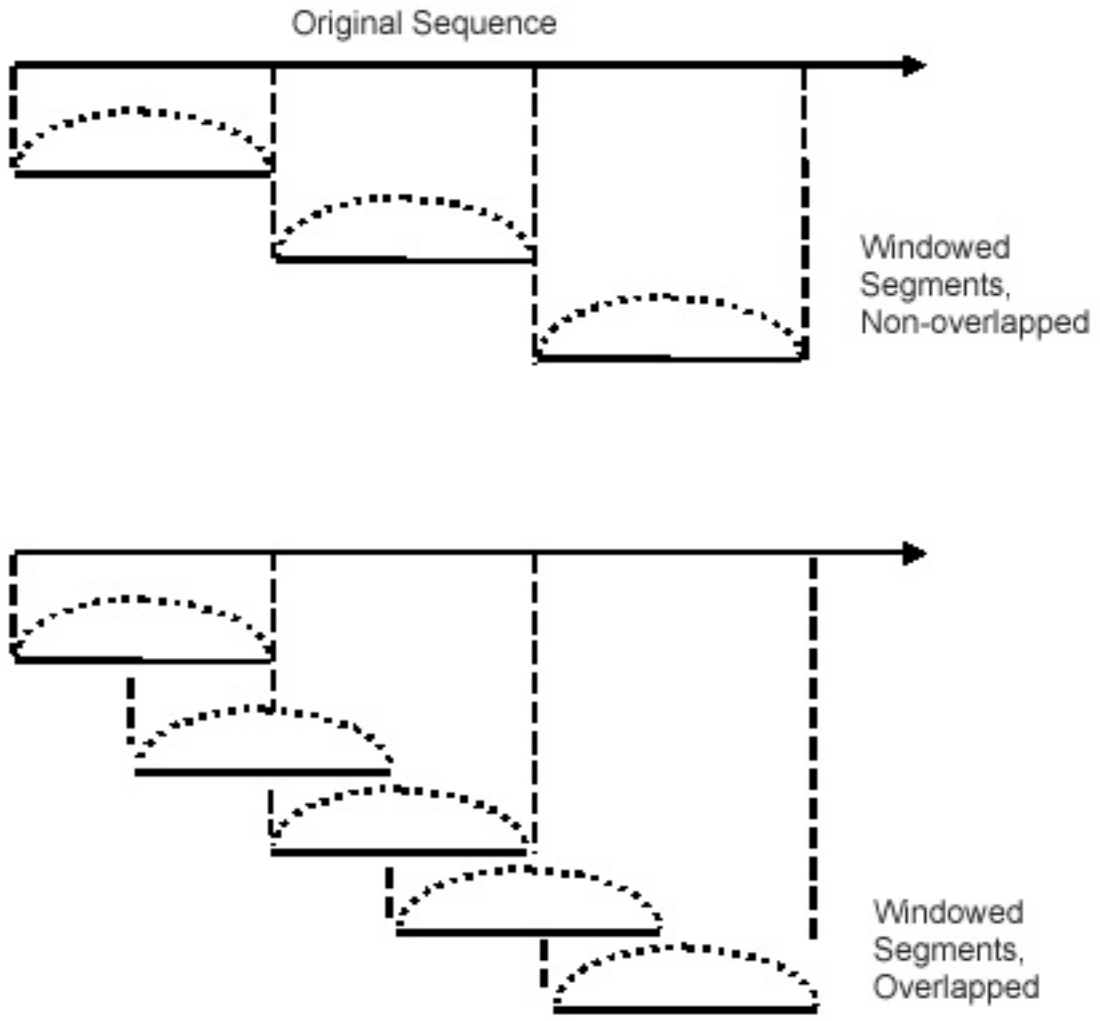

Figure 8-2.

Fast Fourier Transform

Three variations of the discrete Fourier transform have been given in this chapter. The solution to any of these transforms requires a great deal of processing steps for a given time history. Fast Fourier transform methods have been developed, however, to greatly reduce the required steps. These methods typically require that the number of time history data points be equal to 2^N,

where N is some integer. The derivation method is via a butterfly algorithm, as shown, for example, in Reference 8-8.

Records with sample numbers which are not equal to an integer power of 2 can still be processed via the fast Fourier transform method. Such a record must either be truncated or padded with zeroes so that its length becomes an integer power of 2.

Summary

Time history data is subdivided into segments to increase the statistical-degrees-of-freedom by broadening the frequency bandwidth. Next, a window is applied to each segment to taper the ends of the data. Finally, overlapping is used to recover degrees-of-freedom lost during the window operations. The effect of these steps is to increase the accuracy of the power spectral density data. Nevertheless, there are some tradeoffs as shown in the following examples.

References

8-1. W. Thomson, Theory of Vibration with Applications, Second Edition, Prentice-Hall, New Jersey, 1981.

8-2. C. Harris, editor; Shock and Vibration Handbook, 3rd edition; R. Randall, "Chapter 13 Vibration Measurement Equipment and Signal Analyzers," McGraw-Hill, New York, 1988.

8-3. MAC/RAN Applications Manual Revision 2, University Software Systems, Los Angeles, CA, 1991.

8-4. Vibration Testing, Introduction to Vibration Testing, Section 9 (I), Scientific-Atlanta, Spectral Dynamics Division, San Diego, CA, Rev 5/72.

8-5. Walpole and Myers, Probability and Statistics for Engineers and Scientists, Macmillan, New York, 1978.

8-6. R. Randall, Frequency Analysis, Bruel & Kjaer, Denmark, 1987.

8-7. TSL25, Time Series Language for 2500-Series Systems, GenRad, Santa Clara, CA, 1981.

8-8. F. Harris, Trigonometric Transforms, Scientific-Atlanta, Spectral Dynamics Division, Technical Publication DSP-005 (8-81), San Diego, CA.

CHAPTER 9

SAMPLE RATE CRITERIA AND THE NYQUIST RULE

Introduction

An understanding of sample rate criteria requires some preliminary consideration of filtering, however. Lowpass filtering of the *analog* signal is necessary to prevent an error source called aliasing. Aliasing is covered in Chapter 10.

Eventually, the accelerometer data is passed through an analog-to-digital converter. The proper sampling rate must be selected to ensure that the digitized data is accurate.

This chapter gives guidelines for choosing the sampling rate. It also briefly covers amplitude resolution.

Sampling Rate, First Requirement

The first requirement is that the sampling rate must be greater than the maximum analysis frequency. Industry guidelines for this requirement, as discussed in Reference 9-1, are summarized in Table 9-1.

Table 9-1. Sampling Rate First Requirement

(minimum sampling rate) $\geq$ (N)(maximum analysis frequency)

Analysis Type	N
Frequency Domain	2
Time Domain	10

Fourier transforms and power spectral density functions are used in frequency domain analysis.

The shock response spectrum (SRS) is an example of a time domain analysis.

Frequency Domain

The frequency domain requirement in Table 9-1 is based on the fact that at least two time-domain coordinates per cycle are required to resolve a sine wave for analytical purposes.

The Nyquist frequency is equal to one-half the sampling rate. The frequency domain analysis thus extends up to the Nyquist frequency.

Note that some conservative sources specify a value of N = 2.5 for frequency domain analysis.

Time Domain

Reference 9-1 gives the following guideline:

> Unlike other spectral quantities evolving from the discrete Fourier transform computations, the SRS is essentially a time domain quantity. Hence, the digital sampling rate given by Rs = 1/(delta t), introduces errors beyond those associated with aliasing about the Nyquist frequency. Thus, Rs must be high enough to accurately describe the response of the SRS oscillators. To minimize potential error, it is recommended that the SRS computations be performed with a sampling rate of Rs $\geq$ 10 fh, where fh is the highest natural frequency of the SRS computation.

A sampling rate of 100,000 samples per second is thus required for a shock response spectrum analysis extending to 10,000 Hz per this guideline. Again, the SRS is calculated in the time domain, even though the SRS peaks levels are represented as function of natural frequency.

Sampling Rate, Second Requirement

The second requirement is that the sampling rate must be greater than the maximum frequency present in the source energy at the measurement location. This requirement is necessary to prevent aliasing.

The guidelines for the second requirement are summarized in Table 9-2.

Table 9-2. Sample Rate Second Requirement (minimum sampling rate) $\geq$ (M)(maximum frequency in source energy)	
Analysis Type	M
Frequency Domain	2
Time Domain	10

Note the similarity between Tables 9-1 and 9-2.

Shannon's sampling theorem states that a sampled time signal must not contain components at frequencies above the Nyquist frequency. Again, the Nyquist frequency is equal to one-half the sampling rate. Shannon's theorem applies to frequency domain analysis.

Lowpass Filtering

In many cases, the maximum expected frequency is unknown. Thus, lowpass filtering can be used as a precaution to ensure compliance with the requirement in Table 9-2.

Summary

Note that the maximum source energy frequency may be independent of the maximum analysis frequency. Thus, the first and second requirements may be independent.

A common example of this independence occurs in rocket vehicle vibration testing.

Avionics components are typically subjected to power spectral density specifications which are defined up to 2000 Hz. The test specifications assume that the components are immune to vibration above 2000 Hz. The same specifications, however, assume that the components must be tested up to 2000 Hz to verify their integrity, even if the expected flight levels occur at a lower frequency domain.

The component test specifications are derived, in part, from measured or predicted flight levels. Note that a rocket vehicle is excited by aerodynamic turbulence and motor pressure oscillations during its powered flight. The content of this energy may be well below, or perhaps above, 2000 Hz.

An engineer designing a telemetry system must thus consider the expected flight vibration environments as well as post-flight analytical needs.

Amplitude Resolution

Amplitude resolution is considered in this chapter as a supplementary topic.

Analog-to-digital conversion systems have amplitude resolution, which is measured in bits.

The amplitude resolution is one part in 2^(number of bits). Thus, a 12-bit system has a resolution of one part in 4096.

Consider a 12-bit system set up to measure a full scale amplitude of 10 V peak-to-peak. The resolution is (10 V / 4096) = 2.4 mV. This example is shown in Table 9-3, along with two other cases.

Table 9-3.
Example for 10 V peak-to-peak

Bit Resolution	Voltage Resolution (mV)
8	39.1
12	2.4
16	0.15

Note that telemetry data is sometimes given in terms of bits, where the bits are in integer format. The user must apply a scale factor to the bit values. The scale factor might convert the bit values to volts, or to some engineering unit.

The voltage resolution is proportional to the G level for an accelerometer. For example, consider the following configuration:

1. An accelerometer has a 10 V peak-to-peak range.
2. The accelerometer sensitivity is 10 G/volt (0.010 G /mV).
3. The accelerometer signal is applied to a 12 bit acquisition system

In this case, the accelerometer data would have an amplitude bit resolution of 0.024 G. This would cause a measured sine wave to have a "stair-step" appearance if the peak amplitude were below, say, 0.2 G.

The bit resolution for a data acquisition system is usually fixed. The user can manipulate the resolution by choosing an accelerometer with a particular sensitivity. The user may also have control over the full-scale voltage value.

References

9-1. IES Handbook for Dynamic Data Acquisition and Analysis, Institute of Environmental Sciences, Illinois. *Particularly, paragraphs 3.7.2 and 5.5.3.5.*

9-2. R. Randall, Frequency Analysis Third edition, Bruel & Kjaer, 1987.

CHAPTER 10

ALIASING

Introduction

Again, engineers collect accelerometer data in a variety of settings. The accelerometers measure the data in analog form. The accelerometer may have an integral mechanical lowpass filter. Furthermore, the signal conditioning unit may have an analog lowpass filter.

Eventually, the accelerometer data is passed through an analog-to-digital converter. The proper sampling rate must be selected to ensure that the digitized data is accurate. Sampling rate guidelines were given in Chapter 9.

Lowpass filtering of the analog signal is necessary to prevent an error called aliasing.[1] The purpose of this chapter is to discuss aliasing.

Aliasing Examples

The following examples show the consequences of failure to comply with the sampling rate guidelines in Chapter 9. An aliasing error results.

Consider a sine wave sampled at 2000 samples per second. The Nyquist frequency is thus 1000 Hz. The Nyquist frequency is also the upper limit for a frequency domain calculation, per the Chapter 9 guidelines.

The power spectral density function of a 200 Hz sine wave sampled at this rate is given in Figure 10-1. As expected, a spectral line appears at 200 Hz.

The power spectral density of an 1800 Hz sine wave is given in Figure 10-2. Note that aliasing occurs. The 1800 Hz signal is folded about the Nyquist frequency such that a spectral line appears at 200 Hz. The Nyquist frequency thus forms a line of symmetry.

The power spectral density of a 200 Hz sine wave appears to equal that of an 1800 Hz sine wave. Again, this error occurs due to inadequate sampling rate.

The time histories for each of these sine waves are given in Figure 10-3. Note that the 1800 Hz sine wave appears to equal a 200 Hz sine wave with a 180 degree phase difference.

---

[1] An optical analogy of aliasing occurs in certain old western movies where stagecoach wheels appear to spin backwards.

The alias frequency is summarized in equation (10-1).

$$\text{Alias frequency} = S_f - E_f, \quad \text{if} \quad \frac{1}{2}S_f < E_f < S_f \tag{10-1}$$

where

S_f is the sample rate

E_f is the energy frequency

In addition, aliasing will occur if the energy frequency is above the sample rate. A separate formula is required, however.

Lowpass Filtering

Aliasing can be prevented by lowpass filtering the analog data.

Consider a stage separation test or a launch vehicle flight. The maximum expected frequency in the source energy is essentially unknown. Thus, there is no proper means to set the sampling rate, other than setting it at some exceedingly high value.

The simple solution is to pass the analog data through a lowpass filter as shown in the flowchart.

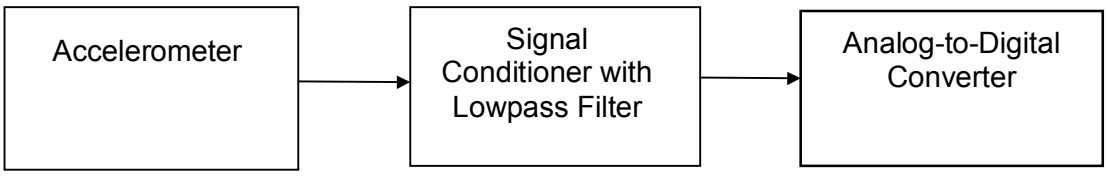

The lowpass filter removes the high-frequency energy from the signal. This filter is often called an "anti-aliasing" filter.

The filter can be part of the signal conditioning system. Typically, a Butterworth filter is used. The Butterworth filter has a roll-off which attenuates the signal by 3 dB at the cut-off frequency.

The cut-off frequency is typically set at, or slightly above, the maximum analysis frequency.

Recommended Filtering Parameters

Let f_c be the cutoff frequency.

Let f_N be the Nyquist frequency.

Reference 8-1 gives the following guidelines:

(1) A lowpass anti-aliasing filter with a cutoff rate of at least 60 dB/octave should be used for the analog-to-digital conversion of all dynamic data.

(2) With a 60 dB/octave cutoff rate, the half-power point cutoff frequency of the filter should be set at $f_c \leq 0.6\, f_N$.

If the anti-aliasing filter has a more rapid cutoff rate, a higher cutoff frequency can be used, but the bound $f_c \leq 0.8\, f_N$ should never be exceeded.

Telemetry Design Example

Ideally, the sampling rate could be chosen after the maximum excitation and analysis frequencies were identified. Practical considerations often require a reverse approach.

Consider a telemetry system for a launch vehicle. Several accelerometers will be mounted in the vehicle. The data will be digitized on-board the vehicle. The digitized signal will be sent via a radio link to a ground station.

The flight dynamic environments are unknown. The maximum sampling rate, however, is 4000 samples per second for each accelerometer channel. This sampling rate is constrained by the available radio link bandwidth and other considerations.

Given this constraint, choose an analog lowpass filter with a cut-off frequency at 2000 Hz. This frequency does not meet the strict guidelines in Reference 10-1, which would set the cut-off frequency at 1200 Hz. Some compromise is often required in telemetry system design, however. In this case, the cut-off frequency is set higher than the guidelines in order to capture additional data beyond 1200 Hz.

The lowpass filter is placed between the accelerometer and the vehicle's analog-to-digital converter.

Now consider that the vehicle has flown and the digital data has been received at the ground station.

Power spectral density functions of the flight data can be calculated up to 2000 Hz, per Table 10-1. Some roll-off may appear starting at about 1600 Hz depending on the filter characteristics, but this is a practical trade-off.

Table 10-1. Sampling Rate First Requirement

(minimum sampling rate) $\geq$ (N)(maximum analysis frequency)

Analysis Type	N
Frequency Domain	2
Time Domain	10

Recall that Fourier transforms and the power spectral density functions are used in frequency domain analysis.

On the other hand, the shock response spectrum is a time domain function.

Shock response spectra of the flight data can be calculated accurately up to 200 Hz, per Table 10-1. This frequency can be extended somewhat if greater error margins are allowed.

This telemetry system will thus yield usable vibration data.

On the other hand, the telemetry system will yield marginal shock data. The resulting shock data may be adequate to characterize motor ignition and launch shock, which are typically dominated by energy below 2000 Hz. Unfortunately, the telemetry data will be inadequate to characterize high-frequency pyrotechnic shock from stage separation events.

Stage separation shock must thus be measured during ground development tests prior to flight. Data acquisition systems with high sampling rates can be used during ground tests.

Reference

10-1. IES Handbook for Dynamic Data Acquisition and Analysis, Institute of Environmental Sciences, Illinois.

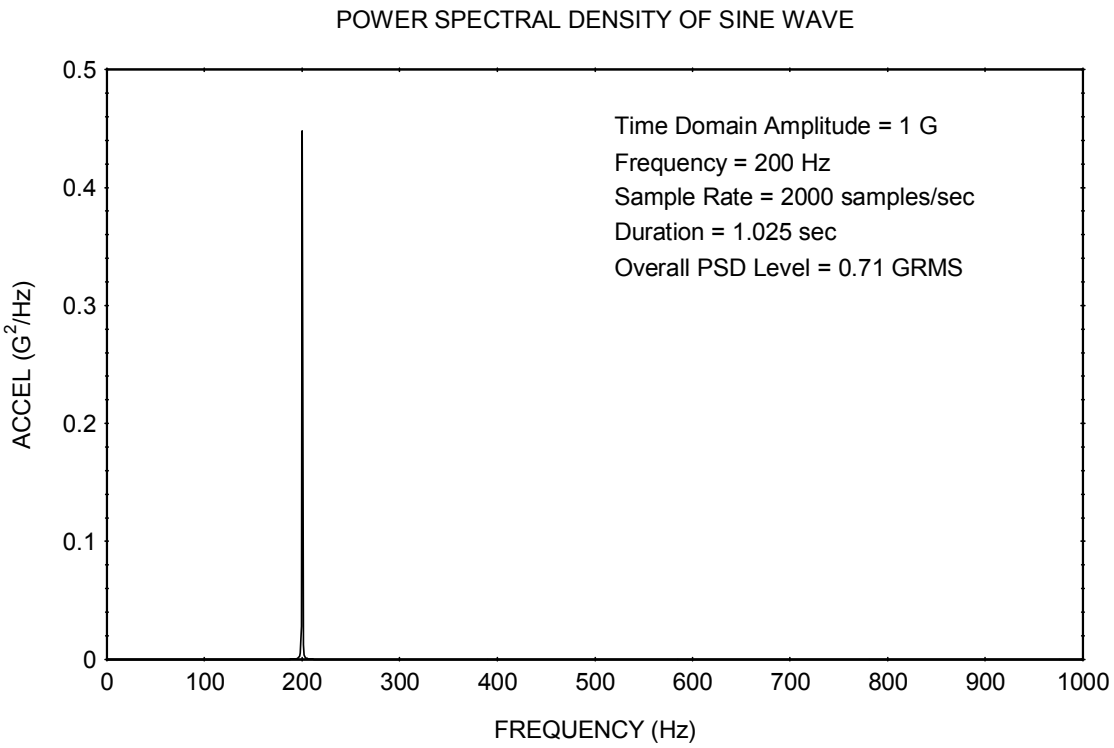

Figure 10-1.

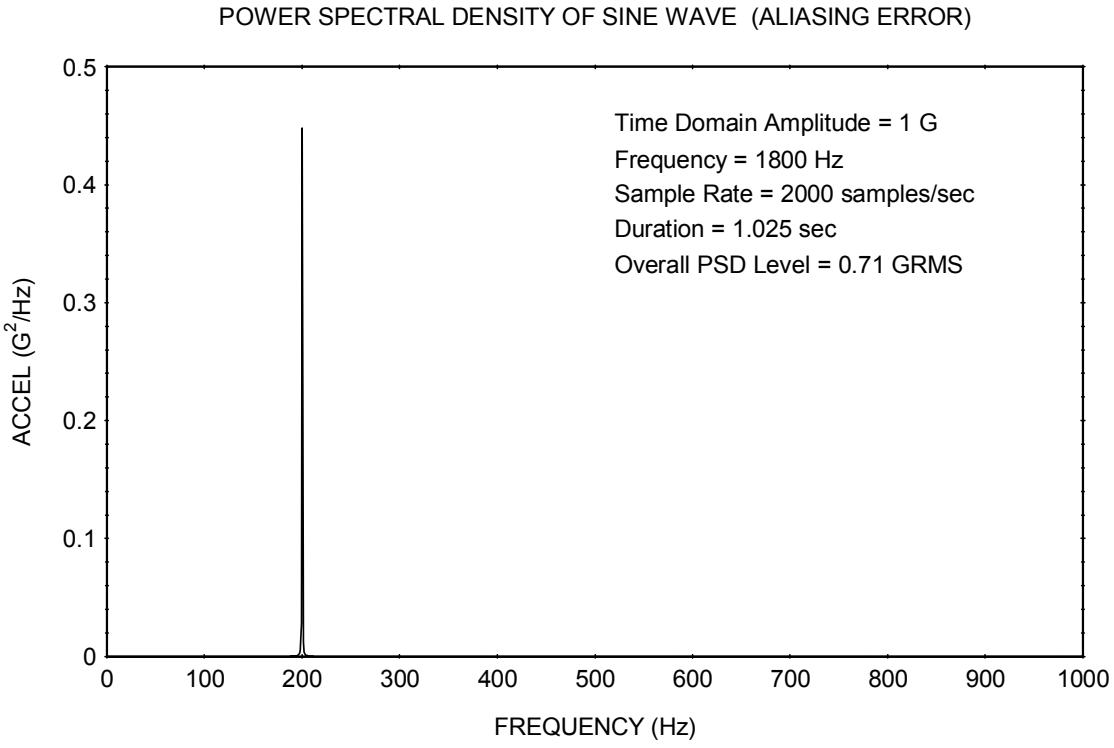

Figure 10-2.

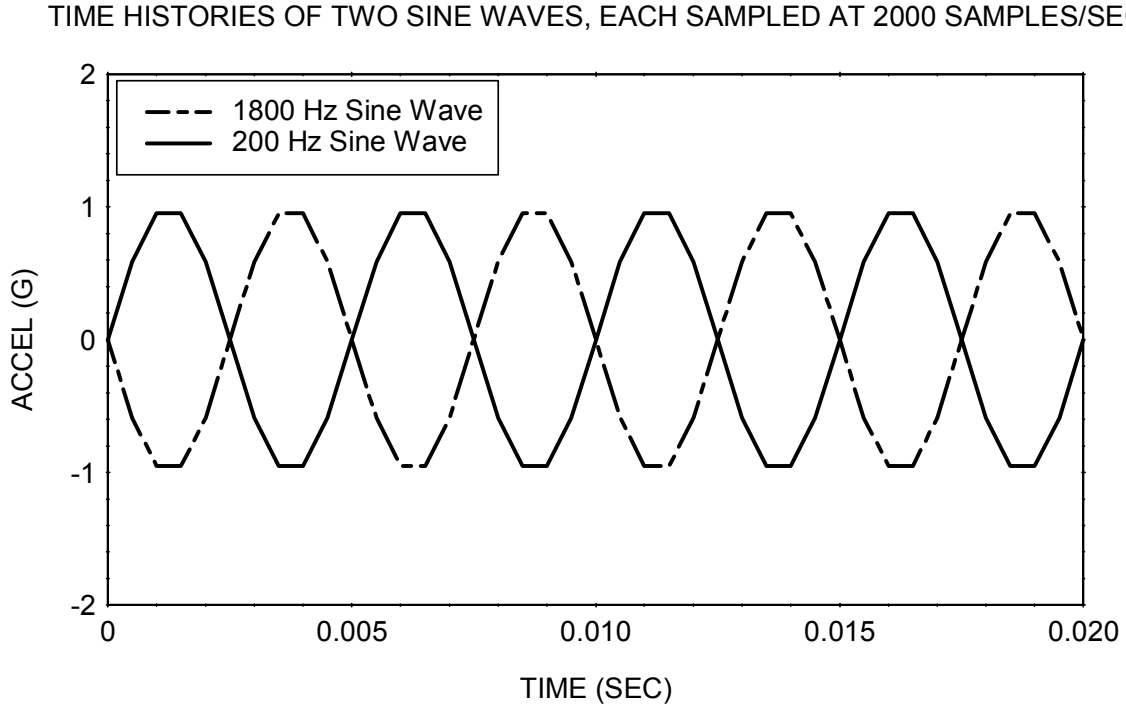
TIME HISTORIES OF TWO SINE WAVES, EACH SAMPLED AT 2000 SAMPLES/SEC
1800 Hz Sine Wave
200 Hz Sine Wave
ACCEL (G)
2
1
0
-1
-2
0
0.005
0.010
0.015
0.020
TIME (SEC)

Figure 10-3.

CHAPTER 11

FILTERING BASICS

Filtering

The purpose of this chapter is to demonstrate the use of filtering using a Butterworth filter as an example. A Butterworth filter is one of several common infinite impulse response (IIR) filters. The derivation underlying Butterworth filters is given in Chapters 12 and 14.

The Butterworth filter can be used either for highpass, lowpass, or bandpass filtering.

A highpass filter is a filter which allows the high-frequency energy to pass through. It is used to remove low-frequency energy from a signal.

A lowpass filter is a filter which allows the low-frequency energy to pass through. It is thus used to remove high-frequency energy from a signal.

A bandpass filter may be constructed by using a highpass filter and lowpass filter in series.

A Butterworth filter is characterized by its cut-off frequency. The cut-off frequency is the frequency at which the corresponding transfer function magnitude is –3 dB, equivalent to 0.707.

A Butterworth filter is also characterized by its order. A sixth-order Butterworth filter is the filter of choice for this tutorial. Further details on the significance of order are given in References 11-1 and 11-2.

A property of Butterworth filters is that the transfer magnitude is –3 dB at the cut-off frequency regardless of the order. Other filter types, such as Bessel, do not share this characteristic, however.

Consider a lowpass, sixth-order Butterworth filter with a cut-off frequency of 100 Hz. The corresponding transfer function magnitude is given in Figure 11-1.

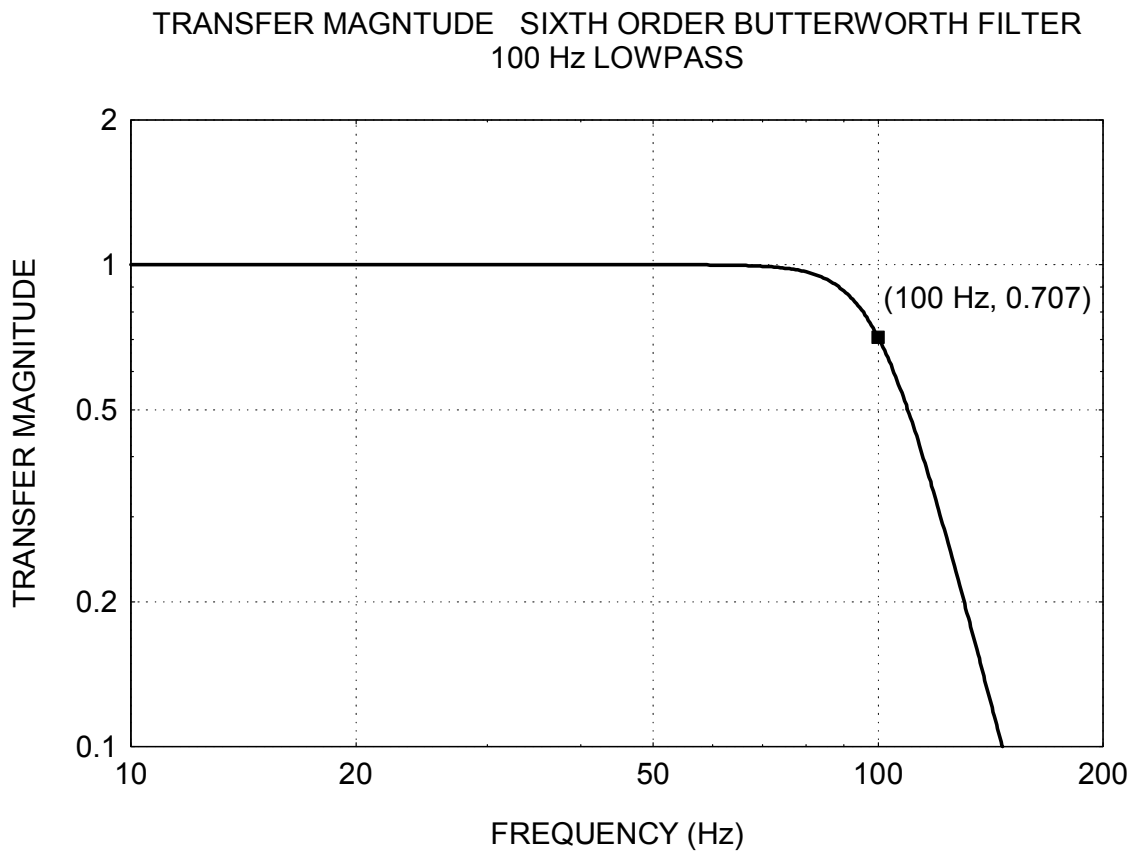

Figure 11-1.

Note that the curve in Figure 11-1 has a gradual roll-off beginning at about 70 Hz. Ideally the transfer function would have a rectangular shape, with a corner at (100 Hz, 1.00). This ideal is never realized in practice, however, due to stability concerns. Thus, a compromise is usually required to select the cut-off frequency.

The transfer function in Figure 11-1 also has a corresponding phase relationship, but this is not shown. The transfer function could also be represented in terms of a complex function, with real and imaginary components.

A transfer function magnitude plot for a sixth-order Butterworth filter with a cut-off frequency of 100 Hz is shown in Figure 11-2.

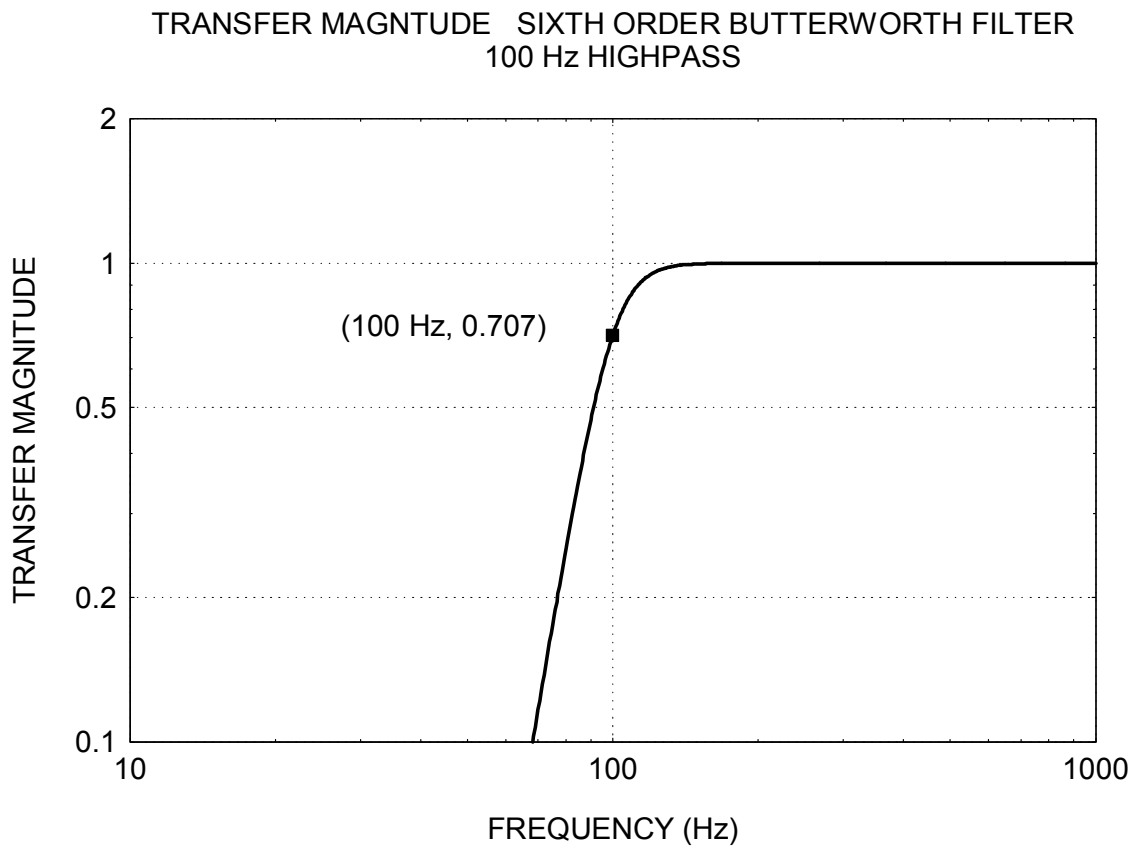

Figure 11-2.

The curves in Figures 11-1 and 11-2 suggest that filtering could be achieved as follows:

1. Take the Fourier transform of the input time history.
2. Multiply the Fourier transform by the filter transfer function, in complex form.
3. Take the inverse Fourier transform of the product.

The above frequency domain method is valid. Nevertheless, the filtering algorithm is usually implemented in the time domain for computational efficiency, as explained in Chapter 12.

Seismic Filtering Example

Figure 11-3. Lehman Seismometer

The boom is a horizontal pendulum. It has a period of 14.2 seconds, equivalent to a natural frequency of 0.071 Hz. A sensor at the free end measures the displacement. The boom length is 64 inch. The total frame height is 35 inch. The boom has a knife edge that pivots against a bolt head in the lower cross-beam of the frame.

The boom is suspended from the frame by a wire cable. The cable is attached to the top cross-beam of the frame. The other end of the cable is attached to the boom, about two-thirds of the distance from the pivot to the free end of the boom. The pivot point is offset from the top cable attachment point. Thus, the boom oscillates as if it were a swinging gate.

The plate supporting the frame has three adjustable mounting feet. The feet can be adjusted to tune the pendulum to the desired natural frequency. Furthermore, the wire cable has a turnbuckle which is used to adjust height of the free end of the boom. The detached frame in the center of the figure is used for assembly and to limit the displacement during tuning.

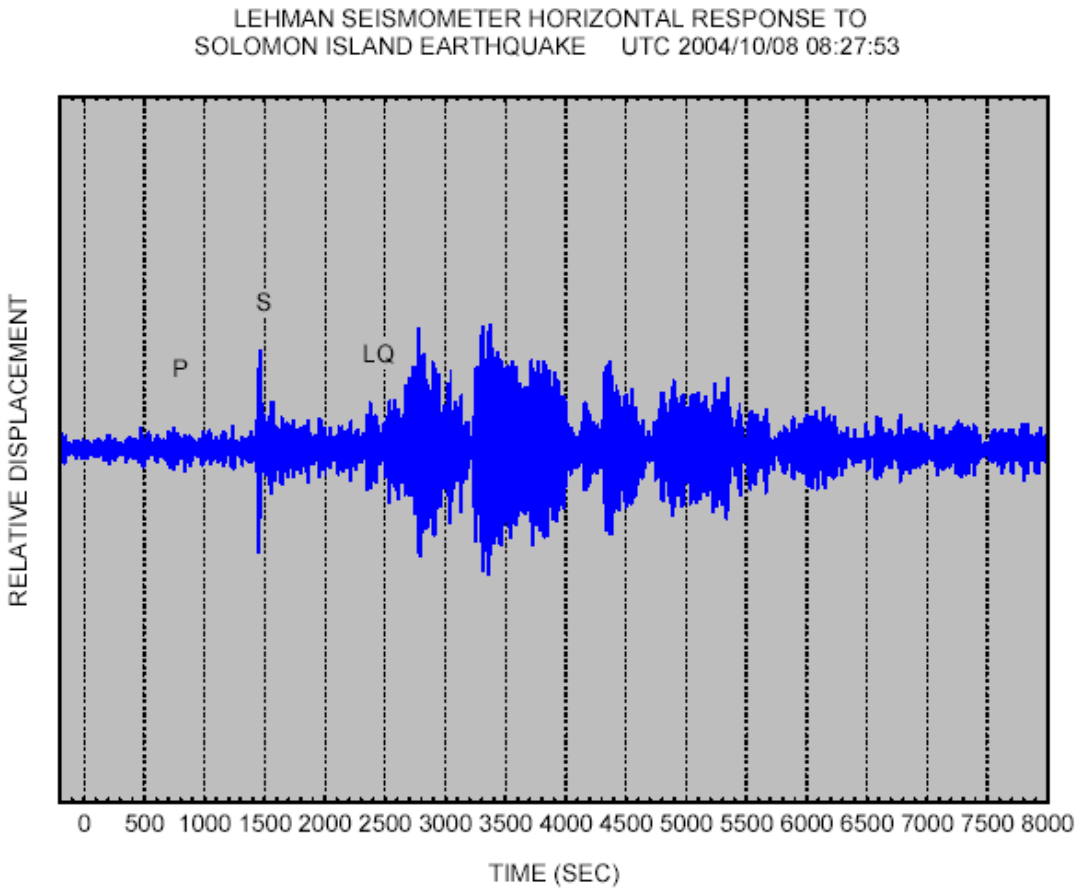

Figure 11-4.

The Solomon Island Earthquake occurred on October 8, 2004, with a magnitude of 6.8. The time history is shown in Figure 11-4 as recorded on the Lehman seismometer in Mesa, Arizona. The time history shows that the Earth is remarkably reverberant. The oscillations last well over one hour.

The time is referenced to the earthquake occurrence using USGS data. The plot's Y-axis is labeled as relative displacement because it is the response of the boom relative to the ground. Further calculation would be required to estimate the true ground motion.

The phase components are

P	primary wave
S	secondary or shear wave
LQ	Love wave

The P-wave is indiscernible against the background microseismic noise. Nevertheless, it can be extracted by additional filtering, as shown in the next figure.

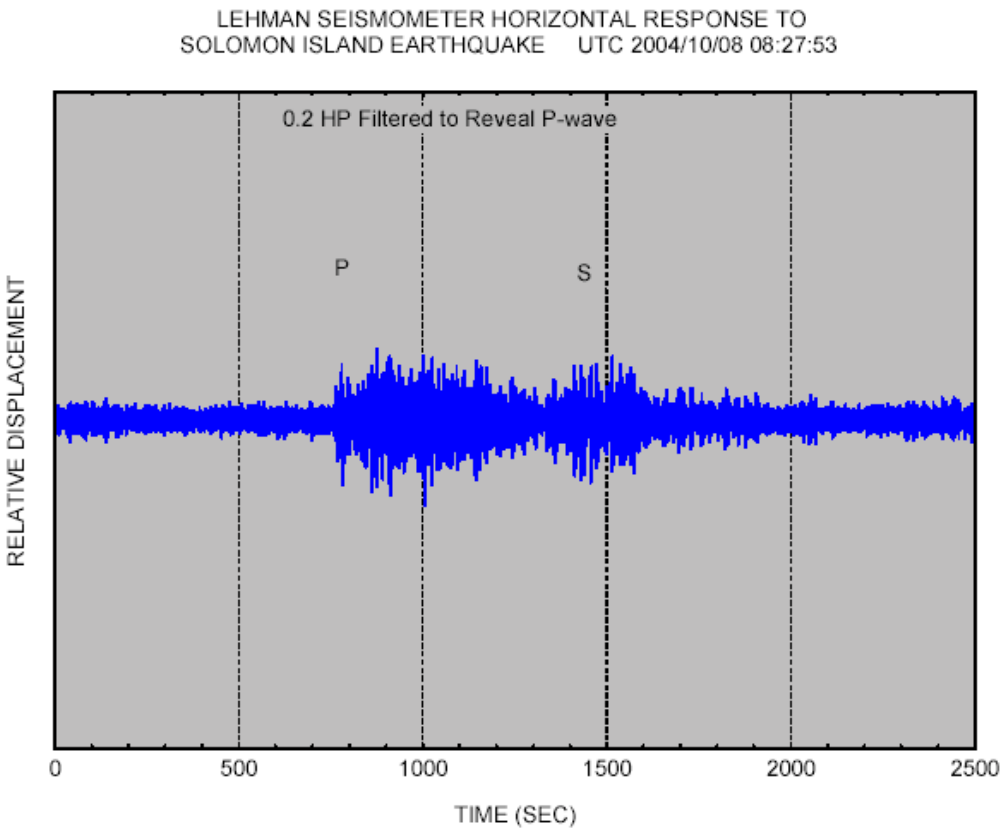

Figure 11-5.

The data in Figure 11-5 is highpass filtered with a cut-off frequency of 0.2 Hz, clarifying the arrival of the P-wave. The P-wave is a longitudinal wave. It is a structural-borne sound wave. It is the fastest of the various seismic waveforms.

References

11-1. Stearns and David, Signal Processing Algorithms in Fortran and C, Prentice Hall, Englewood Cliffs, New Jersey, 1993.

11-2. Himelblau, Piersol, et al., IES Recommended Practice 012.1: Handbook for Dynamic Data Acquisition and Analysis, Institute of Environmental Sciences, Mount Prospect, IL.

CHAPTER 12

DIGITAL FILTER DESIGN

Z-Transform

A useful tool for designing digital filters is the *z-transform*. The two-sided z-transform X(z) of a time history sequence x_k is defined as

$$X(z) = \sum_{k=-\infty}^{\infty} x_k z^{-k} \tag{12-1}$$

The z-transform method is used to derive a transfer function H(z). This transfer function relates the output Y(z) to the input X(z) as follows

$$H(z) = \frac{Y(z)}{X(z)} \tag{12-2}$$

Digital filters are based on this transfer function, as shown in the block diagram in Figure 12-1. Note that x_k and y_k are the time domain input and output, respectively.

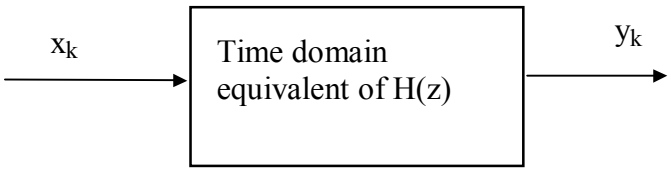

Figure 12-1. Filter Block Diagram

The transfer function can be represented by a series of a_n and b_n coefficients as follows

$$H(z) = \frac{b_0 + b_1 z^{-1} + \cdots + b_L z^{-L}}{1 + a_1 z^{-1} + \cdots + a_L z^{-L}} \tag{12-3}$$

The coefficients are constants which determine the system response. Note the H(z) defines the direct form transfer function for an Lth-order, linear, time-invariant digital system.

Note that

$$z = \exp(j\omega T) \tag{12-4}$$

The T variable is the time step. By substitution,

$$H(\omega) = \frac{b_0 + b_1\left[\exp(j\omega T)\right]^{-1} + \cdots + b_L\left[\exp(j\omega T)\right]^{-L}}{1 + a_1\left[\exp(j\omega T)\right]^{-1} + \cdots + a_L\left[\exp(j\omega T)\right]^{-L}} \tag{12-5}$$

With some manipulation, equations (12-1) through (12-3) can be used to derive the time domain equivalent of H(z) as

$$y_k = \left\{\sum_{n=0}^{L} b_n x_{k-n}\right\} - \left\{\sum_{n=1}^{L} a_n y_{k-n}\right\} \tag{12-6}$$

Equation (12-6) is recursive because the output at any time index k depends on the output at previous times.

Filter Impulse Response Class

Digital filters are classified according to their impulse response: infinite impulse response (IIR) and finite impulse response (FIR).

FIR filters are feedforward filters. IIR filters are feedback filters.

Each class can be implemented in the time domain. The theory underlying each of these classes is discussed in Reference 12-1.

The familiar Bessel, Butterworth, and Chebyshev filters are all examples of IIR filters. Signal processing software typically uses this class of filters.

This report will focus on the IIR class. The Bessel filter is discussed briefly in Chapter 13. The Butterworth filter is discussed in detail in Chapter 14.

IIR Filter Design, Phase Correction

Ideally, a filter should provide linear phase response. This is particularly desirable if shock response spectra calculations are required. IIR filters, however, do not have a linear phase response, for reasons discussed in Reference 12-1. A number of methods are available, however, to correct the phase response. One method is based on time reversals and multiple filtering as shown in Figure 12-2.

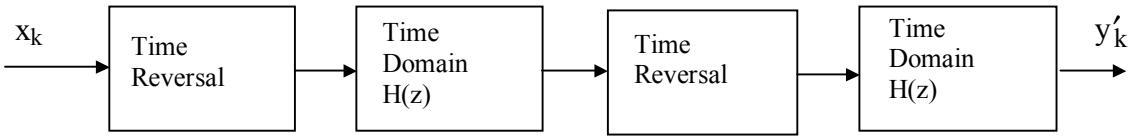

Figure 12-2. Phase Correction Method

Reference

12-1. Stearns and David, Signal Processing Algorithms in Fortran and C, Prentice Hall, Englewood Cliffs, New Jersey, 1993.

CHAPTER 13

BESSEL FILTERS

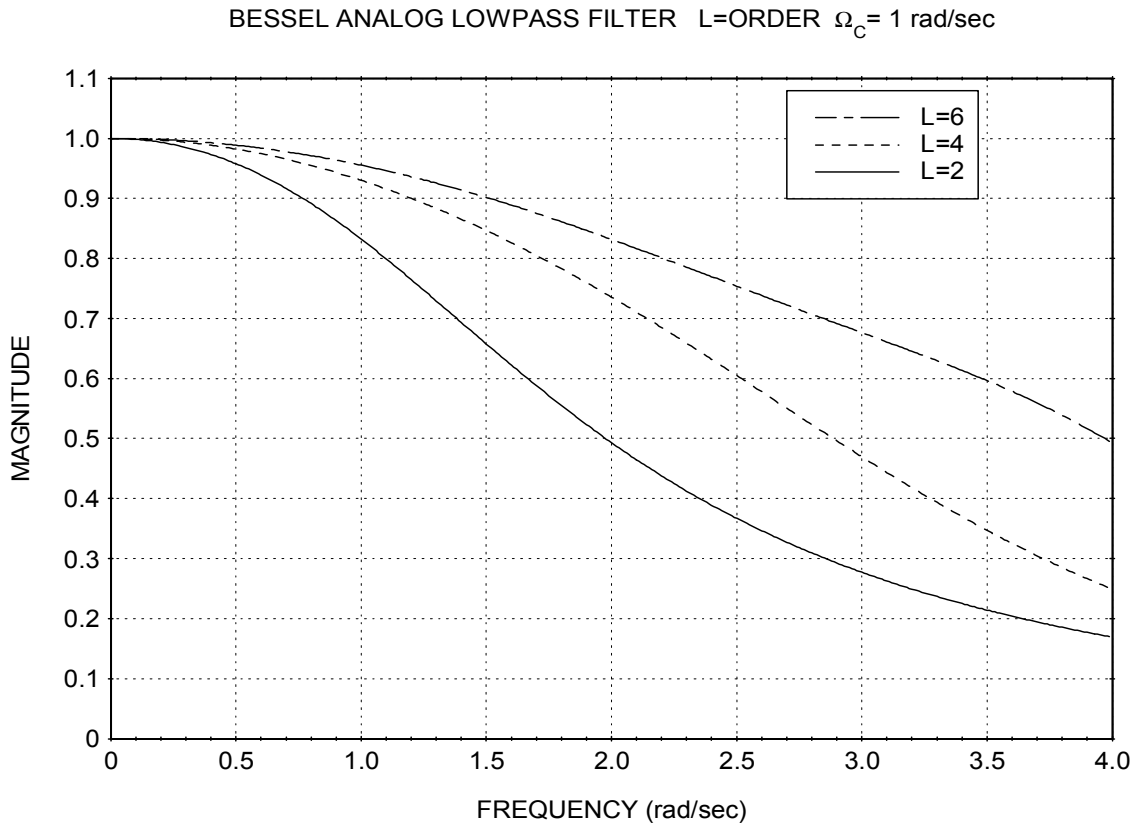

Figure 13-1. Bessel Filter Transfer Magnitude

Bessel filters use the direct-form transfer function as shown in Figure 13-1. Other filters, however, use a cascade approach, as explained later in this report.

An analog Bessel filter has a nearly linear phase response. This property translates only approximately into to the digital version, however.

Bessel filter transfer functions tend to have a very gradual roll-off beyond the cut-off frequency. Another characteristic is that a lower order provides more attenuation above the cutoff frequency.

The analog Bessel lowpass filter transfer function for order L is defined by the following two equations.

$$c_k = \frac{(2L-k)!}{2^{L-k}\, k!\,(L-k)!} \tag{13-1}$$

$$H_L(s) = \frac{c_0}{c_L\, s^L + \cdots + c_0} \tag{13-2}$$

The transfer function can be calculated by setting $s = j\Omega$.

CHAPTER 14

BUTTERWORTH FILTERS

Analog Transfer Function Magnitude

Butterworth filters are often used as anti-aliasing filters. For example, the Pegasus vehicle has on-board analog anti-aliasing filters which are 4-pole Butterworth.

The Lth-order lowpass analog Butterworth filter magnitude response is

$$\left|P_L(\Omega)\right| = \frac{1}{\sqrt{1+\Omega^{2L}}}, \quad L \geq 1 \tag{14-1}$$

Equation (14-1) is normalized to have a cutoff frequency Ω_c equal to 1 radian/sec.

A characteristic of equation (14-1) is that all curves pass through the coordinate $\left(1, \frac{1}{\sqrt{2}}\right)$, regardless of the order. Note that other filter types do not necessarily have this same characteristic.

Equation (14-1) is graphed in Figure 14-1 for three cases.

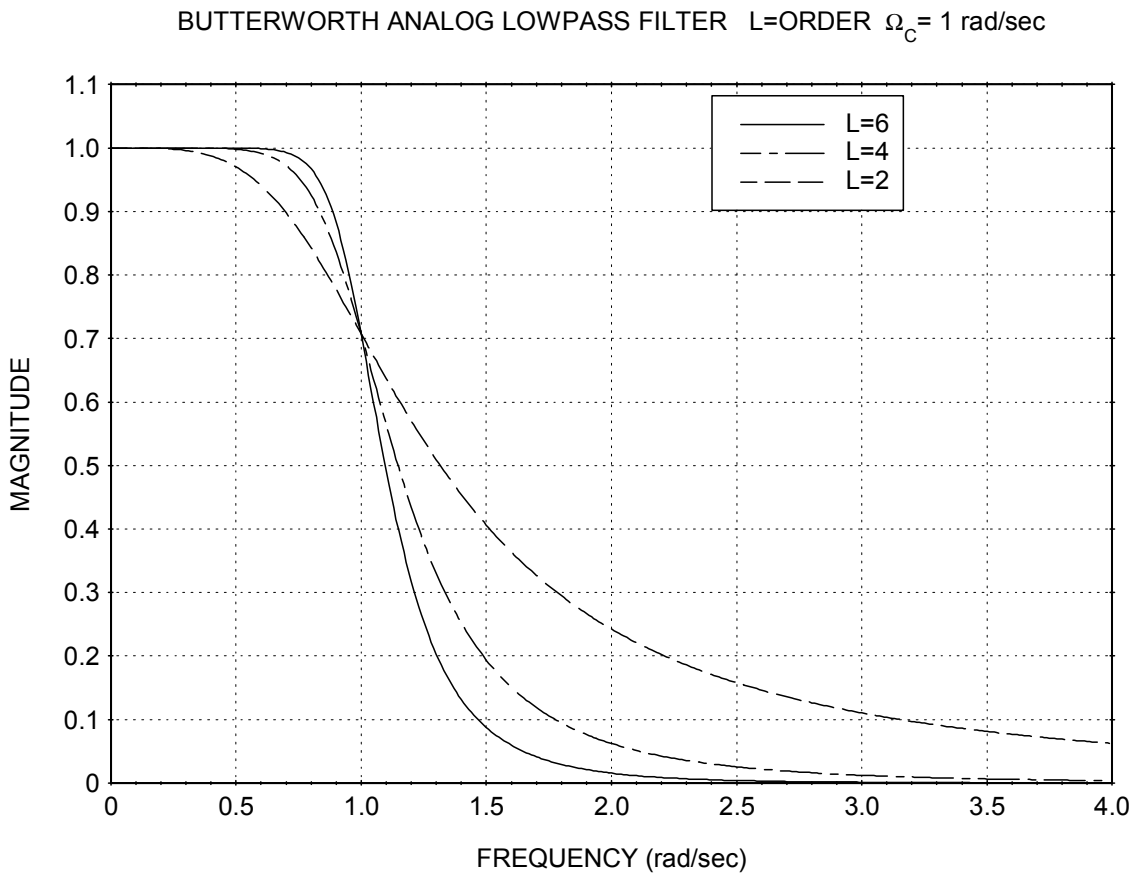

Figure 14-1. Butterworth Filter Transfer Magnitude

An Lth-order filter has a total of 2L poles. Only the L poles in the left half of the s-plane are used, however, to form a stable filter.

The poles s_k are given by

$$s_k = \exp\left(\frac{j\,(2k + L - 1)\pi}{2L}\right), \quad 1 \le k \le 2L \tag{14-2}$$

$$s_k = \cos\left(\frac{(2k + L - 1)\pi}{2L}\right) + j\sin\left(\frac{(2k + L - 1)\pi}{2L}\right), \qquad 1 \le k \le 2L \tag{14-3}$$

Again, only the poles in the left half s-plane are used. Effectively, only the poles for $1 \le k \le L$ are used.

Note that the same pole equations are used for both lowpass and highpass filter designs.

The poles are inserted into the following transfer function

$$H(s) = \frac{1}{(s - s_1)(s - s_2)\ldots(s - s_L)} \tag{14-4}$$

The conventional implementation is to apply the filter in a cascade manner rather than fully expanding the denominator in equation (14-4). Each section of the cascade is a second order-section $H_k(s)$ given by

$$H_k(s) = \frac{1}{(s - s_k)(s - s_{L+1-k})} \tag{14-5}$$

Note that the sections are arranged to match the complex conjugate pairs of the poles.

The analog transfer function for a lowpass Butterworth filter with even order can now be written as

$$H(s) = \prod_{k=1}^{L/2} H_k(s) \tag{14-6}$$

Sixth-order Butterworth Example

A sixth-order lowpass Butterworth filter has the poles given in Table 14-1. Only the poles on the left half of the s-plane are given.

Table 14-1. Sixth-order Lowpass Butterworth Filter	
k	s_k Pole
1	$\cos\left(\frac{7\pi}{12}\right) + j\sin\left(\frac{7\pi}{12}\right)$
2	$\cos\left(\frac{9\pi}{12}\right) + j\sin\left(\frac{9\pi}{12}\right)$
3	$\cos\left(\frac{11\pi}{12}\right) + j\sin\left(\frac{11\pi}{12}\right)$
4	$\cos\left(\frac{13\pi}{12}\right) + j\sin\left(\frac{13\pi}{12}\right)$
5	$\cos\left(\frac{15\pi}{12}\right) + j\sin\left(\frac{15\pi}{12}\right)$
6	$\cos\left(\frac{17\pi}{12}\right) + j\sin\left(\frac{17\pi}{12}\right)$

Note the following complex conjugate pairings:

$$\begin{aligned} s_4 &= s_3{}^* \\ s_5 &= s_2{}^* \\ s_6 &= s_1{}^* \end{aligned} \tag{14-7}$$

Apply the poles into equation (14-6).

$$H_1(s) = \frac{1}{(s - s_1)(s - s_6)} \tag{14-8}$$

$$H_1(s) = \frac{1}{(s - s_1)(s - s_1{}^*)} \tag{14-9}$$

$$H_1(s) = \frac{1}{\left\{s - \left[\cos\left(\frac{7\pi}{12}\right) + j\sin\left(\frac{7\pi}{12}\right)\right]\right\}\left\{s - \left[\cos\left(\frac{7\pi}{12}\right) - j\sin\left(\frac{7\pi}{12}\right)\right]\right\}} \tag{14-10}$$

$$H_1(s) = \frac{1}{\left\{s - \cos\left(\frac{7\pi}{12}\right) - j\sin\left(\frac{7\pi}{12}\right)\right\}\left\{s - \cos\left(\frac{7\pi}{12}\right) + j\sin\left(\frac{7\pi}{12}\right)\right\}} \tag{14-11}$$

$$H_1(s) = \frac{1}{\left\{s - \cos\left(\frac{7\pi}{12}\right)\right\}^2 + \left\{\sin\left(\frac{7\pi}{12}\right)\right\}^2} \tag{14-12}$$

$$H_1(s) = \frac{1}{s^2 - 2\cos\left(\frac{7\pi}{12}\right)s + 1} \tag{14-13}$$

Similarly,

$$H_2(s) = \frac{1}{s^2 - 2\cos\left(\frac{9\pi}{12}\right)s + 1} \tag{14-14}$$

$$H_3(s) = \frac{1}{s^2 - 2\cos\left(\frac{11\pi}{12}\right)s + 1} \tag{14-15}$$

Normalized Frequency Parameter

Now consider a generic stage.

$$H_g(s) = \frac{1}{s^2 - \alpha s + 1} \tag{14-16}$$

Define a frequency parameter Ω_c as

$$\Omega_c = \tan(\pi f_0 T) \tag{14-17}$$

Note that T is the time segment duration. It is thus the inverse of the sampling rate. Furthermore, f_0 is the filter cutoff frequency.

Apply the frequency parameter to the generic transfer function.

$$\hat{H}_g(s) = H_g(s)\Big|_{s=s/\Omega_c} = H_g\left(\frac{s}{\Omega_c}\right) \tag{14-18}$$

$$\hat{H}_g(s) = \frac{1}{\left(\frac{s}{\Omega_c}\right)^2 - \alpha\left(\frac{s}{\Omega_c}\right) + 1} \tag{14-19}$$

$$\hat{H}_g(s) = \frac{{\Omega_c}^2}{s^2 - \alpha\Omega_c s + \Omega_c} \tag{14-20}$$

Z-transform of Butterworth Filter

The bilinear transform is defined by

$$s = \frac{z-1}{z+1} \tag{14-21}$$

The purpose of this function is to transform an analog filter into the z-domain. The frequency transformation in equation (14-17) actually follows from the bilinear transformation in equation (14-21). The derivation is given in Appendix B.

Substitute the bilinear transform into the transfer function in equation (14-20).

$$\hat{H}_g(s) = \frac{{\Omega_c}^2}{\left[\frac{z-1}{z+1}\right]^2 - \alpha\Omega_c\left[\frac{z-1}{z+1}\right] + \Omega_c} \tag{14-22}$$

$$\hat{H}_g(s) = \frac{{\Omega_c}^2[z+1]^2}{[z-1]^2 - \alpha\Omega_c[z-1][z+1] + \Omega_c[z+1]^2} \tag{14-23}$$

$$\hat{H}_g(s) = \frac{{\Omega_c}^2\left[z^2 + 2z + 1\right]}{\left[z^2 - 2z + 1\right] - \alpha\Omega_c\left[z^2 - 1\right] + \Omega_c\left[z^2 + 2z + 1\right]} \tag{14-24}$$

$$\hat{H}_g(s) = \frac{\Omega_c{}^2 z^2 + 2\Omega_c{}^2 z + \Omega_c{}^2}{z^2 - 2z + 1 - \alpha\Omega_c z^2 + \alpha\Omega_c + \Omega_c{}^2 z^2 + 2\Omega_c{}^2 z + \Omega_c{}^2} \tag{14-25}$$

$$\hat{H}_g(s) = \frac{\Omega_c{}^2 z^2 + 2\Omega_c{}^2 z + \Omega_c{}^2}{\left[-\alpha\Omega_c + \Omega_c{}^2 + 1\right] z^2 + \left[+2\Omega_c{}^2 - 2\right] z + \left[\Omega_c{}^2 + \alpha\Omega_c + 1\right]} \tag{14-26}$$

$$\hat{H}_g(s) = \frac{\Omega_c{}^2 z^2 + 2\Omega_c{}^2 z + \Omega_c{}^2}{\left[\Omega_c{}^2 - \alpha\Omega_c + 1\right] z^2 + 2\left[\Omega_c{}^2 - 1\right] z + \left[\Omega_c{}^2 + \alpha\Omega_c + 1\right]} \tag{14-27}$$

$$\hat{H}_g(s) = \frac{\{b_0\} z^2 + \{2b_0\} z + \{b_0\}}{z^2 + \left\{\frac{2\left[\Omega_c{}^2 - 1\right]}{\left[\Omega_c{}^2 - \alpha\Omega_c + 1\right]}\right\} z + \left\{\frac{\left[\Omega_c{}^2 + \alpha\Omega_c + 1\right]}{\left[\Omega_c{}^2 - \alpha\Omega_c + 1\right]}\right\}} \tag{14-28a}$$

where

$$b_0 = \frac{\Omega_c{}^2}{\left[\Omega_c{}^2 - \alpha\Omega_c + 1\right]} \tag{14-28b}$$

Recall equation (12-3).

$$H(z) = \frac{b_0 + b_1 z^{-1} + \cdots + b_L z^{-L}}{1 + a_1 z^{-1} + \cdots + a_L z^{-L}} \tag{14-29}$$

Set L=2.

$$H(z) = \frac{b_0 + b_1 z^{-1} + b_2 z^{-2}}{1 + a_1 z^{-1} + a_2 z^{-2}} \tag{14-30}$$

Multiply through by z^2,

$$H(z) = \frac{b_0 z^2 + b_1 z + b_2}{z^2 + a_1 z + a_2} \tag{14-31}$$

Again,

$$b_0 = \frac{\Omega_c{}^2}{\left[\Omega_c{}^2 - \alpha\Omega_c + 1\right]} \tag{14-32}$$

$$b_1 = \frac{2\Omega_c{}^2}{\left[\Omega_c{}^2 - \alpha\Omega_c + 1\right]} \tag{14-33}$$

$$b_2 = b_0 \tag{14-34}$$

$$a_1 = \frac{2\left[\Omega_c{}^2 - 1\right]}{\left[\Omega_c{}^2 - \alpha\Omega_c + 1\right]} \tag{14-35}$$

$$a_2 = \frac{\left[\Omega_c{}^2 + \alpha\Omega_c + 1\right]}{\left[\Omega_c{}^2 - \alpha\Omega_c + 1\right]} \tag{14-36}$$

The coefficients can be inserted into equation (14-1). The resulting recursive equation for a filter section is

$$y_k = \left[b_0 x_k + b_1 x_{k-1} + b_2 x_{k-2}\right] - \left[a_1 y_{k-1} + a_2 y_{k-2}\right] \tag{14-37}$$

Equation (14-37) represents one of three cascade stages for a sixth-order filter. Note that there is a unique set of coefficients for each of these stages.

Equation (14-37) is applied six times if refiltering is used for phase correction, again assuming a sixth-order filter.

Highpass Butterworth Filter

Recall the generic transfer function for a lowpass filter stage

$$H_g(s) = \frac{1}{s^2 - \alpha s + 1} \tag{14-38}$$

The lowpass filter H can be transformed into a highpass filter J by changing s to 1/s.

$$J_g(s) = \frac{1}{\left(\frac{1}{s^2}\right) - \left(\frac{\alpha}{s}\right) + 1} \tag{14-39}$$

$$J_g(s) = \frac{s^2}{1 - \alpha s + s^2} \tag{14-40}$$

$$J_g(s) = \frac{\left(\frac{s}{\Omega_c}\right)^2}{1 - \alpha\left(\frac{s}{\Omega_c}\right) + \left(\frac{s}{\Omega_c}\right)^2} \tag{14-41}$$

$$J_g(s) = \frac{s^2}{{\Omega_c}^2 - \alpha\Omega_c s + s^2} \tag{14-42}$$

Recall the bilinear transform

$$s = \frac{z-1}{z+1} \tag{14-43}$$

By substitution,

$$\hat{J}_g(s) = \frac{\left[\frac{z-1}{z+1}\right]^2}{(\Omega_c)^2 - \alpha\Omega_c\left[\frac{z-1}{z+1}\right] + \left[\frac{z-1}{z+1}\right]^2} \tag{14-44}$$

$$\hat{J}_g(s) = \frac{[z-1]^2}{\Omega_c{}^2[z+1]^2 - \alpha\Omega_c[z+1][z-1] + [z-1]^2} \tag{14-45}$$

$$\hat{J}_g(s) = \frac{\left[z^2 - 2z + 1\right]}{\Omega_c{}^2\left[z^2 + 2z + 1\right] - \alpha\Omega_c\left[z^2 - 1\right] + \left[z^2 - 2z + 1\right]} \tag{14-46}$$

$$\hat{J}_g(s) = \frac{\left[z^2 - 2z + 1\right]}{\left[\Omega_c{}^2 - \alpha\Omega_c + 1\right]z^2 + \left[2\Omega_c - 2\right]z + \left[\Omega_c{}^2 + \alpha\Omega_c + 1\right]} \tag{14-47}$$

$$\hat{J}_g(s) = \frac{\{b_0\}z^2 + \{-2b_0\}z + \{b_0\}}{z^2 + \left\{\frac{\left[2\Omega_c{}^2 - 2\right]}{\left[1 - \alpha\Omega_c + \Omega_c{}^2\right]}\right\}z + \left\{\frac{\left[1 + \alpha\Omega_c + \Omega_c{}^2\right]}{\left[1 - \alpha\Omega_c + \Omega_c{}^2\right]}\right\}} \tag{14-48a}$$

where

$$b_0 = \frac{1}{1 - \alpha\Omega_c + \Omega_c{}^2} \tag{14-48b}$$

Recall the z-transform

$$H(z) = \frac{b_0 z^2 + b_1 z + b_2}{z^2 + a_1 z + a_2} \tag{14-49}$$

Thus the highpass filter coefficients are thus

$$a_1 = \frac{2\left[-1+\Omega_c{}^2\right]}{\left[1-\alpha\Omega_c+\Omega_c{}^2\right]} \tag{14-50}$$

$$a_2 = \frac{\left[1+\alpha\Omega_c+\Omega_c{}^2\right]}{\left[1-\alpha\Omega_c+\Omega_c{}^2\right]} \tag{14-51}$$

$$b_0 = \frac{1}{1-\alpha\Omega_c+\Omega_c{}^2} \tag{14-52}$$

$$b_1 = \frac{-2}{1-\alpha\Omega_c+\Omega_c{}^2} \tag{14-53}$$

$$b_1 = -2\,b_0 \tag{14-54}$$

$$b_2 = b_0 \tag{14-55}$$

Again, the coefficients are inserted into the following filter equation for an individual stage

$$y_k = \left[b_0 x_k + b_1 x_{k-1} + b_2 x_{k-2}\right] - \left[a_1 y_{k-1} + a_2 y_{k-2}\right] \tag{14-56}$$

Equation (14-56) represents one of three cascade stages for a sixth-order filter. Note that there is a unique set of coefficients for each of these stages.

CHAPTER 15

FILTER NUMERICAL STABILITY

Numerical Stability

The following criteria are taken from Reference 15-1. The criteria apply to a cascade filter implementation. Note that the stability of each stage must be evaluated separately.

The filter tends to become unstable if the product $\left(f_0 T \right)$ is very small. This comes about because the filter weights require more digits for a very small $\left(f_0 T \right)$ product.

Recall the z-transform

$$H(z) = \frac{b_0 z^2 + b_1 z + b_2}{z^2 + a_1 z + a_2} \tag{15-1}$$

Define stability coordinates

$$(x, y) = (-a1, -a2) \tag{15-2}$$

The coordinates must fall inside the triangle shown in Figure 15-1. The coordinate (0.6, -0.4) is used as an example in Figure 15-1.

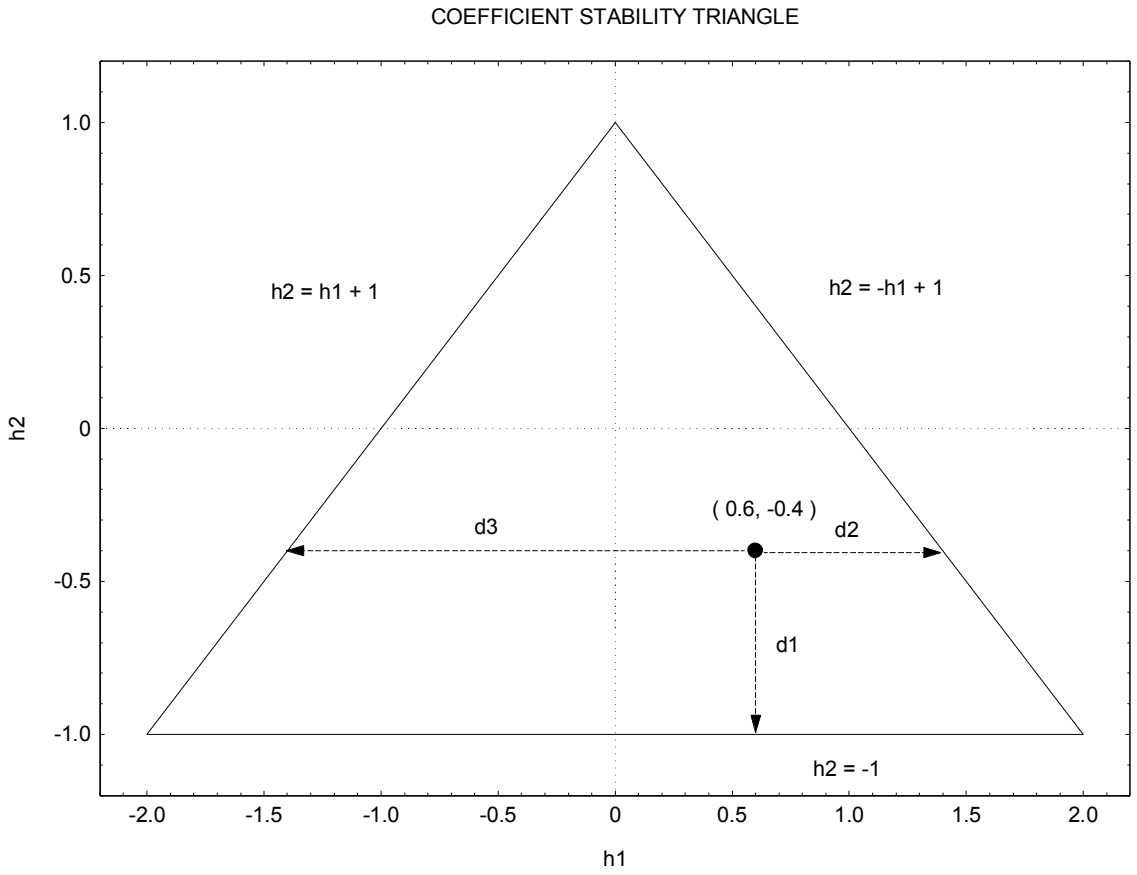

Figure 15-1. Coefficient Stability Triangle

The filter is stable is the coordinate pair is within the triangle. The filter becomes unstable if the pair is on a border or outside the triangle.

Three distance parameters are shown in Figure 5-1. For this example,

d1 = 0.6

d2 = 0.8

d3 = 2.0

The key distance is the smallest of the three values, denoted as d. For this example, d = 0.6.

The stability criteria for d are shown in Table 15-1.

Table 15-1. Stability Criteria	
Size of d	Stability Comment
$d > 5.0(10^{-6})$	Good Stability
$5.0(10^{-6}) \geq d > 0$	Marginally Unstable
$d \leq 0$	Unstable

Actually, the criteria in Table 15-1 apply to computers with word lengths greater than 32 bit. The $5.0(10^{-6})$ threshold should be increased for computers with smaller word lengths.

Also note that the cutoff frequency must be less than the Nyquist frequency, which is one-half of the sampling rate. The filter becomes unstable in the limiting case where the cutoff frequency is equal to the Nyquist frequency.

Reference

15-1. Stearns and David, Signal Processing Algorithms in Fortran and C, Prentice Hall, Englewood Cliffs, New Jersey, 1993.

CHAPTER 16

DETAILED FILTERING EXAMPLE

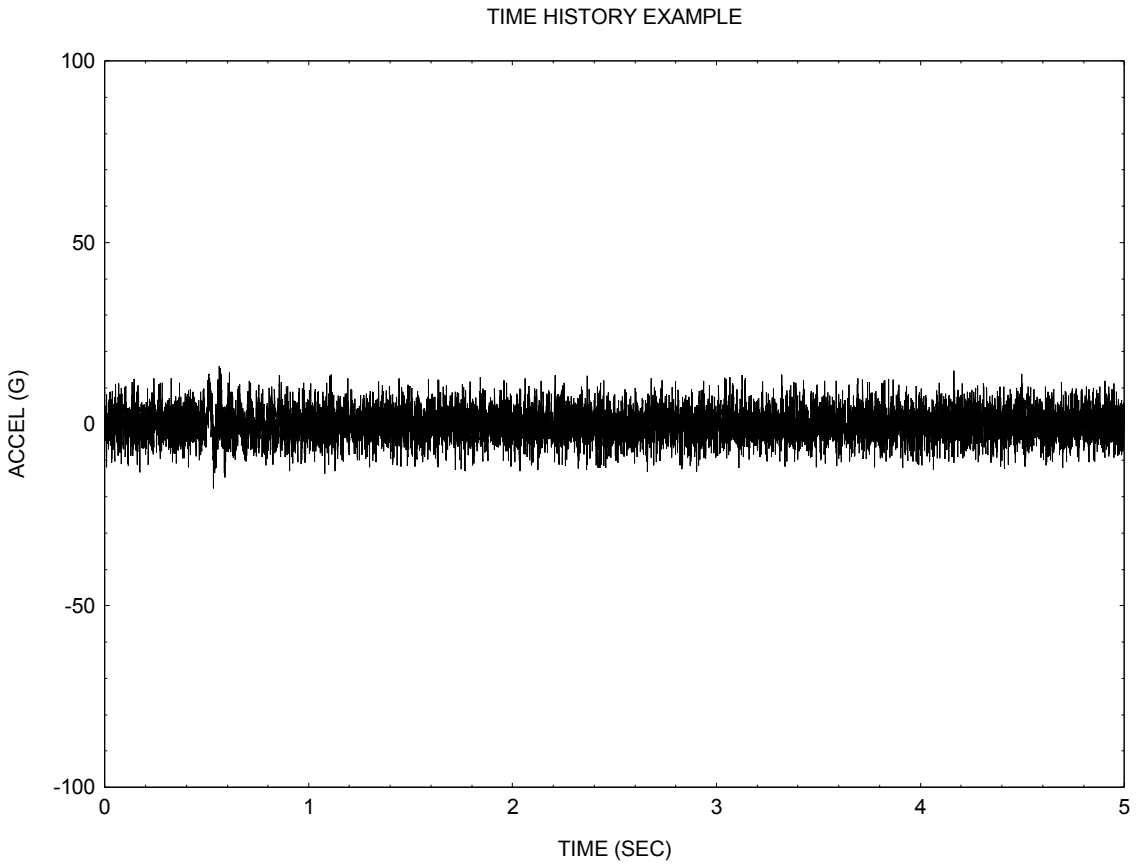

Figure 16-1. Synthesized Time History, Raw Data

Time History Example

A synthesized time history is shown in Figure 16-1. The sample rate is 2000 samples per second. The time increment is thus 0.0005 seconds. The signal is largely white noise, but a possible transient event appears near 0.6 seconds.

The raw data was lowpass filtered at 30 Hz using a 6^{th} order Butterworth filter with refiltering for phase correction. The resulting time history clarifies the transient, as shown in Figure 16-2.

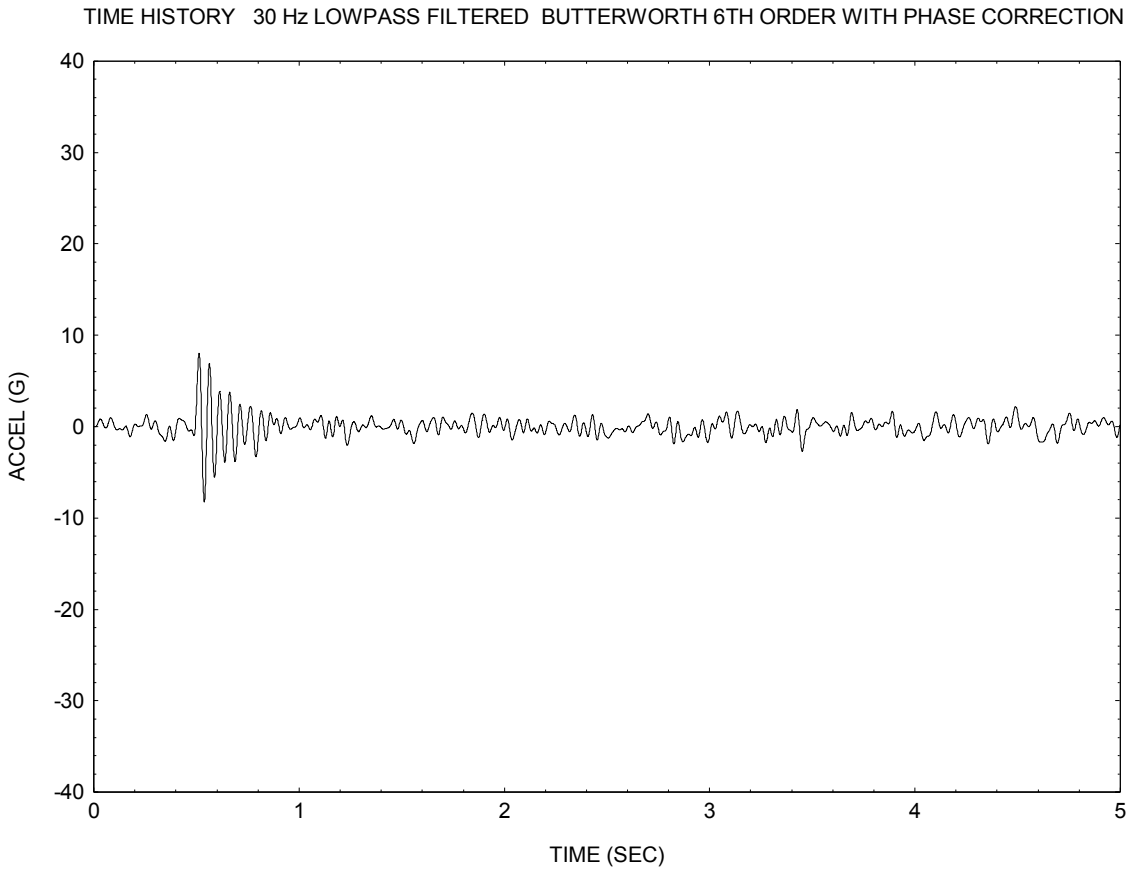

Figure 16-2. Filtered Time History

The transient is a 20 Hz sinusoid with 5% damping.

The digital filter transfer function is shown in Figure 16-3. The transfer function includes the refiltering effects.

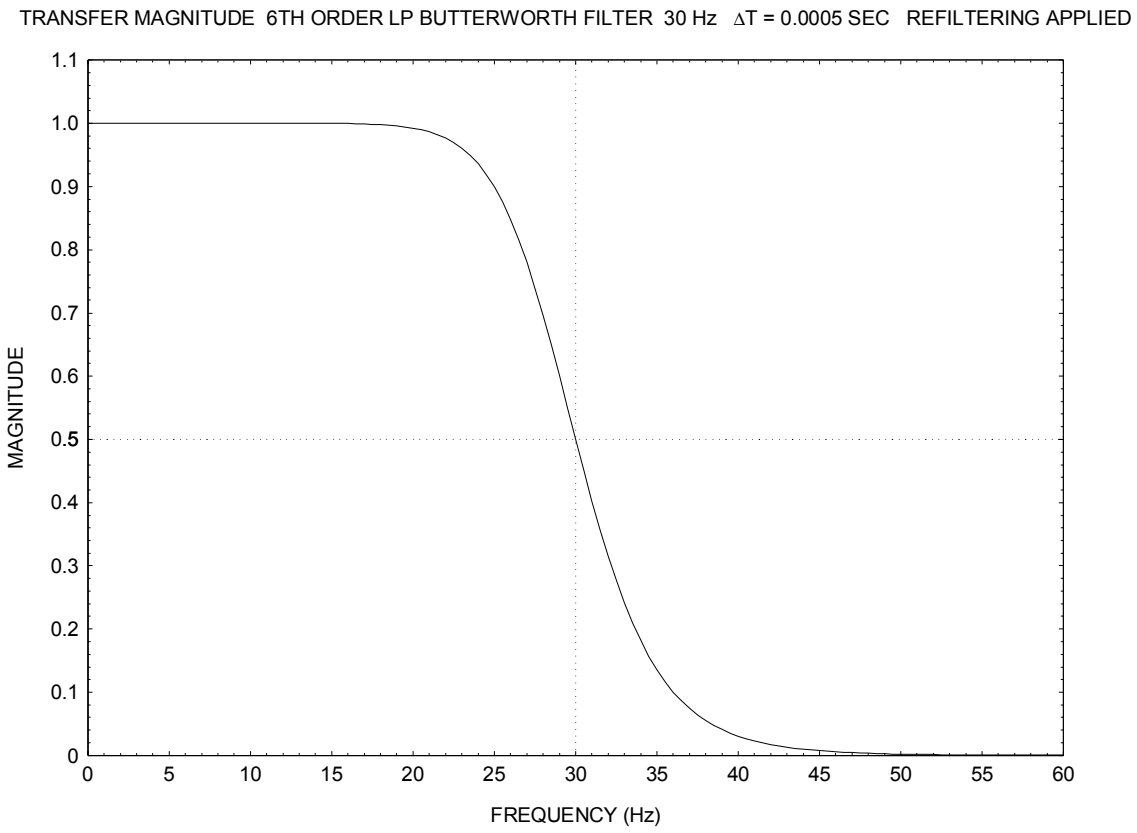

Figure 16-3. Transfer Magnitude

Note that refiltering decreases the -3 dB point to -6 dB at the cutoff frequency of 30 Hz.

The poles are those shown in Table 14-1. The filter coefficients are shown in Table 16-1.

Table 16-1. Filter Coefficients		
Stage	Denominator	Numerator
1	a(1)= -1.943779 a(2)= 0.9524443	b(0)= 0.2166255E-02 b(1)= 0.4332509E-02 b(2)= 0.2166255E-02
2	a(1)= -1.866892 a(2)= 0.8752146	b(0)= 0.2080568E-02 b(1)= 0.4161135E-02 b(2)= 0.2080568E-02
3	a(1)= -1.825209 a(2)= 0.8333458	b(0)= 0.2034114E-02 b(1)= 0.4068227E-02 b(2)= 0.2034114E-02

The stability results are shown in Figure 16-3. The plot is focused on the lower right corner of the triangle. Each of the three coordinates is close to the right leg of the triangle. Nevertheless, each coordinate is sufficiently inside the boundary to yield good stability.

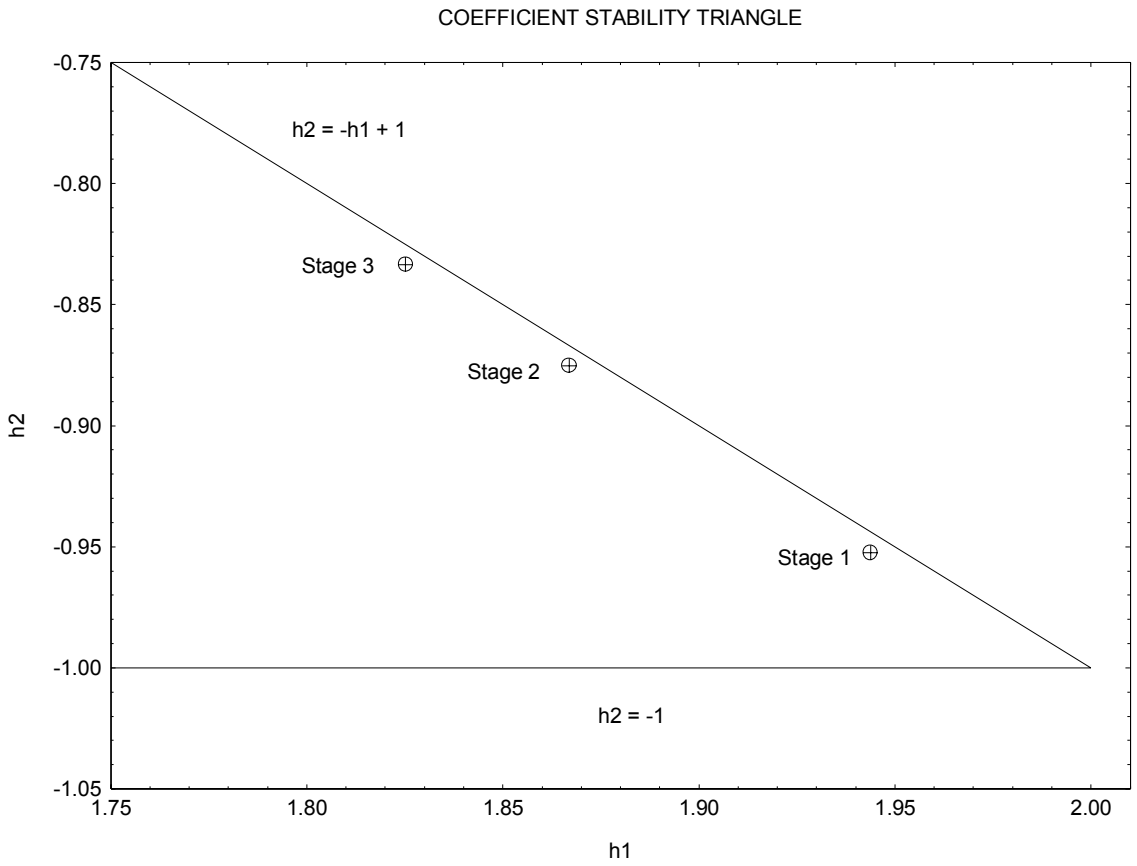

Figure 16-3. Stability Results

CHAPTER 17

POWER SPECTRAL DENSITY VIA SUCCESSIVE BANDPASS FILTERING

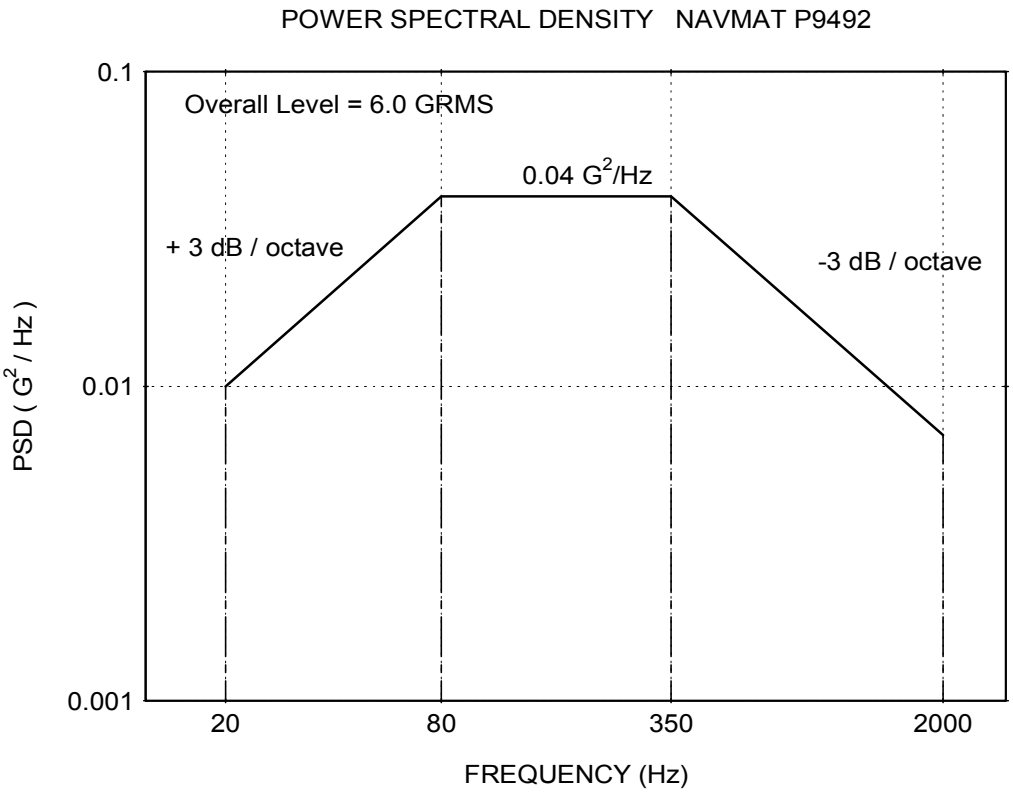

Figure 17-1.

A power spectral density can be calculated using bandpass filtering a shown in the following example.

The NAVMAT P9492 power spectral density is shown in Figure 17-1. A time history was synthesized to satisfy this specification, using the method in Reference 17-1. The synthesized time history is shown in Figure 17-2.

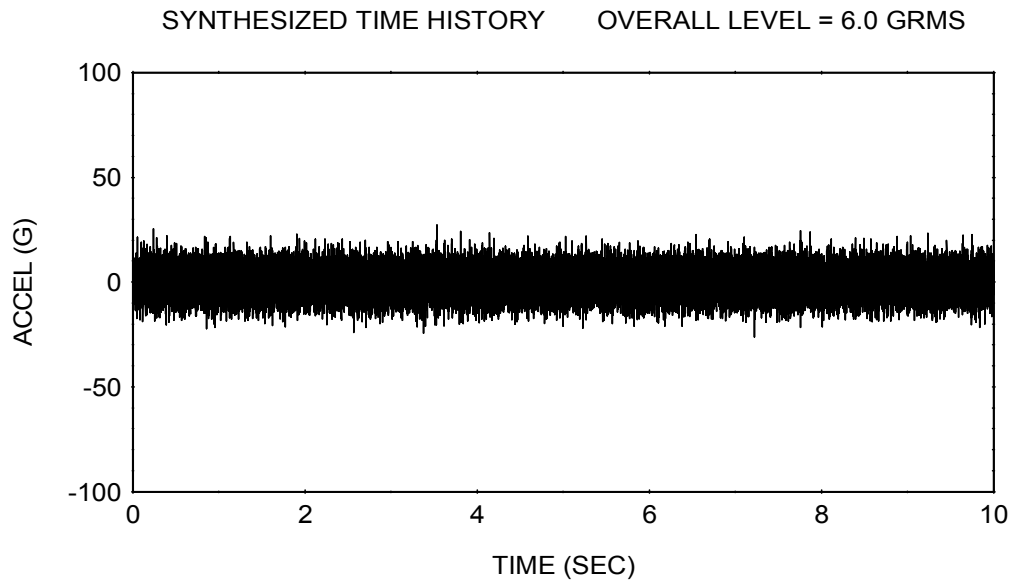
SYNTHESIZED TIME HISTORY
OVERALL LEVEL = 6.0 GRMS
100
50
0
-50
-100
ACCEL (G)
0
2
4
6
8
10
TIME (SEC)

Figure 17-2.

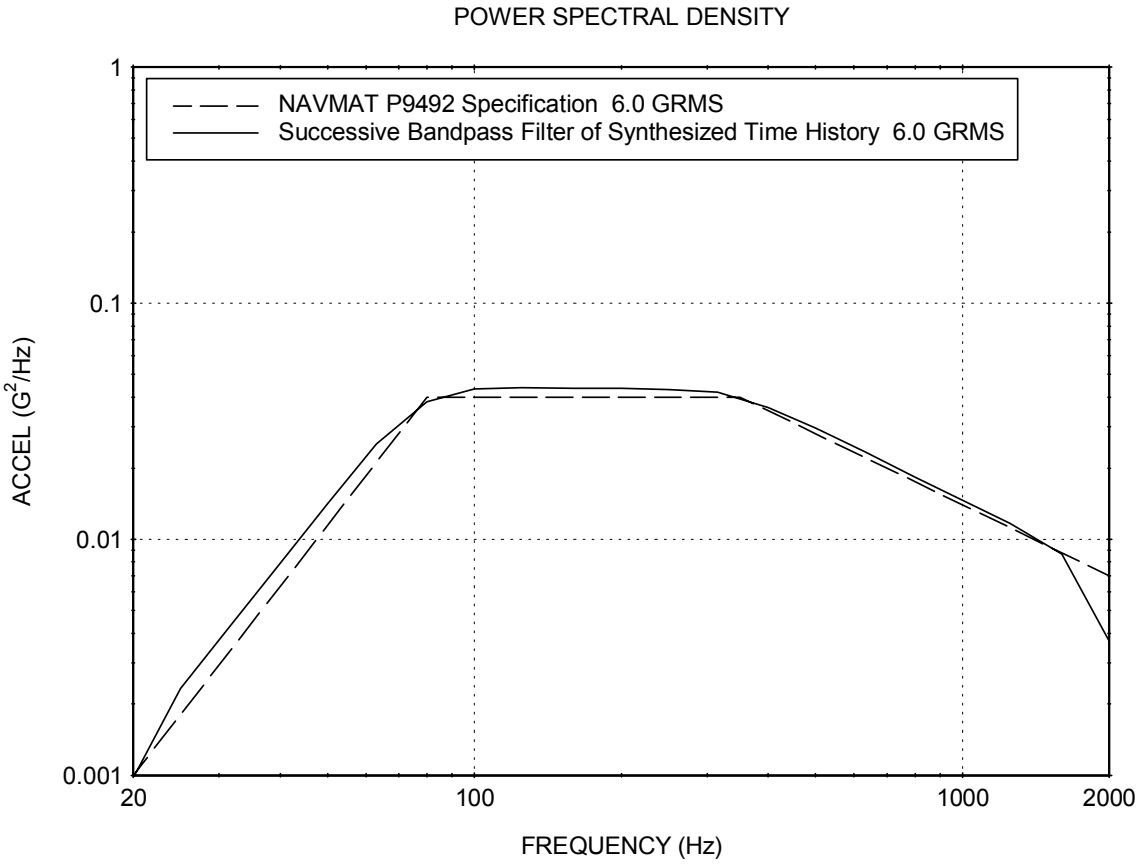

Figure 17-3.

A power spectral density of the synthesized time history was calculated by bandpass filtering the time history over successive one-third octave bands. The filter was a Butterworth sixth order filter. The RMS value was calculated for each band. The resulting power spectral density is shown in Figure 17-3 along with the specification. The calculation details are shown in Table 17-1.

Again, G^2/Hz is an abbreviation for GRMS^2/Hz.

Table 17-1. Successive Bandpass Filtering Results					
Center Freq (Hz)	Lower Freq (Hz)	Upper Freq (Hz)	Bandwidth (Hz)	GRMS	PSD(G^2/Hz)
20	17.82	22.45	4.631	0.067	9.73E-04
25	22.27	28.06	5.789	0.116	2.33E-03
31.5	28.06	35.36	7.294	0.177	4.28E-03
40	35.64	44.9	9.263	0.271	7.93E-03
50	44.54	56.12	11.58	0.405	1.42E-02
63	56.13	70.72	14.59	0.608	2.53E-02
80	71.27	89.8	18.53	0.841	3.82E-02
100	89.09	112.2	23.16	1.001	4.33E-02
125	111.4	140.3	28.95	1.128	4.40E-02
160	142.5	179.6	37.05	1.268	4.34E-02
200	178.2	224.5	46.31	1.420	4.35E-02
250	222.7	280.6	57.89	1.579	4.31E-02
315	280.6	353.6	72.94	1.749	4.19E-02
400	356.4	449	92.63	1.830	3.62E-02
500	445.4	561.2	115.8	1.850	2.96E-02
630	561.3	707.2	145.9	1.849	2.34E-02
800	712.7	898	185.3	1.843	1.83E-02
1000	890.9	1122	231.6	1.838	1.46E-02
1250	1114	1403	289.5	1.838	1.17E-02
1600	1425	1796	370.5	1.790	8.65E-03
2000	1782	2245	463.1	1.310	3.71E-03

Reference

17-1. T. Irvine, A Method for Power Spectral Synthesis Rev B, Vibrationdata Publications, 200.

APPENDIX A

FOURIER TRANSFORM OF A SINE FUNCTION

Consider a sine wave

$$x(t) = A \sin\left[2\pi \hat{f}\, t\right] \tag{A-1}$$

where

$$-\infty < t < \infty$$

The Fourier transform is calculated indirectly, by considering the inverse transform. Note that the sine wave is a special case in this regard.

Recall

$$x(t) = \int_{-\infty}^{\infty} X(f) \exp\left[+ j 2\pi f t\right] df \tag{A-2}$$

Thus

$$A \sin\left[2\pi \hat{f}\, t\right] = \int_{-\infty}^{\infty} X(f) \exp\left[+ j\, 2\pi f t\right] df \tag{A-3}$$

$$A \sin\left[2\pi \hat{f}\, t\right] = \int_{-\infty}^{\infty} X(f) \left\{\cos\left[2\pi f t\right] + j \sin\left[2\pi f t\right]\right\} df \tag{A-4}$$

Let

$$X(f) = P(f) + j\, Q(f) \tag{A-5}$$

where

P(f) and Q(f) are both real coefficients

and

$$-\infty < f < \infty.$$

$$A \sin\left[2\pi \hat{f}\, t\right] = \int_{-\infty}^{\infty} \left\{P(f) + j\, Q(f)\right\} \left\{\cos\left[2\pi f t\right] + j \sin\left[2\pi f t\right]\right\} df \tag{A-6}$$

$$A\sin\left[2\pi\hat{f}t\right] = \int_{-\infty}^{\infty}\left\{P(f)\cos\left[2\pi f t\right] - Q(f)\sin\left[2\pi f t\right]\right\}df + j\int_{-\infty}^{\infty}\left\{P(f)\sin\left[2\pi f t\right] + Q(f)\cos\left[2\pi f t\right]\right\}df \tag{A-7}$$

Equation (A-7) can be broken into two parts

$$A\sin\left[2\pi\hat{f}t\right] = \int_{-\infty}^{\infty}\left\{P(f)\cos\left[2\pi f t\right] - Q(f)\sin\left[2\pi f t\right]\right\}df \tag{A-8}$$

$$0 = j\int_{-\infty}^{\infty}\left\{P(f)\sin\left[2\pi f t\right] + Q(f)\cos\left[2\pi f t\right]\right\}df \tag{A-9}$$

Consider equation (A-8)

$$A\sin\left[2\pi\hat{f}t\right] = \int_{-\infty}^{\infty}\left\{P(f)\cos\left[2\pi f t\right] - Q(f)\sin\left[2\pi f t\right]\right\}df \tag{A-10}$$

Now assume

$$P(f)=0 \tag{A-11}$$

With this assumption,

$$A\sin\left[2\pi\hat{f}t\right] = -\int_{-\infty}^{\infty}Q(f)\sin\left[2\pi f t\right]df \tag{A-12}$$

Now let

$$Q(f)= q_1(f) + q_2(f) \tag{A-13}$$

$$A\sin\left[2\pi\hat{f}t\right] = -\int_{-\infty}^{\infty}\left[q_1(f) + q_2(f)\right]\sin\left[2\pi f t\right]df \tag{A-14}$$

$$A\sin\left[2\pi\hat{f}t\right] = -\int_{-\infty}^{\infty}\left[q_1(f)\right]\sin\left[2\pi f t\right]dt - \int_{-\infty}^{\infty}\left[q_2(f)\right]\sin\left[2\pi f t\right]df \tag{A-15}$$

$$A\sin\left[2\pi\hat{f}t\right] = -\int_{-\infty}^{\infty}\left[q_1(f)\right]\sin\left[2\pi f t\right]dt + \int_{-\infty}^{\infty}\left[q_2(f)\right]\sin\left[-2\pi f t\right]df \tag{A-16}$$

Equation (A-14) is satisfied by the pair of equations

$$q_1(f) = -\frac{A}{2}\delta\left(f - \hat{f}\right) \tag{A-17}$$

$$q_2(f) = \frac{A}{2}\delta\left(-f - \hat{f}\right) \tag{A-18}$$

where δ is the Dirac delta function.

By substitution,

$$Q(f) = \frac{-A}{2}\delta\left(f - \hat{f}\right) + \frac{A}{2}\delta\left(-f - \hat{f}\right) \tag{A-19}$$

Verification must be made that equation (A-9) is satisfied. Recall

$$0 = j\int_{-\infty}^{\infty}\left\{P(f)\sin\left[2\pi f t\right] + Q(f)\cos\left[2\pi f t\right]\right\}df \tag{A-20}$$

$$0 \stackrel{?}{=} j\int_{-\infty}^{\infty}\left\{0\sin\left[2\pi f t\right] + \left\{\frac{-A}{2}\delta\left(f - \hat{f}\right) + \frac{A}{2}\delta\left(-f - \hat{f}\right)\right\}\cos\left[2\pi f t\right]\right\}df \tag{A-21}$$

$$0 \stackrel{?}{=} j\left\{\frac{-A}{2}\cos\left[2\pi\hat{f}\ t\right] + \frac{A}{2}\cos\left[-2\pi\hat{f}\ t\right]\right\} \tag{A-22}$$

$$0 \stackrel{?}{=} j\left\{\frac{-A}{2}\cos\left[2\pi\hat{f}\ t\right] + \frac{A}{2}\cos\left[2\pi\hat{f}\ t\right]\right\} \tag{A-23}$$

$$0 = 0 \tag{A-24}$$

Recall the time domain function

$$x(t) = A\sin\left[2\pi\hat{f}\,t\right] \tag{A-25}$$

where $-\infty < t < \infty$

The Fourier transform is thus

$$X(f) = \frac{-jA}{2}\delta\left(f - \hat{f}\right) + \frac{jA}{2}\delta\left(-f - \hat{f}\right) \tag{A-26}$$

$$X(f) = \left\{\frac{jA}{2}\right\}\left\{-\delta\left(f - \hat{f}\right) + \delta\left(-f - \hat{f}\right)\right\} \tag{A-27}$$

APPENDIX B

FILTER ARGUMENT

Consider the points at $s = j\Omega_0$ on the s-plane and $z = \exp[j\omega_0]$ on the z-plane.

By substitution in to equation (14-21),

$$j\Omega_0 = \frac{\exp[j\omega_0] - 1}{\exp[j\omega_0] + 1} \tag{B-1}$$

$$j\Omega_0 = \frac{\cos[\omega_0] + j\sin[\omega_0] - 1}{\cos[\omega_0] + j\sin[\omega_0] + 1} \tag{B-2}$$

$$\Omega_0 = \frac{\cos[\omega_0] + j\sin[\omega_0] - 1}{j\cos[\omega_0] - \sin[\omega_0] + j} \tag{B-3}$$

$$\Omega_0 = \frac{\cos[\omega_0] - 1 + j\sin[\omega_0]}{-\sin[\omega_0] + j\{\cos[\omega_0] + 1\}} \tag{B-4}$$

$$\Omega_0 = \left\{\frac{\cos[\omega_0] - 1 + j\sin[\omega_0]}{-\sin[\omega_0] + j\{\cos[\omega_0] + 1\}}\right\}\left\{\frac{-\sin[\omega_0] - j\{\cos[\omega_0] + 1\}}{-\sin[\omega_0] - j\{\cos[\omega_0] + 1\}}\right\} \tag{B-5}$$

$$\Omega_0 = \left\{\frac{\{\cos[\omega_0] - 1\}\{-\sin[\omega_0] - j\{\cos[\omega_0] + 1\}\} + \{j\sin[\omega_0]\}\{-\sin[\omega_0] - j\{\cos[\omega_0] + 1\}\}}{\sin^2[\omega_0] + \{\cos[\omega_0] + 1\}^2}\right\} \tag{B-6}$$

$$\Omega_0 = \left\{ \frac{-\cos[\omega_0]\sin[\omega_0] + \sin[\omega_0] - j\left\{\cos^2[\omega_0] - 1\right\}}{\sin^2[\omega_0] + \cos^2[\omega_0] + 2\cos[\omega_0] + 1} \right\}$$

$$+ \left\{ \frac{\cos[\omega_0]\sin[\omega_0] + \sin[\omega_0] - j\sin^2[\omega_0]}{\sin^2[\omega_0] + \cos^2[\omega_0] + 2\cos[\omega_0] + 1} \right\}$$

(B-7)

$$\Omega_0 = \left\{ \frac{2\sin[\omega_0]}{2\cos[\omega_0] + 2} \right\} \tag{B-8}$$

$$\Omega_0 = \left\{ \frac{\sin[\omega_0]}{\cos[\omega_0] + 1} \right\} \tag{B-9}$$

$$\Omega_0 = \tan\left[\frac{\omega_0}{2} \right] \tag{B-10}$$

$$\Omega_0 = \tan[\pi f_0 T] \tag{B-11}$$